NTIS #PB96-129036

SSC-383

OPTIMUM WELD-METAL STRENGTH FOR HIGH STRENGTH SHIP STRUCTURES

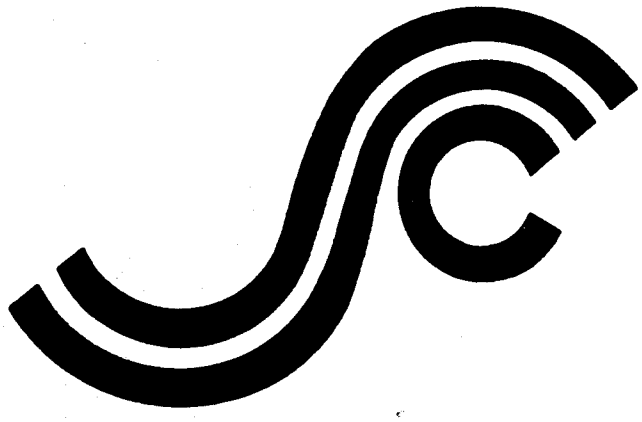

SHIP STRUCTURE COMMITTEE

1995

SHIP STRUCTURECOMMITTEE

The SHIP STRUCTURE COMMITTEE is constituted to prosecute a research program to improve the hull structures of ships and other marine structures by an extension of knowledge pertaining to design, materials, and methods of construction.

RADM J. C. Card, USCG (Chairman)
Chief, Office of Marine Safety, Security
and Environmental Protection
U. S. Coast Guard

Mr. Thomas H. Peirce
Marine Research and Development
Coordinator
Transportation Development Center
Transport Canada

Mr. Edwin B. Schimler
Associate Administrator for Ship-
building and Technology Development
Maritime Administration

Dr. Donald Liu
Senior Vice President
American Bureau of Shipping

Mr. Robert McCarthy
Director, Survivability and Structural
Integrity Group (SEA O3P)
Naval Sea Systems Command

Mr. Thomas Connors
Acting Director of Engineering (N7)
Military Sealift Command

Dr. Ross Grahm
Head, Hydronautics Section
Defence Research Establishment-Atlantic

EXECUTIVE DIRECTOR

CDR Stephen E. Sharpe, USCG
U. S. Coast Guard

CONTRACTING OFFICER TECHNICAL REPRESENTATIVE

Mr. William J. Siekierka
Naval Sea Systems Command

SHIP STRUCTURESUBCOMMITTEE

The SHIP STRUCTURE SUBCOMMITTEE acts for the Ship Structure Committee on technical matters by providing technical coordination for determinating the goals and objectives of the program and by evaluating and interpreting the results in terms of structural design, construction, and operation.

MILITARY SEALIFT COMMAND

Mr. Robert E. Van Jones (Chairman)
Mr. Rickard A. Anderson
Mr. Michael W. Touma
Mr. Jeffrey E. Beach

MARITIME ADMINISTRATION

Mr. Frederick Seibold
Mr. Richard P. Voelker
Mr. Chao H. Lin
Dr. Walter M. Maclean

U. S. COAST GUARD

CAPT George Wright
Mr. Walter Lincoln
Mr. Rubin Sheinberg

AMERICAN BUREAU OF SHIPPING

Mr. Glenn Ashe
Mr. John F. Conlon
Mr. Phillip G. Rynn
Mr. William Hanzelek

NAVAL SEA SYSTEMS COMMAND

Mr. W. Thomas Packard
Mr. Charles L. Null
Mr. Edward Kadala
Mr. Allen H. Engle

TRANSPORT CANADA

Mr. John Grinstead
Mr. Ian Bayly
Mr. David L. Stocks
Mr. Peter Timonin

DEFENCE RESEARCH ESTABLISHMENT ATLANTIC

Dr. Neil Pegg
LCDR Stephen Gibson
Dr. Roger Hollingshead
Mr. John Porter

SHIP STRUCTURE SUBCOMMITTEE LIAISON MEMBERS

SOCIETY OF NAVAL ARCHITECTS AND MARINE ENGINEERS
Dr. William Sandberg

CANADA CENTRE FOR MINERALS AND ENERGY TECHNOLOGIES
Dr. William R. Tyson

U. S. NAVAL ACADEMY
Dr. Ramswar Bhattacharyya

U. S. MERCHANT MARINE ACADEMY
Dr. C. B. Kim

U. S. COAST GUARD ACADEMY
LCDR Bruce R. Mustain

U. S. TECHNICAL ADIVSORY GROUP TO THE INTERNATIONAL STANDARDS ORGANIZATION
CAPT Charles Piersall

NATIONAL ACADEMY OF SCIENCES - MARINE BOARD
Dr. Robert Sielski

NATIONAL ACADEMY OF SCIENCES - COMMITTEE ON MARINE STRUCTURES
Dr. John Landes

WELDING RESEARCH COUNCIL
Dr. Martin Prager

AMERICAN IRON AND STEEL INSTITUTE
Mr. Alexander D. Wilson

OFFICE OF NAVAL RESEARCH
Dr. Yapa D. S. Rajapaske

MASSACHUSETTS INSTITUTE OF TECHNOLOGY

CAPT Alan J. Brown

STUDENT MEMBER
Mr. Jason Miller
Massachusetts Institute of Technology

Member Agencies:

American Bureau of Shipping
Defence Research Establishment Atlantic
Maritime Administration
Military Sealift Command
Naval Sea Systems Command
Transport Canada
United States Coast Guard

Ship Structure Committee

An Interagency Advisory Committee

Address Correspondence to:

Executive Director
Ship Structure Committee
U.S. Coast Guard (G-MMS/SSC)
2100 Second Street, S.W.
Washington, D.C. 20593-0001
Ph:(202) 267-0003
Fax:(202) 267-4816

SSC-383
SR-1343

18 December 1995

OPTIMUM WELD-METAL STRENGTH FOR HIGH STRENGTH SHIP STRUCTURES

The production of high strength steel hulls is highly impacted by the need for extensive pre- and post-weld heat soak for the weldments. This has been further impacted by the assumption that a weldment must have a higher strength than the base plate in order to prevent failures from initiating in the weld. This project was intended to look at the possibility of undermatching these weldments in order achieve productivity gains.

The large test facilities available at Lehigh University allowed for full scale wide plate tests of representative welds using a variety of base metals and percentages of undermatching. Through the analysis of the results, the report recommends several applications for which the use of undermatched welds with high strength steels may be appropriate.

J. C. CARD
Rear Admiral, U.S. Coast Guard
Chairman, Ship Structure Committee

Technical Report Documentation Page

1. Report No.	2. Government Accession No.	3. Recipient's Catalog No.
SSC 383	PB96-129036	

4. Title and Subtitle	5. Report Date
"Optimum Weld-Metal Strength for High-Strength Steel Structures"	July 1995
	6. Performing Organization Code
7. Author(s)	8. Performing Organization Report No.
Robert J. Dexter and Matthew Ferrell	ATLSS Report No. 95-08
9. Performing Organization Name and Address ATLSS Engineering Research Center Lehigh University 117 ATLSS Drive Bethlehem, PA 18015-4729	10. Work Unit No. (TRAIS)
	11. Contract or Grant No. DTCG23-92-R-E01014-1
12. Sponsoring Agency Name and Address Ship Structure Committee U.S. Coast Guard 2100 Second St., SW Washington, DC 20593	13. Type of Report and Period Covered Final Report
	14. Sponsoring Agency Code

15. Supplementary Notes

Sponsored by the Ship Structure Committee and its member agencies

16. Abstract

This report provides data and analysis to support the acceptance of undermatched welds in high-strength steel in shipbuilding. Wide-plate tensile tests made from HSLA-100 steel plate (690 MPa minimum yield strength) with transverse groove welds demonstrated that moderately-undermatched joints (actual weld yield strength up to 12 percent less than actual base-plate yield strength) can achieve strength and ductility as high as overmatched welds. Welds undermatched between 18 and 28 percent exhibited full strength but minimal ductility. Relatively coarse-mesh elastoplastic finite-element analysis adequately reproduced the behavior observed in the experiments. Wide-plate specimens were prepared with various controlled intentional defects in both moderately-undermatched and overmatched welds. These defect specimens exhibited remarkable performance and there was no consistent difference between the results of the moderately-undermatched welds and the overmatched welds. When loaded in shear, groove welds undermatched up to 28 percent developed the required minimum shear strength of the HSLA-100 plate and had excellent ductility. Guidelines and commentary for design, finite-element analysis, selection of weld filler metal and welding procedure for various types of joints are given to facilitate the use of high-strength steel with optimum weld metal properties.

17. Key Words	18. Distribution Statement
Ship structure, undermatched weld, strength ductility, weld defects, finite element	Available from: National Technical Information Service Springfield, VA 22161 Distribution unlimited

19. Security Classif. (of this report)	20. Security Classif. (of this page)	21. No. of Pages	22. Price
Unclassified	Unclassified	126	$27.00 Paper $12.50 Microf.

Form DOT F 1700.7 (8-72) Reproduction of completed page authorized

United States Department of Commerce
Technology Administration
National Institute of Standards and Technology
Metric Program, Gaithersburg, MD 20899

METRIC CONVERSION CARD

Approximate Conversions to Metric Measures

Symbol	*When You Know*	*Multiply by*	*To Find*	*Symbol*
LENGTH				
in	inches	2.5	centimeters	cm
ft	feet	30	centimeters	cm
yd	yards	0.9	meters	m
mi	miles	1.6	kilometers	km
AREA				
in^2	square inches	6.5	square centimeters	cm^2
ft^2	square feet	0.09	square meters	m^2
yd^2	square yards	0.8	square meters	m^2
mi^2	square miles	2.6	square kilometers	km^2
	acres	0.4	hectares	ha
MASS (weight)				
oz	ounces	28	grams	g
lb	pounds	0.45	kilograms	kg
	short tons (2000 lb)	0.9	metric ton	t
VOLUME				
tsp	teaspoons	5	milliliters	mL
Tbsp	tablespoons	15	milliliters	mL
in^3	cubic inches	16	milliliters	mL
fl oz	fluid ounces	30	milliliters	mL
c	cups	0.24	liters	L
pt	pints	0.47	liters	L
qt	quarts	0.95	liters	L
gal	gallons	3.8	liters	L
ft^3	cubic feet	0.03	cubic meters	m^3
yd^3	cubic yards	0.76	cubic meters	m^3
TEMPERATURE (exact)				
°F	degrees Fahrenheit	subtract 32, multiply by 5/9	degrees Celsius	°C

Approximate Conversions from Metric Measures

Symbol	*When You Know*	*Multiply by*	*To Find*	*Symbol*
LENGTH				
mm	millimeters	0.04	inches	in
cm	centimeters	0.4	inches	in
m	meters	3.3	feet	ft
m	meters	1.1	yards	yd
km	kilometers	0.6	miles	mi
AREA				
cm^2	square centimeters	0.16	square inches	in^2
m^2	square meters	1.2	square yards	yd^2
km^2	square kilometers	0.4	square miles	mi^2
ha	hectares (10,000 m^2)	2.5	acres	
MASS (weight)				
g	grams	0.035	ounces	oz
kg	kilograms	2.2	pounds	lb
t	metric ton (1,000 kg)	1.1	short tons	
VOLUME				
mL	milliliters	0.03	fluid ounces	fl oz
mL	milliliters	0.06	cubic inches	in^3
L	liters	2.1	pints	pt
L	liters	1.06	quarts	qt
L	liters	0.26	gallons	gal
m^3	cubic meters	35	cubic feet	ft^3
m^3	cubic meters	1.3	cubic yards	yd^3
TEMPERATURE (exact)				
°C	degrees Celsius	multiply by 9/5, add 32	degrees Fahrenheit	°F

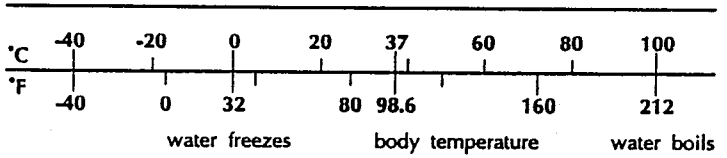

Table of Contents

List of Tables

List of Figures

Acknowledgements

This work was supported by the interagency Ship Structure Committee under contract DTCG23-92-R-EO1014-1. The authors are grateful for the guidance of the Project Technical Committee, especially the Chairman Allen Manuel of NAVSEA and the Technical Advisor Jim Sawhill of Newport News Shipbuilding. The survey of ship weld details, economic analysis, and preparation of the first series of test specimens was done by Bath Iron Works Corporation under the direction of David Forrest. In addition to the authors, many others at Lehigh have contributed to this research, especially Eric Kaufmann and David Schnalzer. Professors John Fisher and Alan Pense provided guidance and advice. Several undergraduate students at Lehigh University contributed to the project, especially Kenneth Gilvary, Sheri Mignone, and Erika Frykhammer. The authors are also grateful for the work of the technical staff at Fitz Laboratory and the photography of Richard Sopko.

1.0 INTRODUCTION

The material properties of weld metal, in approximate order of importance, are weldability, fracture toughness, ductility, and strength. All of these properties are affected in different ways by the chemistry of the weld filler metal and the welding procedures. The weld filler metals and weld procedures must be carefully selected in order to produce welds with an optimum balance of these material properties.

Weldability can be thought of as the ability to easily and repeatedly produce quality welds without strict procedure controls and without onerous preheating requirements. For shipbuilding steels, the primary weldability issue is the resistance of the weld and heat-affected zone (HAZ) to hydrogen-assisted cracking. Weldability is provided for in shipbuilding specifications by limits on the chemistry and processing of the steel as well as the weld consumables. Shipyards and individual welders refine their welding procedures to achieve good weldability.

Typically, steel, weld consumables, and weld procedures which result in good weldability also result in a weldment with good fracture toughness and ductility. Steel and weld-metal specifications further screen out materials with inadequate fracture toughness by having a requirement for minimum Charpy vee-notch (CVN) energy at specified temperatures. Weld metal with better CVN typically is more weldable as well.

High-strength steel plates and weld filler metals have been developed for ships requiring improved weldability and higher fracture toughness. For example, copper-precipitation-hardening steels are produced in the U.S. such as ASTM A710, i.e. "Low Carbon Age-Hardening Nickel-Copper-Chromium-Molybdenum-Columbium and Nickel-Copper-Columbium Alloy Steels". The U.S. Navy has been the primary market for the A710 steel plates. The military specification for this steel (Mil-S-24645A (SH)), Steel Plate, sheet, or coil age-hardening alloy, structural, high yield strength, (HSLA-80 and HSLA-100)) provides for two grades known as HSLA-80 (560 MPa yield) and HSLA-100 (690 MPa yield). The military specification has more stringent CVN requirements than ASTM A710, e.g. for HSLA-100, 80 Joules is required at -84°C and 107 Joules is required at -18°C. The military specification requires additional fracture testing, e.g. the plate must pass the explosion-bulge test at -18°C and pass the nil-ductility test at -68°C.for HSLA-80 (at a temperature to be specified for HSLA-100). Because of the superior fracture properties, this steel is ideal for connections with transverse welds and/or other notches or stress concentrations loaded in tension.

While strength is of obvious importance, it is rated last in the above list of weld metal properties because it is easily controlled through specifications and testing by weld consumable manufacturers. Consequently, inadequate strength is rarely the cause of structural failure. Furthermore other limit states such as fatigue, deflection, compression stability, or weld distortion may often control the scantlings, and therefore the strength of the steel cannot be fully exploited.

Ductility of weld metal is required to allow yielding and redistribution of the stresses in structures. Ductility is critical to the safe operation of ships because it enables the ships to maintain integrity in the event of fabrication defects, deterioration, damage, extreme loads, or accidents. Ductility is expressed in terms of the "ductility factor", which is defined here as the ratio of the total deformation at failure to the deformation at yielding. The measure of deformation can be the overall displacement of a structural element, rotation at a joint, or strain. Ductility is determined by the structural details as well as the material properties. Therefore, elongation or reduction in area in the tensile test is a poor indicator of structural ductility. Because welded structures have notches and discontinuities, good fracture toughness is probably more important for structural ductility than the elongation or reduction in area in a tensile test.

Full-scale tests show that properly proportioned and detailed welded steel structural assemblages can consistently exceed their yield strength, achieve the calculated fully-plastic "limit load", and deform in a ductile manner to a total displacement many times larger than the displacement at the yield point [39]. Because of this ductility, design specifications for bridges, buildings, and a variety of other steel structures have evolved which are based on the plastic limit load rather than an allowable stress. Examples of such limit-state design specifications include the "Load and Resistance Factor Design (LRFD) Specification for Structural Steel Buildings" from the American Institute of Steel Construction (AISC) and the "AASHTO LRFD Bridge Design Specifications" from the American Association of State Highway and Transportation Officials. LRFD specifications: 1) have a quantifiable level of reliability which is approximately equal for all limit states; and, 2) are typically more efficient than allowable stress specifications. The trend in ship design is also moving toward limit state design [41].

The required level of ductility is usually not explicitly specified in design codes. Ductility is indirectly assured by detailing and workmanship requirements and by allowing only specific materials. There are a few references to acceptable levels of ductility on a structural scale in the literature. Wells' criterion for good performance from wide-plate tests in the early 60's was a ductility factor of 4. In a recent paper by Rudi Denys [40], a criterion for acceptability of defective welds is proposed to assure pipeline integrity. Denys proposes that wide-plate tests are acceptable if there is greater than 0.8 percent strain over the gage length. For a steel with a yield point of about 350 MPa, this is equivalent to a ductility factor between 4 and 5.

The welding codes that govern fabrication of ships and other steel structures such as buildings and bridges often require that the weld metal yield strength match or exceed that of the parent plate, i.e. the weld is overmatched. This is done primarily to protect the weld from localization of plastic strain in the event that the yield load of the structure is exceeded, i.e. to force the plastic deformation to occur primarily in the parent plate. The overmatching requirement is dependent on the type of joint, and typically applies to joints where weld failure could be catastrophic. For example, the American Welding Society (AWS) Structural Welding Code D1.1 [3] only requires matching weld metal for groove welds subjected to tension normal to the effective area. For non-critical members and joints subjected to certain types of loading this matching requirement is waived and undermatched weld metal may be used. However, in order to preclude the possibility of a mixup, it is considered preferable to use only one type of consumable on a particular job.

For Navy ships, the welding filler materials are specified in Section 10 of MIL-STD-1689A(SH), "Fabrication, Welding, and Inspection of Ship Structure". These filler materials are overmatched, and MIL-STD 1689 states that these overmatching filler materials should be used for all types of joints, "unless otherwise approved". In fact, many applications of undermatched welds have been approved on a case-by-case basis for HSLA-100 and HY-100.

An overmatching requirement presents no problems for the common, low-strength steels now typically used in most structural applications. However, the increased use of high-strength steels (yield strengths in excess of 690 MPa) in shipbuilding and civil structures has indicated a number of disadvantages of the high-strength overmatching weld metals, e.g. lower fracture toughness and greater susceptibility to hydrogen-assisted cracking. The greater susceptibility to hydrogen-assisted cracking is mitigated with stringent control of the weld process including significant preheat and interpass temperature requirements. For high-strength steels such as HSLA-100, the use of undermatched weld metal will significantly reduce welding costs and will probably also result in a joint with improved fracture resistance and ductility as well.

However, in the event that a member is yielded in tension or in tension from bending, yielding and strain localization in an undermatched weld may be a potential problem which limits overall ductility. Fortunately, two phenomena occur which mitigate the yielding in moderately undermatched weld metal: 1) strain-hardening which increases the flow stress; and, 2) constraint. The effect of constraint is discussed in detail in subsequent Sections. Both phenomena contribute to the spreading of plasticity and the associated achievement of reasonable overall member ductility.

In summary, the primary weld-metal properties which can be controlled and are quantifiable, and therefore can be optimized, are the CVN notch toughness and the yield strength. The objective is to obtain the maximum possible ductility of the structural system and minimize the cost of welding. It was determined in this project that for the HSLA-100 steel, optimum weld-metal properties are obtained with the undermatched 100S-1 weld wire (minimum 690 MPa ultimate strength), with some restrictions on the maximum heat input.

This report addresses outstanding issues relevant to acceptance of undermatched welds in shipbuilding. The objectives of the research were to:

1. summarize the current knowledge regarding the performance of structural members with undermatched welds (relative to corresponding overmatched welds) when subjected to service loading as well as unanticipated loading that causes yielding.

2. assess the criticality of typical ship welded joints and determine candidate joints for potential undermatching.

3. determine how much undermatching of critical joints in surface ship structure can be tolerated without significantly affecting the performance of the structure.

4. develop failure criteria for undermatched joints and prepare guidelines for the acceptance of undermatched welds in structures.

The approach to this research is described below:

1. A summary of the current state of knowledge was developed by extensive literature review, conference attendance, and personal communication with those researchers currently involved in research concerning undermatched welds. This information is discussed in Chapter 2.

2. Joint criticality was determined by a major shipyard (Bath Iron Works) and this assessment is also discussed in Chapter 2.

3. The performance of undermatched welds was determined with full-scale testing (Chapter 3) and finite-element analysis (Chapter 4).

4. The findings from the testing and analysis are synthesized and developed into design and welding guidelines in Chapter 5.

5. The conclusions of this research are presented in Chapter 6.

2.0 BACKGROUND

2.1 Weld Yield Strength Variations

2.1.1 Practice of Overmatching

The concept of requiring overmatching weld metal was supported by the work of Hartbower and Pellini [14,15]. Hartbower and Pellini conducted explosion bulge tests on both overmatched and undermatched weldments. These tests examined the deformation and fracture behavior of welds subjected to high strain rate, multiaxial loading conditions. The results showed that the effect of the undermatched weld was to concentrate strain in the weld such that the weld strain is much higher than the nominal strains in the parent plate remote from the weld, while overmatching had the opposite effect. Additionally, the overmatched welds exhibited ductile fracture at lower temperatures than undermatched welds (The criterion for ductile fracture was defined as achieving a ten percent thickness reduction prior to fracture.) Only half of the overmatched specimens developed cracks in the weld, and those cracks that formed were perpendicular to the axis of the weld, arresting in the base plate. The undermatched welds, in contrast, all fractured in the weld parallel to the weld axis, which is undesirable. It was concluded, therefore, that welds should be overmatched to shield defects from excessive strains.

However, the work of Hartbower and Pellini was with steels of 260 MPa to 360 MPa yield strengths, low- to medium-strength by current standards. The overmatching requirement presents no difficulty for steels at these relatively low strength levels, as overmatching weld metals with good weldability and toughness, not very susceptible to hydrogen cracking, are readily available. The increased use of high-strength steels has spurred research into the possible use of undermatching weld metal in order to have weld metal with greater fracture toughness and resistance to hydrogen cracks.

In order to generate acceptance of undermatched welds, a database of undermatched weld performance must be generated. Four areas of interest are:

1. strength and ductility;
2. fracture performance;
3. fatigue resistance; and
4. compression stability (various buckling modes).

Additionally, the cost savings associated with fabricating undermatched welds compared to overmatched welds must be quantified and demonstrated.

2.1.2 Unintentional Undermatch

Though overmatched welds may be specified, welded joints produced using overmatching electrodes may have soft zones, i.e., zones of lower yield strength, which are unintentional and are not considered. The welds may unknowingly be undermatched because the base

plate has much higher yield strength than the minimum specified yield strength (MSYS). For example, the specifications for HSLA-100 (MIL-S-24645A(SH)) requires the yield strength to remain in the range 690 to 900 MPa. Tensile data for HSLA-100 steel collected from the steel mills by Naval Surface Warfare Center is shown in Figure 2-1. The mean yield strength of the HSLA-100 is about 745 MPa and the coefficient of variation is about 5.5 percent. These data show that HSLA-100 commonly ranges up to 815 MPa which is 18 percent greater than the MSYS.

Also, the weld itself may have much lower strength than expected. Often the filler metal certification tests are performed on welds in thicker plates than the application, which means the cooling rate and strength may be lower in the application. For example, a recent study at General Dynamics Electric Boat Division [5] examined weld undermatch in relatively thin section HY-100 steel (690 MPa yield). Thirty specimens were fabricated with overmatching Mil-120S-1 and Mil-12018-M2 electrodes (minimum 830 MPa ultimate) using a number of weld processes and specimen thicknesses from 9 mm to 16 mm. The results are shown in Table 2-1. Only 11 percent of the weld metal coupons achieved the required 704 MPa yield strength and the average for all processes and thicknesses was nearly 60 MPa below that value. This represents a nominal undermatch of six to seven percent, i.e. the yield strength of the weld metal was six to seven percent less than the MSYS. The lowest weld metal strength was obtained for shielded-metal-arc welding (SMAW) in 9 mm thick plate, i.e. the average yield strength was 613 MPa. Actually, it is the undermatch relative to the actual yield strength which is the most important parameter. The actual undermatch could be up to 32 percent if SMAW process was used in 9 mm plate which is at the high end of the allowable yield strength (900 MPa). Without specific guidelines governing the potential impact of unintentional soft zones on structural performance, these soft zones are a potential hazard.

2.1.3 Soft Zones in the HAZ

Even if the weld itself is overmatched, zones of low-strength material can occur in the heat-affected zone (HAZ) when micro-alloyed steels produced with advanced processing or auxiliary heat treatment (e.g. HSLA or TMCP steels) are welded. The thermal cycles applied to the steel during welding essentially negates the effects of the processing. The softening is generally most significant in the grain-refined region, i.e. the region which is reheated only momentarily above the austenite transformation temperature.

Examples of softening found in the literature are shown in Table 2-2. The maximum softening is about 25 percent below the actual base metal yield strength and the maximum width of the softened region is 8 mm. Though little experimental work has been done on the effect of HAZ soft zones on weldment performance, the analogy between soft zones in the HAZ and undermatched welds is clear. However, soft zones in the HAZ are much more narrow than an undermatched weld zone. Therefore, the HAZ soft zones are generally thought to be much less detrimental to ductility and strength than undermatched welds [7].

2.2 Advantages of Undermatching High-strength Steel

2.2.1 Hydrogen Cracking

The most significant disadvantage, in terms of cost, of welding high-strength steels with overmatching weld metal is the possibility of hydrogen cracking, also referred to as cold cracking since it may occur after the weld has cooled. Though the process of hydrogen cracking is not fully understood, there are three primary factors which are necessary for its occurrence: 1) diffused hydrogen in the weld; 2) tensile residual and/or applied stresses; and, 3) a crack-sensitive microstructure. Hydrogen can cause cracking in the heat-affected zone (HAZ), surface cracks at the weld toe, and transverse cracks within the weld itself.

The sensitivity of the microstructure in these areas is determined primarily by the carbon and to a lesser extent other alloys. The base metal can be processed to increase strength without increasing carbon. In fact, modern low-carbon high-strength steels are produced by advanced processing techniques, such as controlled-rolling or precipitation hardening, which are very resistant to hydrogen cracking in the base metal or HAZ. However, in order to overmatch 690 MPa MSYS steel such as HSLA-100, filler metals (such as the 120S-1 wire) must have a higher alloy than the base metal. When these high-alloy weld metals cool, they tend to form a more crack-sensitive microstructure with a high proportion of martensite. Also, the higher alloy content of the weld metal may delay the transformation of the weld relative to the base metal. This delay in weld transformation may inhibit diffusion of the hydrogen out of the weld, further increasing the potential for hydrogen cracking. Costly weld procedures must be strictly followed in order to prevent cracking of this 120S-1 weld metal.

Undermatching will decrease the potential for hydrogen cracking because the lower-strength weld requires less alloying. As the undermatched weld cools, it transforms to a less crack-sensitive microstructure. Undermatching can also reduce the amount of residual stress in the weldment. It has been shown that in highly restrained welds, the peak magnitude of the tensile residual stresses are on the order of the yield strength of the weld metal [8]. Therefore, by reducing the strength of the weld metal, the magnitude of the tensile residual stresses is also reduced. Undermatched weld metal, therefore, mitigates two of the three primary factors which contribute to hydrogen cracking.

It has been shown previously and was confirmed in this project that the HSLA-100 steel can be welded without preheat and interpass temperature requirements if the less-susceptible but slightly-undermatched 100S-1 weld metal is. used.

2.2.2 Welding Productivity

The procedures used to fabricate high-strength steels are strictly controlled to minimize the probability of hydrogen cracking. The preheat and interpass temperatures must be carefully monitored. Electrodes and flux must be carefully handled to minimize the introduction of hydrogen into the weld. Also, rigorous non-destructive evaluation (NDE) is required (typically 48 hours after welding due to the delayed nature of hydrogen cracking) to ensure sound welds. These procedures increase both fabrication costs and production time. Undermatched welds, due to their resistance to hydrogen cracking, will reduce the more costly aspects of these procedures. For example, if the probability of hydrogen cracking is diminished, the NDE requirements could be relaxed, saving both time and expense.

Undermatched welds will only be accepted when a clear economic benefit from undermatching is established. A number of researchers [13,29] have demonstrated that a reduction of preheat can be obtained using undermatched welds, though the economic benefit was not quantified. The most comprehensive review of the economics of fabrication, criteria for weldment performance, and factors affecting weldment performance was developed by the National Materials Advisory Board (NMAB) [17]. The report examined welding procedures and specifications for HY steels used primarily for Naval ship construction. The NMAB investigation concluded that there are economic advantages to moderate undermatching (10% or less based on MSYS) including reduced preheat, relaxed NDE due to lower hydrogen cracking potential, and increased deposition of weld metal. NMAB found no justification for the overmatching requirement for HY steels, concluding that higher toughness and lower residual stresses of the undermatched weld metal offset the probability of weld metal fracture due to strain concentration in the weld. NMAB recommends that undermatching be considered, but that the ability of matched and undermatched weldments to meet performance requirements be verified experimentally with tensile, explosion bulge, and dynamic tear testing.

In this project, Bath Iron Works (BIW) reviewed the potential cost savings and other practical advantages of undermatching. The model for the cost savings is based on the HSLA-80 fabrication (9 to 18 mm thickness) at BIW facilities in the Arleigh Burke (DDG-51) class of Aegis destroyer. The calculations relied partially upon cost data from a 1989 Navy study. It was attempted to estimate the possible savings in undermatching HSLA-100 based on these data. The results estimate that a six percent reduction of the fabrication labor costs could be achieved. The breakdown of these savings is: 1) one percent labor savings due to reduced preheat; 2) four percent overhead cost savings (facilities, energy, heating devices, and maintenance); and, 3) one percent material cost savings (filler metal). These results are very sensitive to the assumptions, e.g. the facility or the hull. The results were also not entirely consistent with the 1989 Navy study.

Jim Sawhill of Newport News Shipbuilding reports that the cost savings are much greater than this for the thick plates (with higher preheats) in aircraft carrier decks. Also, in reaction to hydrogen-cracking which recently occurred with HY-100/120S-1 weldments in the Seawolf submarine, the requirements for 120S-1 have become tighter and more expensive since BIW completed their study. These tighter requirements for 120S-1 wire are applied to surface ships and HSLA-100 as well. Therefore the cost savings is greater than BIW estimated in their study. In any case, every shipbuilder agrees the savings are very significant.

2.3 Behavior of Undermatched Welds

2.3.1 Strength and Ductility

The first major project investigating the performance of undermatched welds is the work of the Soft Joint Committee of the Japan Welding Engineering Society. This research, primarily the work of Satoh and Toyoda, has made a significant contribution to the acceptance of undermatched welds. Satoh and Toyoda [30,32] published a series of papers describing the behavior of flat-plate and round bar tensile coupons with a uniform zone of low strength material. This investigation concluded that performance of the welded bars and plates was dependent of the ratio of soft layer thickness to plate thickness or bar diameter, that is, relative thickness. For specimens with large soft zones (relative thickness greater than one), the ultimate strength of the welded joint approached that of the soft layer while narrower weldments achieved base plate strength. An additional study [28] demonstrated the importance of the plate width-to-thickness (w/t) ratio. For joints with low relative thickness, a $w/t > 5$ yielded "infinite" plate results, i.e., achieved full base plate strength, but these joints exhibited lower strengths for $w/t < 5$.

Satoh and Toyoda conducted similar research [31] on joints in heavy plates (70 mm thickness) confirming the effect of w/t ratio. This work was motivated by the desire to undermatch the welds in thick HT80 pipes (760 MPa ultimate strength) comprising penstocks for a dam. In a sufficiently wide welded joint, joint strength equivalent to the base plate strength was achievable for undermatch up to 10 percent. (Unless otherwise stated, undermatch will be given in terms of the actual base plate strength as opposed to the MSYS). The ductility of these plates with 10 percent undermatched welds was also found to be comparable to similar plates with overmatched welds. However, joints which were undermatched by 34 percent achieved only 22 percent of the parent plate's ductility, yet reached 94 percent of the base plate's ultimate strength. Additional studies [29] showed that by using an 18 percent undermatching electrode, welding preheat could be reduced by 25°C for 760 MPa tensile strength steel without an appreciable difference in strength or ductility compared to overmatched weldments. Generally, the results of Soft Joint Committee research indicate that for butt-welds in these relatively thick plates, welds could be undermatched as much as 18 percent are achievable without a significant loss of strength or ductility.

The two primary factors that can help an undermatched weld achieve the full strength of the base plate (and spread the plastic deformation) are strain hardening and constraint. Since there is little strain hardening in these weld metals, constraint is the primary factor. Constraint is developed at the interface of the weld and base plate. Consider a butt weld loaded normal to the weld axis. If the weld is softer than the adjacent base plate, it will yield first. As strain localizes in the soft weld, it will begin deform as shown in Figure 2-2. Because the adjacent base plate is unyielded it will constrain the deformation of the soft weld. The weld will begin to develop tension is both the width and thickness directions, in addition to tension in the longitudinal direction due to the applied load.

When the weld experiences tension in two or three material directions, the mean stress or hydrostatic stress in the weld is increased.

Yielding of a material is governed by the Von-Mises Yield Criterion:

$$\sigma_y = \sqrt{\frac{3}{2}\,\sigma'_{ij}\,\sigma'_{ij}} \qquad (1)$$

where; σ_y is the yield stress, and
σ'_{ij} is the deviatoric stress tensor.

This yield criterion is represented in three dimensions as the yield surface shown in Figure 2-3. The magnitude of deviatoric stress is dependent on the hydrostatic stress as given by:

$$\sigma'_{ij} = \sigma_{ij} - \sigma_{kk} \qquad (2)$$

where; σ'_{ij} is the deviatoric stress tensor,
σ_{ij} is the applied stress tensor, and
σ_{kk} is the hydrostatic stress.

Therefore, as the hydrostatic stress is increased by constraint, the magnitudes of the deviatoric stresses, which govern yielding, are reduced. Thus, because of constraint, larger stresses are required to further increase plastic strain. An apparent increase in the weld metal strength is observed, and increases in applied load can be achieved.

The relatively thin plates (25 mm thickness and less) used in surface ships do not develop significant constraint through the thickness and are therefore in a state of plane stress with principal in-plane stresses σ_{11} and σ_{22}. In this case, the Von-Mises Yield Criterion, i.e. Equation (1), can be simplified to an elliptical yield surface:

$$\sigma_y = \sqrt{\sigma_{11}^2 - \sigma_{11}\sigma_{22} + \sigma_{22}^2} \qquad (3)$$

In the absence of constraint through the thickness, the maximum constraint is that associated with a plate of infinite width in the direction transverse to the axial loading. In this case, when a butt weld which is transverse to the axial loading begins to yield, there can be no strain in the transverse direction. A stress will develop in the direction transverse to the axial loading (σ_{22}) which is proportional to the axial stress (σ_{11}) by Poisson's ratio, ν which is equal to 0.3:

$$\sigma_{22} = \nu\sigma_{11} \tag{4}$$

In this case:

$$\sigma_y = \sigma_{11}\sqrt{1-\nu+\nu^2} = 0.889\sigma_{11} \tag{5}$$

Therefore, when the weld metal begins to yield:

$$\sigma_{11} = 1.125\sigma_y \tag{6}$$

In other words, because of the transverse tensile stress due to the Poisson effect, the weld metal will not yield until the axial stress approaches 112.5 percent of the uniaxial yield strength. Neglecting strain hardening, the weld will not yield if it is undermatched less than 12.5 percent. Therefore, with negligible strain hardening in the weld metal, the maximum tolerable undermatch in relatively thin plates is about 12.5 percent. The results of this simple analysis are consistent with the results of the wide-plate tests described in Chapter 3, i.e. that welds can be undermatched up to 12 percent in terms of the actual yield strength.and still retain full strength and ductility.

In the event that sufficient constraint can be developed, yielding will eventually spread outside the soft weld, that is, gross-section yielding (GSY) of the weldment will be reached. When GSY is achieved, the full base-plate strength is achieved, even with the undermatched weld. Note that this constraint effect will occur for perfectly plastic yielding, i.e., without strain hardening. Strain hardening is another independent phenomenon that will also raise the load carrying capacity and enhance the spread of plasticity.

The effect of constraint is apparent in the work of Satoh and Toyoda. For example, as the w/t of the weldment is increased, the width constraint increases and the weldment performance reaches that of the base plate. For the relatively thick plates studied by Satoh and Toyoda, there was also significant constraint through the thickness. They described the through-thickness constraint in terms of the relative thickness. As the weld gap is increased, the weld loses the benefit of thickness constraint. Only very narrow gap welds benefit from thickness constraint, i.e. for most common weld geometries the thickness constraint is minimal.

The gas transmission pipeline industry has been a leader in the use of steels above 500 MPa yield strength. This industry has sponsored significant research on undermatched welds, particularly girth welds which are made from one-side in the field. Both field welding and one-sided welding are factors which significantly increase the risk of hydrogen cracking. In order to get good penetration, cellulosic electrodes (e.g. E7010) are preferred. These electrodes liberate large amounts of hydrogen relative to other electrodes. Fortunately, pipeline girth welds are also highly constrained. A pipeline must have hoop strain compatibility at the weld interface, which provides even higher constraint than a wide plate. Glover [13] showed that using an undermatched root pass and nominally matched fill passes, the preheat necessary to prevent hydrogen cracking of the root pass can be reduced. Transverse weld tension tests (flat-strap specimens) showed that the yield point of the plate with an undermatched weld was higher than the minimum specified yield strength of the base plate.

Dexter and Lundin [7] showed in full-scale pipe tests, welds up to 16 percent undermatched perform as well as overmatched welds, i.e. the pipes developed the full strength of the base metal and can withstand more than 5 percent nominal elongation without failure. Oshawa et al [25] conducted burst tests of full-scale pipe with 15 percent undermatched welds and found the burst pressure was in good agreement with the calculated value which assumed an homogenous pipe with base metal properties. This is higher than the 12.5 percent limit for wide plates because pipes develop axisymmetric constraint which is even higher than the constraint provided by an infinitely wide plate.

2.3.2 Fracture Performance

The research discussed in Section 2.3.1 validates the use of slightly undermatched welds, within certain limits. The performance of undermatched welds which have significant defects has not been considered. The requirement for overmatching is generally intended to protect such defects from large strain concentration.

A significant amount of work has been done to characterize the fracture behavior of weldments, including the effects of heterogeneity of micro-structure and material properties. Denys [6] has examined the effect of weld undermatching on the nominal axial elongation of wide-plate tension tests with transverse butt-welds with flaws. The fracture strain is reduced for undermatched welds relative to overmatched welds for flaws

which are less than 10 percent of the gross-section tensile area. When flaws exceed 10 percent of the gross tensile area, there was no consistent difference between the fracture strains for undermatched and overmatched welds. The fracture occurred at low strains, i.e., 1 to 3 times the yield strain, regardless of the weld metal strength.

Analogous results were obtained numerically by Prinaris [27]. Using two-dimensional, finite-element models of through-crack center-cracked panels, Prinaris found that large cracks produced net-section yielding in all cases, but the behavior of small-cracked specimens was dependent on the degree of undermatch. As the undermatching increases, small flaws become more critical.

A large amount of research into the fracture behavior of undermatched welds has been performed at GKSS Research Center. Petrovski et al. [26] in a study of small surface cracks in center-cracked tensile panels found that cracks in the weld metal significantly reduced the stain capacity of the welded joint, but this was not the case for cracks in the HAZ and base plate. However, the level of undermatch was so severe (30%) that spread of plasticity from the weld was not possible.

Kocak et al. [19] found that the fracture behavior of highly under- and overmatched transverse weld metals with large through-thickness cracks was generally identical to the parent plate. However, the undermatched weld experienced loss of both strength and ductility for a smaller crack. Schwalbe [35], describes the Engineering Treatment Model (ETM), which is an analytical method to assess flaws in welded joints which accounts for strength mismatch effects. He found that the performance of center-cracked weldments was dependent not only on the degree of undermatch, but the amount of strain hardening of both the base plate and the weld metal. As the work hardening of the weld metal increases, the applied crack-driving force decreases, reducing the detrimental effect of undermatching. Additionally, using the ETM methodology, the required amount of weld metal toughness can be estimated. Schwalbe found that the applied crack-driving force for a 20% undermatched welded joint is nearly 2.5 times the applied crack-driving force for an equivalent crack in the parent plate. This finding indicates the weld metal toughness should be 2.5 times greater than the parent plate toughness to ensure a uniform resistance to fracture in the undermatched weld.

The fracture research on undermatched welds indicates that there is a significant effect of undermatching on wide-plate tests with small transverse through-thickness or surface cracks along the centerline of the weld. These findings have been widely publicized leading to general reluctance to accept undermatched welds. However, this specimen geometry is unrealistic. Most welding cracks occur along the fusion line or in the HAZ. Fatigue cracks occur at the weld toe and typically propagate in the HAZ. Most research has shown that undermatching has relatively little effect on such cracks; compared to cracks at the weld centerline which rarely occur. At a recent conference focusing on the behavior of mis-matched welds [34], most of the papers dealt with analysis and testing of specimens with notches or cracks particularly located along the weld centerline. There

were relatively few papers on the strength and ductility of members without cracks or with typical welding discontinuities. The conference concluded with discussion of the current state of knowledge regarding undermatched welds. Undermatching was considered to have an "effect" if the total elongation of the wide-plate test was significantly reduced for undermatched welds compared to overmatched welds. The consensus was that undermatching had a significant effect for small cracks in the middle of the weld. There was typically no undermatching effect for the following conditions:

a. cracks on the fusion line,

b. surface cracks at the root of single-vee groove welds,

c. large cracks, i.e., through cracks greater than 25 percent of the width or surface cracks greater than 15 percent of the area,

d. cracks in welds subjected to a strain gradient, such as, near a stress concentration or for members in bending, and

e. cleavage fracture which occurs below the weld yield strength.

Though undermatching may have an effect, cracks in the middle of the weld are rarely encountered in actual structures. Therefore the case most extensively studied, i.e. cracks along the weld centerline have little applicability to in-service problems, and is primarily of academic interest. The behavior in cases where little undermatching effect is seen can be rationalized as follows. For the first two cases (a and b), these problems occur close to the base metal, therefore the constraint at the interface shields the defect from large strains. These cases are particularly interesting because most welding defects (for example, hydrogen cracking and lack-of-penetration) occur in these locations. Therefore, for typical welding defects, undermatching should not be detrimental.

For the last three cases, undermatching makes little difference because premature failure occurs in any case, regardless of the weld metal strength. For example, both large cracks and strain gradients will cause strain localizations, making the strain localization due to the undermatched weld inconsequential. Most fatigue cracks occur at stress concentrations where there is large strain gradient. Also, in modern high-toughness steel, fatigue cracks typically are quite long before they are detected. Therefore, for practical cases of fatigue cracks, the effect of the undermatch should be insignificant as well.

The previous research has focused primarily on the fracture behavior of cracked undermatched weldments. Therefore the research described in this report was focused on the strength and ductility of full-scale members with undermatched joints with typical welding defects, relative to similar overmatched joints.

2.3.3 Fatigue Resistance

Undermatched welds should have little influence on the low-stress-range, high-cycle fatigue life of a welded structural member. The stresses in a high-cycle fatigue-controlled design are small relative to the yield strength of the undermatched weld or the base plate. It is possible that the presence of defects in the weld may induce locally high strain concentrations which could be increased by the presence of an undermatched weld. However, the lower residual stresses and fewer discontinuities (due to the decreased tendency for hydrogen cracking) may offset this concern.

No research has looked specifically at the fatigue performance of undermatched welded joints in full-scale members. Fisher et al [9] performed a number of tests on welded beams of A514 steel, which were undermatched to maintain constant weld properties over a series of tests examining the fatigue performance of different steel grades. No effect of undermatch was seen as the A514 beams had fatigue life comparable to other overmatched beams.

High-cycle fatigue is the type of loading characteristic of surface ships, but submarines may be loaded in a low-cycle, high-stress-range regime. It is presently believed that even for low-cycle fatigue, the strains in the weld will shakedown to the elastic range after a few cycles and therefore undermatching should not have a detrimental effect.

2.3.4 Compression Stability

In thin ship plate, bucking will initiate in the elastic range and therefore should not be adversely affected by undermatched welds. Plastic strain will occur after initial buckling, and undermatched welds may influence the post-buckling response. It is possible that the reduction in residual stresses may improve compression behavior of undermatched welded members compared to overmatched specimens, however, this has not been demonstrated experimentally.

At this time, there has been no published research on the effect of undermatched welds on member stability. Ongoing research at the Naval Surface Warfare Center [37] on hydrostatic collapse testing of specimens with undermatched welds has shown no significant effect of undermatching up to 18 percent undermatch. Further research, including initial imperfections and defects, is continuing.

2.4 Potential Applications of Undermatched Welds in Surface Ships

As discussed, the undermatching requirement presents no problems for most steel grades. It is therefore necessary to determine which steels, joints, and loading conditions would achieve the greatest benefits from undermatching, and incorporate these findings into the research plan. As part of this project, Bath Iron Works (BIW) conducted a survey of numerous ship types, military and civilian, to determine which ship details could be potentially undermatched. BIW was tasked with determining:

1. high yield stress steel grades present in modern ships;
2. joint types and loadings found; and
3. criticality of each joint type.

The steels, joint types, and loading were used to establish typical materials and geometries. The criticality factor was important because those welds which control the ship's survivability must be assured of obtaining full base plate strength and ductility. It was reasoned that if critical ship joints could be successfully undermatched, less critical joints would also meet requirements if undermatched. Therefore, the testing program should emphasize critical joints and loading conditions for steels which derive the greatest benefits from undermatching.

2.4.1 Plate Material

BIW found the following high-strength steel grades in their survey:

1. ASTM A514F;
2. HY-80 and HY-100 (MIL-S-16216); and
3. HSLA-80 and HSLA-100 (MIL-S-24645).

Undermatching is only an issue for the 690 MPa MSYS steel, and at this time, HY-100 and HSLA-100 have the biggest cost impact on shipbuilding in North America.

HSLA-100 was selected for the experimental program. The HSLA steels are more modern low-alloy steels which have excellent weldability and toughness as well as high strength. The other high-strength steels noted above are much less weldable. Therefore, the HSLA steels are likely to replace the other grades in future applications.

2.4.2 Welding Filler Metal

The standard overmatching weld metal for HSLA-100 is a Mil-120 type electrode (830 MPa ultimate, which is nominally a 10 percent overmatch relative to MSYS). Consumables of this strength are required when joining steels with 690 MPa yield strength by Naval specification [23]. Two undermatching welding wires were also considered. The primary undermatching wire is Mil-100S-1 (690 MPa ultimate strength). The minimum yield strength allowed for this weld metal is 565 MPa, which is nominally a 18 percent undermatch relative to MSYS of the base metal but could be undermatched as much as 37 percent if the base metal was near the maximum allowable yield strength of 900 MPa. By controlling the maximum heat input and the associated minimum cooling rate, 100S-1 welds which are undermatched only about 10 percent relative to MSYS of the base metal can be easily produced. A joint which is nominally undermatched by 10 percent is anticipated to perform well, but the HSLA100/100S-1 system is not generally accepted. Since the 100S-1 weld metal provides good weldability, it is not necessary to undermatch more significantly in practice. However, a second welding wire was used in the experiments in order to investigate highly undermatched joints, i.e. Mil-70S-3 (480 MPa ultimate). The 70S-3 weld metal is nominally 35 percent undermatched with respect to MSYS of the HSLA-100.

2.4.3 Joint Geometry and Loading

BIW found that all AWS [3] prequalified joints were found in ships. The four most frequent types were:

1. butt joints, full penetration;
2. tee joints, partial penetration (fillet and groove);
3. tee joints, full penetration (groove); and
4. corner joints.

The loading conditions for these joints were also determined. Tee joints and corner joints loaded in a direction parallel to the weld axis should present no problems for undermatching. For example, consider the T-joints with loadings shown in Figure 2-4. For T-joints loaded in tension (Figure 2-4a), there is strain compatibility at the weld/base-plate interface. Therefore, even though the undermatched weld yields first, the section will still achieve base plate strength because strain will not localize in the soft weld. For T-joints in shear (Figure 2-4b,c), the size of fillet welds can be increased if additional strength is required. Similarly, groove welds can be reinforced with fillets.

However, in tee joints and corner joints where the primary loading is bending (Figure 2-4d), the effect of the soft weld may be to increase the strain concentration in the weld due to the loading, resulting in high plastic strains and premature failure. Therefore, in cases where the prying load is significant, the joint should not be significantly undermatched unless the design is changed to reduce the prying. In practice, this type of tee joint with significant bending is always designed with brackets to reduce the load on the weld. In this case, the joint can be safely undermatched.

Butt joints and loadings are shown in Figure 2-5. BIW determined that all welds in the hull envelope are critical to water tight integrity of the ship. Typically, these water tight joints are butt joints. The exception is joining of the side shell to the deck and keel, which are corner or Tee joints. Therefore, primary consideration should be given to butt joints.

The loading conditions also reflect the joint criticality. The most critical joints are butt joints in tension in the upper deck and keel at midships. Butt joints in the side shell at the ends of the ship and butt joints in the shear strake and bilge strake are subjected to large shear forces. Thus the performance of undermatched butt joints in shear is also a concern.

Thickness (mm)	Welding Process	Number of Specimens	Avg YS (MPa)	Avg TS (MPa)
	SMAW	10	613	756
9	GMAW	6	702	819
	P-GMAW	6	630	825
	SMAW	8	633	763
13	GMAW	6	657	798
	P-GMAW	6	596	814
	SMAW	3	653	752
16	GMAW	5	704	817
	P-GMAW	4	659	821
ALL SPECIMENS		54	645	793

Table 2-1 Results of All-Weld-Metal Tensile Tests for Welding of Thin Plates with Mil-120S-1 Electrodes Showing the Potential for Unintentional Undermatch in Thin Sections Due to Slow Cooling Rates (after [5]).

Reference	Material	Welding Process	Decrease in Hardness (%)	Width of Soft Zone (mm)
Sbarskaya, et al.	Plate	SMAW	13~21	2.0~4.6
[33]		SAW	17~25	4.6~8.1
Smirnov &Borisov	690 MPa Yield Pipe	GMAW	15	2.8
[36]		SMAW	21	6.4
Ikeda, et al.[18]	X52 Pipe	SMAW	20	-
Aronson[4]	6 mm Plate	GMAW	10	-
Hasimoto, et al.[16]	X80 and X100 Pipe	-	0~13*	1.0~8.1
Lundin[7]	HSLA-80	SMAW	4~17	1.0~5.1
	DQ-80	SMAW	13~17	2.0~6.4
	DQ-125	SMAW	0~17	0.0~3.6
	AC-50	SMAW	0~13	0.0~3.8
Youn and Kim[38]	AC-60	SMAW & SAW	0~13	0.0~7.9

* Indicates Hardness Estimated from Cross-Weld Tension Test.

Table 2-2 Research Demonstrating that Welding High-Strength Steels Produced with Advanced Processing Techniques Can Create Substantial Soft Zones Within the Heat-Affected-Zone (HAZ).

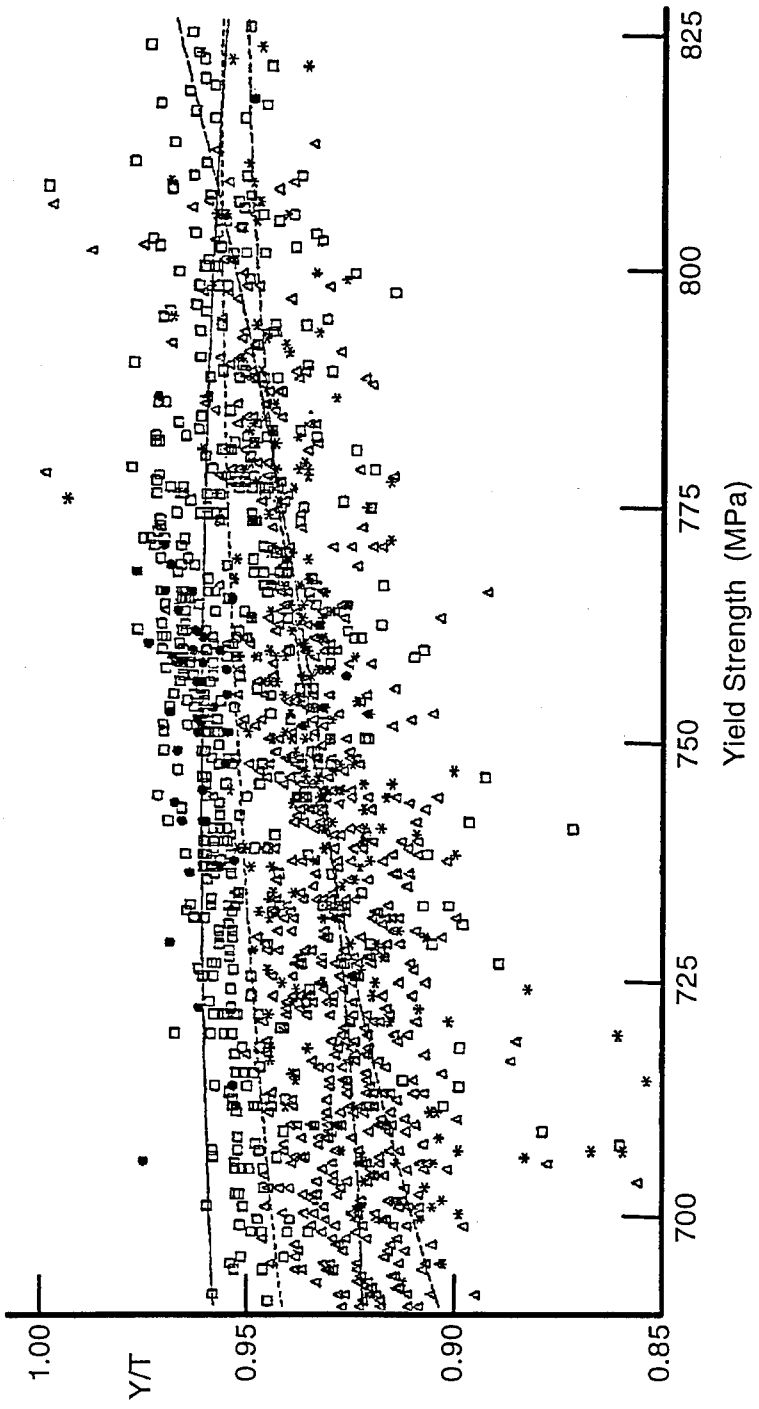

Figure 2-1 Database of Mill-test Tensile Data for HSLA-100. (Provided by NSWC, meaning of the lines is not known.)

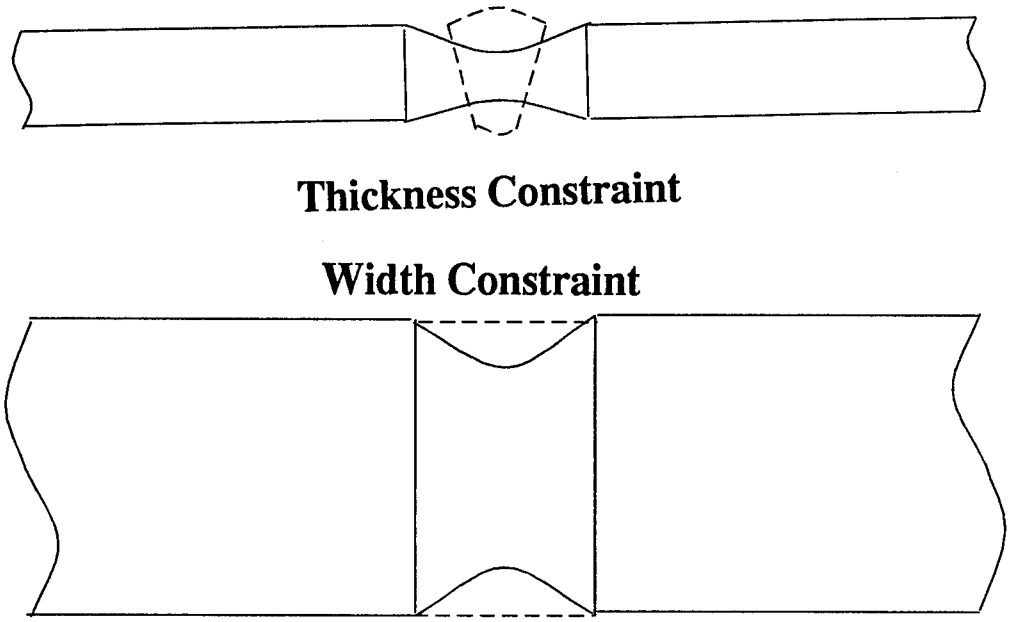

Figure 2-2 Weld Deformations that Lead to the Development of Constraint.

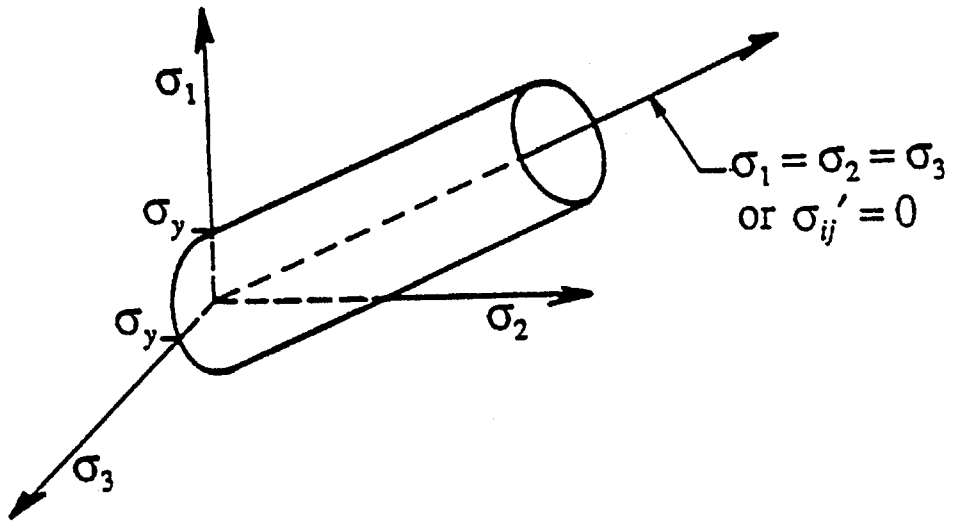

Figure 2-3 Von-Mises Yield Surface.

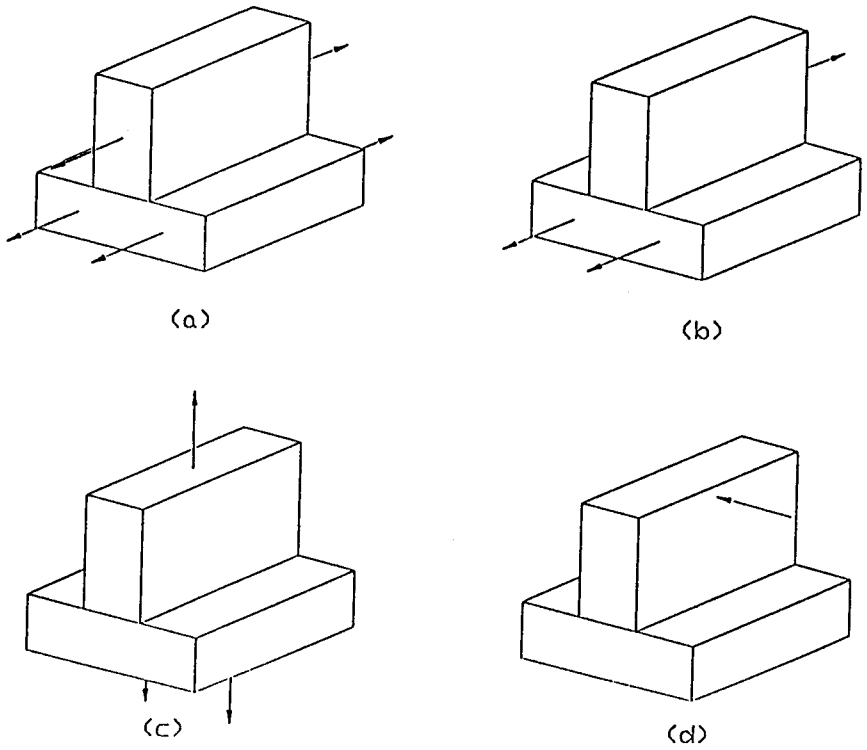

Figure 2-4 Tee Joints and Loadings

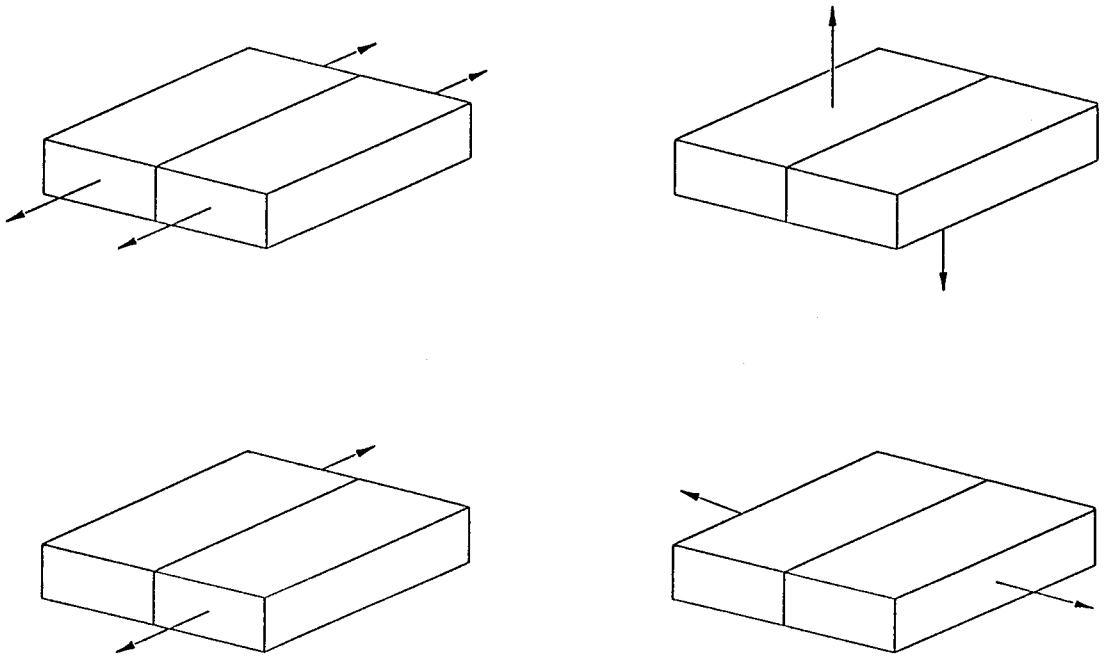

Figure 2-5 Butt Joints and Loadings

3.0 EXPERIMENTAL PROGRAM

As discussed in Section 2.3, a significant portion of the previous research on undermatched welds has involved specimen geometries and defect conditions rarely encountered in actual structures. In many cases, the research examined severe levels of undermatch not expected to perform well in real structural elements. The focus of this research was primarily to qualify undermatched welds for use in Naval surface ships. This was done by examining the performance of welds with moderate, practical degrees of undermatch for the typical critical geometries and loadings found in Naval surface combatants as discussed in Section 2.4.

3.1 Material Characterization Tests

3.1.1 Material Chemistry

For the reasons explained in Section 2.4.1, HSLA-100 was chosen as the base plate for these experiments (the HSLA-100 specification is in Mil-S-24645A). The HSLA-100 is a copper precipitation-hardening steel. The mill report chemical analysis is shown in Table 3-1. The better strength of HSLA-100 is created by modest increases in certain alloys (Mn, Ni, and Mo) over the specified limits for HSLA-80. This chemistry is typical for HSLA-100 plates less than or equal to 25 mm thick. Also, shown in the table are the IIW carbon-equivalent (C_{eq}) and the P_{cm} composition parameter. After a first group of experiments, two series of additional tests were done on a different heat of 13 mm thick HSLA-100, which is shown in Table 3-1 as "new plate".

The filler metal chemistry is shown in Table 3-2. Carbon-equivalencies are also calculated for the filler material. Though C_{eq} is not typically applied to welding electrodes, the C_{eq} serves to demonstrate the significantly greater (~16 percent) alloy content of the 120S-1 weld metal compared the 100S-1 weld metal. As expected, the 70S-3 has much less alloy than either the 120S-1 or the 100S-1.

3.1.2 Charpy Toughness

Charpy toughness was determined for the base material and the weld metals used in the first group of experiments. Figure 3-1 compares the toughness of the HSLA-100 at the three specimen thicknesses. At all thicknesses, the toughness is substantially greater than required.

Weld metal toughness is shown in Figure 3-2. The comparison of the 120S-1 and the 100S-1 welds show that the 100S-1 has 30 percent greater upper-shelf toughness. This degradation in toughness of the 120S-1 relative to the 100S-1 weld, which is an indicator of a degradation in weldability, shows quantitatively an advantage of undermatching. Though the 100S-1 weld metal has greater toughness than the 120S-1 weld metal, the toughness is still less than the HSLA base plate. The 70S-3 weld is expected to have even better toughness but was not tested.

3.1.3 Tensile Properties

Tensile properties of the HSLA-100 base plate were determined from 38 mm wide flat specimens and properties of the weld were determined with 6 mm diameter round all-weld-metal (AWM) specimens. Yield strength is calculated at 0.2 percent strain offset. AWM specimens were obtained for the 100S-1 weld at all three thicknesses, and at the 13 mm thickness for the different weld metals.

As shown in Table 3-3, the base plate yield strength for the original 13 mm thick plates ranges from 750 to 813 MPa with an average of 779 MPa. The 9 mm base plate had a yield strength of 747 MPa. The yield strength of the 25 mm base plate was only slightly above allowable at 710 MPa. The trend of lower strength for greater thicknesses is expected since the steel gets much of it strength from controlled rolling.

The pulsed gas-metal-arc welding process (GMAW-P) was used for most of these weldments. The rationale for using the pulsing was that welds in the flat position would usually be made with the submerged-arc welding (SAW) process. Therefore, the GMAW process is used primarily for welding out of position, where the pulsing gives better performance. The plates were welded in the flat position for convenience, however.

As shown in Table 3-9, the heat inputs for the original series of welds were not high. The heat inputs ranged from 0.55 to 1.2 kJ/mm for the fill passes and up to 1.7 kJ/mm for the root pass, well below the allowable heat input at these thicknesses of 1.8 kJ/mm. With the low heat input and no preheat, the cooling rate for the weld was high. According to heat-input vs. strength correlations [24], the 100S-1 weld metal in the first series of tests was expected to have a yield strength of about 690 MPa.

The resulting yield strength of the weld metal ranged from 670 to 750 MPa with an average weld metal strength of 717 MPa. Thus the first series of 13 mm thick plates were undermatched from 9 to 12 percent in terms of the actual yield strength. The second and third series of tests sought to investigate the larger possible undermatch that could occur if the weld is made at much higher heat input. The yield strength for the 100S-1 weld wire is allowed to be as low as 565 MPa, which is 18 percent undermatched with respect to the MSYS of the HSLA-100.

Different HSLA-100 base plates were acquired for the second and third series of tests. Table 3-3 also shows the range of yield strength and tensile strength for the new 13 mm thick plate and the high-heat-input weld metal from the second and third series of tests. The new base plate exhibits significant variation in yield strength (from 712 to 784 MPa). The mean yield strength of the new plate is 740 MPa, whereas the mean yield strength of the 13 mm thick plates from the first series of tests was 780 MPa. The yield strength of this new plate is closer to the 745 MPa yield strength which was the average from the overall database (shown in Figure 2-1). The average ultimate tensile strength of the new base plate was 760 MPa, and the average yield-to-tensile ratio (Y/T) was 0.97.

The target range of weld metal yield strength for the second series of tests was 565 to 600 MPa. Based upon recommendations of Charles Null (NAVSEA), the new plates were welded using 175 degrees C preheat and interpass temperature and a heat input of 2.2 kJ/mm. The maximum permissible heat input for the 13 mm thick plate is 1.8 kJ/mm, however 2.2 kJ/mm can be used on 25 mm thick plates. Exceptions are granted and in certain applications even higher heat-inputs are allowed. Also, the preheat and interpass temperatures are slightly greater than the maximum allowed, which is 150 degrees C. As shown in Table 3-3, the resulting weld metal yield strength ranged from 570 to 610 MPa, almost all within the target range. The average weld metal yield strength was 580 MPa, which is about 22 percent undermatched with respect to the average actual base-plate yield strength. The average weld metal tensile strength was 695 MPa, giving an average Y/T of 0.83.

The third series of tests were welded using the maximum allowable preheat and interpass temperature (150 degrees C) and the maximum allowable heat input (1.8 kJ/mm). Also, the pulsing was not used in welding this third series of test specimens. According to Charles Null, this weld procedure in a 13 mm thick plate should result in a cooling rate of 5 degrees C per second and a yield strength of 610 MPa. This is about 18 percent undermatching in terms of the average actual base plate yield strength (740 MPa). As shown in Table 3-3, the resulting yield strength in the third series of tests ranged from 589 to 611 MPA with an average of 603 MPa, slightly less than anticipated.

3.1.4 Weldment Hardness

Hardness traverses were conducted on weld cross-sections (from the original series of tests only) for the three weld metals and the three thickness of the 100S-1 weldment. There is very little variation through the thickness in the 100S-1 welds, and the weld metal hardness is comparable to the base plate. The amount of softening in the heat-affected zone is from eight to 15 percent with width of 3 mm to 5 mm. These results are consistent with previous research (see Table 2-2) on softening of HSLA steels. Figure 3-3 compares the three weld metals. The 120S-1 and 70S-3 show similar softening. Any difference is probably random variation.

3.2 Fatigue Experiments

3.2.1 Test Matrices and Fabrication

The base plate material for the fatigue tests was HSLA-80 (similar to ASTM A710, Grade A, Class 3). HSLA-80 was chosen because some I-beams were available at no cost and the results could be compared to previous fatigue tests with overmatched welds. The minimum specified yield strength of the steel is 550 MPa and the actual strength was approximately 580 MPa. The weld was produced with a 70S-3 electrode, with a yield strength of 460 MPa. The undermatch for the fatigue tests was approximately 21 percent.

The fatigue specimen design and test set-up is shown in Figure 3-4. The three specimens were fabricated at Lehigh University and various defects were intentionally introduced. One specimen had an incomplete penetration of the web. A second had incomplete penetration of the web, as well as, porosity in the tension flange. The third specimen had no detectable defects in the flange groove weld. The welding was performed in accordance with Mil-Std-1689, with the exception of the intentional defects. Though undermatching of HSLA-80 is of little practical interest, this approach was used for comparison to a large fatigue database [11] for comparable overmatched welds in the same steel.

3.2.2 Test Setup and Procedure

The fatigue specimens were tested at the ATLSS Engineering Laboratory. The minimum stress was 14 MPa and the applied stress range was 165 MPa. These stresses were verified before testing began using a single strain gage. The specimens were then loaded with sinusoidal waveforms at 4 Hertz. The specimens were tested to failure; defined by a 2.5 mm increase in the displacement, which was used to stop the test. This displacement typically corresponded to when the crack had extended through most of the width of the flange.

3.2.3 Results of the Fatigue Experiments

The results of the fatigue tests are compared to results of similar tests with overmatched butt welds generated in previous research [11] in Figure 3-5. The specimen that was welded without intentional defects failed prematurely outside the groove welds. The fatigue crack initiated from a lack-of-fusion defect in the longitudinal fillet weld during previous testing, and was enlarged by the undermatched test. Therefore, only the two tests that yielded useful data are shown.

The Category E fatigue design curve is a lower bound for all these previous data. The two undermatched welds fall at the lower end of life. Beam 1 had lack-of-fusion along the entire depth of the web, 2 mm wide. Beam 2 had similar lack-of-fusion as well as significant porosity in the tension flange. These defects are considerably larger than those found in the overmatched beams accounting for the shorter fatigue life. The purpose of this limited number of fatigue tests was only to identify any potential problems. Unfortunately, the results were inconclusive. A significant number of tests, at least nine, would be required to further resolve this issue.

3.3 Shear Experiments

3.3.1 Test Matrices and Fabrication

The design of the shear specimens is shown in Figure 3-6. The shear test matrix is shown in Table 3-4. The shear tests primarily examined the comparative performance of the three weld metals, with duplicate 100S-1 specimens. The additional specimens were to examine possible loss of weld constraint due weld width or adjacent base-plate stiffness.

All shear specimens were fabricated at Bath Iron Works (a major shipyard) according to the welding procedure shown in Tables 3-5 and 3-6. These welding parameters were chosen at the discretion of the shipyard.All fabrication, welding, and inspection was performed in accordance with MIL-STD-1689.

3.3.2 Test Setup and Procedure

The specimens were measured to find local variations in width or thickness. A one dimensional grid of parallel lines was drawn on one of the welds of the shear specimens for qualitative analysis of the weld deformation. The specimens were instrumented with five rosette-type strain gages, placed along the weld and on both sides of the weld. A single displacement transducer measured displacement of one side of the weld relative to the other. This transducer was placed across the weld, and its exact position was specimen specific. The load and machine cross-head displacement were also recorded.

The specimens were gripped by pneumatic wedge grips in the 2.7 MN universal testing machine at the ATLSS Engineering Laboratory. A fully instrumented, test ready specimen, along with a failed specimen, is shown in Figure 3-7. The specimens were then loaded to one-fourth their nominal yield load to ensure the instrumentation and data acquisition systems were functioning properly. The specimens were then unloaded, and the testing began. The specimens were loaded to failure at a strain rate of $1x10^{-5}$ sec^{-1} to simulate quasi-static conditions.

3.3.3 Results of the Shear Experiments

3.3.3.1 Shear in Butt Joints

Figure 3-8 shows the normalized load-displacement curves for the butt-weld shear specimens. The load is normalized by the load computed with the nominal area and the minimum specified yield strength of the base material in shear. The yield strength in shear is 57.7 percent of the nominal yield strength in tension in accord with the Von-Mises yield criterion. The minimum specified yield strength in tension is 690 MPa. All of the specimens exceeded this minimum strength. The specimen with the 70S-3 weld had an LVDT malfunction during the test so the load-displacement data can not be plotted. The normalized ultimate strength for the 70S-3 weld was 1.2 which is 18 percent greater than what would be expected based on the measured yield strength of the weld metal in tension.

Table 3-7 compares the ultimate strength of the welded joint with ultimate strength of the weld metal in tension (τ_u/σ_u). Fisher et al. [10] found that the mean value of τ_u/σ_u is about 0.84 for fillet welds in shear. The values for these butt-weld tests are substantially below that value. The reason for this is the shear lag present in the short weld.

As shown in Figure 3-9, in addition to the applied shear stress, there are bending stresses in the weld due to the joint eccentricity. This bending was observed experimentally. The strain gage data in Figure 3-9 are axial strains perpendicular to the axis of the weld for the widegap 100S-1 weld specimen. These data indicate zones of tension and compression created by the bending. These compression zones reduce the capacity of the joint by allowing the weld to deform in pure shear. The effect of pure shear, as opposed to simple shear, is that at large deformations, tension can not develop normal to the direction of the applied shear because contraction across the width of the weld is not prevented. Therefore, in pure shear, constraint can not develop and the joint strength is reduced.

This effect is most clearly seen in the widegap 100S-1 weld specimen. Because of the larger eccentricity of this specimen, the bending stresses are increased. This leads to a further reduction in strength as shown by the τ_u/σ_u value which is lower than the standard 100S-1 weld specimens. This effect can be reduced by increasing the joint length which would reduce the magnitude of the bending stresses.

3.3.3.2 Shear in Fillet Welds

In addition to the butt-joint specimens, standard AWS [1] fillet weld qualification test specimens were fabricated and tested. The purpose of these tests was to see if the same strength would be obtained as from the butt-joint tests. The geometry of the specimens is shown with the test matrix in Figure 3-10. As shown, the 120S-1, 100S-1, and 70S-3 weld metals were used, with replicate 100S-1 specimens, including one with a different heat input.

The load-displacement curves from the specimens fabricated with the three weld metals are compared in Figure 3-11. Several 100S-1 specimens were tested and the result in the Figure is typical. Both the 100S-1 and the 120S-1 exceeded the base plate strength, with a negligible decrease in ductility in the 100S-1 specimen. The 70S-3 has ductility comparable to the 100S-1 welds, but achieves about only 75 percent of the required strength. The low strength of severely undermatched fillet welds is not significant because, as discussed in Section 2.4.3, if additional strength is required for fillet joints (as is clearly the case for the 70S-3 weld), the weld size or length can be increased.

The ultimate strengths from fillet weld and groove weld specimens are compared in Table 3-7. The fillet-weld shear test results are not consistent with the behavior of butt-joints in shear. For example, the 70S-3 butt-joint achieved full strength, the fillet weld did not. The inherent differences between the two joint types (constraint, cooling rate, etc.) apparently significantly affect the apparent shear strength of the weld metal.

3.4 Tension Experiments

3.4.1 Test Matrices and Fabrication

Since it appears that transverse butt welds are the primary concern for undermatched welds, the wide-plate tension tests are the primary focus of this research. The purpose of these tests is primarily to qualify the use of undermatched weld metal for butt joints in tension. The design of the tensile specimens is shown in Figure 3-12. These specimens were fabricated as oversize blanks. The cut-away portions provided additional length of weld from which flat strap tensile specimens, all-weld-metal tensile specimens, and weld macros were obtained. The test matrix for the tensile specimens is shown in Table 3-8.

The matrix is composed of two subsets:

1. those specimens which are free of defects; and
2. those which include intentional defects or variations as described in the Table.

The defect free weldments are designed to examine:

1. comparative performance of the 120S-1, 100S-1, and 70S-3 welds with identical configurations, and a reinforced 70S-3 weld;
2. comparative performance of the 100S-1 weld at three thicknesses;
3. comparative performance of the 100S-1 weld with different heat-input;
4. variance in performance of replicate 100S-1 welds;
5. performance of the 100S-1 and 70S-3 welds in joining an HSLA-80 plate to the HSLA-100 plate.

A number of exploratory tests including defects or variations were performed. These tests examined the comparative behavior of under- and overmatched welds. The defects or variations were intentionally introduced and controlled to produce similar conditions in both under- and overmatched specimens. The variants included: lack-of-fusion, undercut, plate misalignment, and joint buttering. As discussed in Section 2.3., previous laboratory tests on undermatched weld have included only ideal notches at the weld centerline, which are not considered relevant to actual weld defects.

All tensile specimens were fabricated according to the welding procedure shown in Table 3-5 and 3-9. All fabrication, welding, and inspection was similar to the shear specimens, with the exception of introduced defects.

3.4.2 Test Setup and Procedure

Data on width and thickness variation and out-of-flatness caused by welding distortion were collected. Additionally, some specimens had punch marks across the weld crown which were measured before the test and at selected displacements. The apparent strain between the punchmarks was used to verify strain readings.

The specimens were extensively instrumented. A total of sixteen high-elongation strain gages (functional to 20 percent strain) were place on both the weld crown and weld root sides of the specimen as indicated in Figure 3-13. Three global (over the 1520 mm gage length) displacement transducers were located on the edges and root side of the specimen to give nominal elongation of the specimen. A local cross-weld displacement transducer (50 mm gage length) was placed on the crown side of the specimen. These are also shown in the figure.

The specimens were bolted to fixtures mounted in clevises in the 22 MN universal testing machine in Fritz Engineering Laboratory. An instrumented specimen, ready for testing, and a fractured specimen are shown in Figure 3-14. The specimens were loaded to one-fourth their nominal yield load (1.33 MN for the 13 mm thick specimens) to ensure the instrumentation and data acquisition systems were functioning properly. The specimens were then unloaded, and the testing began. The specimens were loaded to failure at a strain rate of 1×10^{-5} sec^{-1}. The tests were paused twice just after the initial yielding to determine the static yield point.

3.4.3 Results of the Tension Experiments

3.4.3.1 Global Behavior

The results of the wide-plate tests are summarized in Table 3-10. Table 3-11 compares the results of the wide-plate specimens with 38 mm wide flat-strap cross-weld tension specimens and the results of base and weld metal standard tension tests. This table summarizes only those specimens with different weld metals and thicknesses; replicate specimens are omitted, as well as those with defects.

Specimens 3, 4 and 5 are all 100S-1 welds, 13 mm thick, with comparable heat inputs. Specimen 3 is considered representative and was used in Table 3-11. Figure 3-15 shows the load-elongation curves for the three replicate 13 mm specimens with the 100S-1 weld metal. The load has been normalized by the product of the minimum specified yield strength (690 MPa) and the actual original cross-sectional area. The nominal elongation is the average of the three full gage length LVDTs mounted on the back and edges of the specimen normalized by the 1500 mm gage length. Only one of these specimens fractured in the weld or on the fusion line. The total variation of strength is about 5 percent, though all specimens achieved the required nominal base plate minimum specified yield strength (MSYS). The elongation at fracture ranges from 6.7 to 8.0 percent over the 1500 mm gage length, i.e. the natural variation in elongation among replicate specimens is about 18 percent. Overall elongation greater than six percent is excellent ductility for a plate with a transverse groove weld. As discussed in the introduction, welds are rarely expected to tolerate more than one or two percent strain.

The effect of thickness is shown in Figure 3-16. The 9 mm thickness, which fractured in the base plate, performed identically to the 13 mm thick plates. The 25 mm plate demonstrated lower strength and greater ductility. The reduced strength was due to the lower strength of the 25 mm thick base plate. This specimen fractured in the base plate. The effect of thickness was confounded by the effect of base plate strength and level of undermatch. At modest levels of undermatch, it seems the overall strength and ductility is controlled by the base plate properties. It is possible that the greater elongation of the 25 mm specimens is associated with the greater Charpy toughness for this base plate thickness (see Figure 3-1).

The 100S-1 weld metal was also tested with the widest allowable root opening (5 mm) and 10 or 13 mm side-wall buttering on each joint edge (the maximum permissible buttering is 13 mm). The total gap at the weld root varied from 25 to 31 mm. Both wide-gap specimens fractured in the base plate. There was no significant difference in strength or ductility attributable to the widegap. Unfortunately, as indicated in Table 3-11, the widegap weld metal had unusually high yield strength. It is possible there was less dilution of the weld metal in the widegap joints because of the built-up buttering layers. The C and Mn of the weld metal is greater than the base metal, therefore dilution could lower the weld metal strength in this case.

The load elongation curves for the three weld metals are shown in Figure 3-17. The figure shows that the behavior of the 100S-1 weld and the 120S-1 weld specimens are within the same scatter band. The strength was identical and the elongation was only slightly greater (about 8.7 percent) which is not significant considering the overall variability. The 70S-3 weld exhibited the same load deflection behavior up to about 1.2 percent strain. At this point, the specimen fractured due to strain localization in the weld.

The second series of tests used the 100S-1 weld metal at much higher heat input as explained in Section 3.1.3. The behavior of the tests in the second series was similar to the behavior of the 70S-3 welds, i.e. the wide-plate tests developed sufficient strength but negligible ductility. Therefore, a third series of tests was conducted on three of these specimens. Since there was virtually no plastic strain in the second series of tests, the welds were cut off and the plates were rewelded to make specimens with a slightly smaller gage length. Specimens 25, 26, and 27 were chosen since these had the smallest fracture strain.

All of the tests in the second and third series exceeded the MSYS by at least 10 percent which exceeds the average actual base plate yield strength, i.e. the undermatched weldments could achieve the full strength of the base plate or 100 percent joint efficiency. The small flat strap specimens indicated that full base plate strength is not achieved. The wide-plate tests develop constraint which enables the weld metal to withstand higher stresses than in the flat-strap specimens. All of the new tests and the 70S-3 weldment tested earlier exhibited very limited ductility. The overmatched welds and the welds undermatched up to 13 percent in the previous series of tests exhibited total nominal elongations exceeding 6 percent, which is greater than 16 times the yield strain of the base plate (which is about 0.36 percent). These new specimens fractured between 0.4 to 0.8 percent strain, i..e. from 1 to 2 times the yield strain of the base plate.

The behavior of the tests in the second and third series was similar to the behavior of the previously tested 70S-3 weldment in that the plastic strain had begun to localize in the weldment and that little or no plastic strain occurred in the base plate. This is in contrast to the slightly undermatched welds, where the weld strain and base-plate strain accumulated at comparable rates. Therefore, it appears that welds which are undermatched 18 percent or more will tend to fail prematurely due to strain localization in the weld, whereas we know that welds that are undermatched up to 13 percent will spread the plastic strain uniformly throughout the plate and give very good ductility. The dividing line between these two types of behavior is somewhere between 13 and 18 percent undermatching. This finding is consistent with the simple analysis in Section 2.3.1 which showed that the constraint in an a wide plate would allow up to 12.5 percent undermatching. The additional few percent undermatch that were tolerated by the wide plates is probably due to strain hardening, which was ignored in the simple analysis.

There was no significant difference between the 70S-3 specimen with the 3 mm reinforcement and that with the reinforcement ground flush. Based on previous research [7], this reinforcement was expected to dramatically improve the performance of this 70S-3 weld. This lack of improvement may be due to lower weld metal strength for the reinforced specimen due to variation in the weld procedure. Thus, the effect of the reinforcement was negated, which confounded the attempt to estimate its benefits.

Comparative tests were also performed on the slightly undermatched (low-heat-input) 100S-1 and 120S-1 welds with the following intentional defects:

1. simulated undercut (UC) consisting of a machined notch 1.6 mm deep and 3 mm wide along the fusion line;
2. simulated lack-of-fusion or incomplete penetration defect (IP) consisting of a thin strip of metal 3 x 9 x 152 mm which was tacked to the side wall and welded over; and
3. misalignment with the plates parallel but offset 3 mm.

Figure 3-18 shows weld macrosections for a typical standard specimen as well as these variations.

The specimens with the simulated undercut developed the yield strength of the base plate material based on the gross cross-sectional area. Both specimens fractured at the notch, though the nominal elongation of the 120S-1 specimen was significantly reduced while the ductility of the 100S-1 specimen was not affected. The undermatched weld was apparently beneficial in this case, though the result may be random.

The specimens with lack-of-fusion defects fractured at about 0.7 percent elongation over the whole gage length in both the 100S-1 weld and the 120S-1 weld. This elongation represents a ductility factor of about 2.3 times the yield strain, which is good considering the severity of the defect. The measured defect size was approximately 5 x 170 mm in the 120S-1 weld and 5 x 165 mm for the 100S-1 weld, indicating the net fused area was only 90 percent of the gross-section area. Although the 100S-1 specimen yielded at a gross nominal stress that was a few percent below the MSYS, before fracturing the gross nominal stress exceeded the MSYS. The specimen with the 120S-1 weld yielded at a gross-section nominal stress which exceeded minimum specified base plate strength.

The mis-aligned joints attained full base plate strength with only minor decreases in ductility. The elongation was reduced to 5.5 percent on average versus 7.7 percent on average for the joints with no defects. The 100S-1 weld exhibited greater ductility, though this result is probably due to random variation.

The dissimilar plates performed as expected. The loads for both the 100S-1 and 70S-3 welds were not significantly different and exceeded the minimum specified HSLA-80 strength. Both specimens fractured in the lower strength HSLA-80 plate.

3.4.3.2 Local Behavior and Fracture Criterion

The high-elongation strain gages performed very well. In general, the strain gages were in agreement with strains measured at the punch marks and with an LVDT (with a 67 mm gage length) which spanned the welds. In most locations, three gages were used across the width of the specimens (see Figure 3-13). The results of the three gages in any row were typically consistent, therefore the gages were typically averaged together. These gages gave interesting data on the heterogeneity of the strain in the plates.

Figure 3-19 shows strain gage data for the 120S-1 overmatched weld specimen (Specimen 2). The Figure shows the weld strains and the average base metal strains measured at various distances from the weld axis as a function of nominal specimen elongation. The upper and lower (indicating position in the test machine) base plate are the averages of the gages 375 mm from the weld axis on either plate. The mid-height gages were located just off the weld 32 mm from the weld centerline. The weld crown and weld root gages were located on the weld axis.

The specimens all exhibited angular distortion which is typical of single-vee welds due to shrinkage. The distortion would be expected to cause additional strain in the weld crown upon straightening. The effect of this distortion could be detected in the history of the strain in the gages at the weld root. The strain in these gages went into compression slightly due to the specimen straightening before going into tension due to the overall elongation. Figure 3-19 shows that the weld root strain was greater than the weld crown strain. This relative distribution of strain (i.e. root strain greater than crown strain) was observed on most tests. One exception was the 25 mm specimen which had was a double-vee weld.

The greater strain in the weld root can be explained if it is assumed that the vee-shaped weld is stretched transversely such that the same displacement occurs at the weld crown and at the weld root. Such stretching would occur if yielding initiates in the weld and most of the elongation is due to deformation of the weld zone. Then the strain in the relatively narrow root must be larger to achieve comparable displacement to the weld crown. Moire fringe photographs of wide-plate tests with mismatched single-vee groove welds typically show identical fringe patterns on both surfaces, indicating displacement compatibility through the thickness [6].

As shown in Figure 3-19, the strain in the weld was within the same scatter band as the strain in the base plate. With the exception of the lower base plate gages, the average strain was in good agreement with the overall nominal elongation which confirmed that the strain was uniform and the measurements reliable. In this particular experiment, the strain in the lower base plate gages exhibits some relative increase or localization which is an indication of the necking and fracture which occurred in the base plate near these gages. For these materials, regardless of whether the specimen fractures in the weld or in the base plate, fracture typically occurs soon after the plates attain about six percent nominal elongation, i.e. a ductility factor of about 18 times the yield deformation.

Even though this specimen and several others fractured in the base plate, this should not be interpreted as an inconclusive test on the weld metal. In these cases where the specimens fracture in the base plate, the weld metal undergoes significant strains about the same magnitude as the average base plate strain, i.e. up to 18 times the yield strain. This level of performance is much greater than the minimum acceptable levels of ductility which, as discussed in the Introduction, are about 4 or 5 times the yield deformation. Therefore, even though the weld did not fracture in some cases, the excellent performance was adequately demonstrated.

The normal-matched 100S-1 widegap specimen had behavior similar to the overmatched weld. Figure 3-20 shows that strains in the widegap specimen localized in the upper base plate, though the general behavior was similar. However, the widegap specimen does not show a difference in strain between the weld crown and weld root. This is in agreement with the concept of displacement compatibility discussed above. The root of the widegap welds, in contrast to the standard specimens, is proportionally closer in width to the crown. Displacement compatibility can therefore be maintained without strains in the weld root which are much larger than strain s in the weld crown.

Strain data for one of the moderately undermatched 100S-1 weld specimens (Specimen 4) is shown in Figure 3-21. This specimen shows localization in the mid-height gages. This specimen eventually fractured in the HAZ, and this localization is captured by the mid-height gages. These data suggest that the location of fracture was random. For example, as shown in Figure 3-22, among the replicate 100S-1 weld specimens; Specimen 3 fractured in the weld, Specimen 4 fractured in the HAZ, and Specimen 5 fractured in the base metal remote from the weld. This suggests that the location for fracture is probably influenced by local variations in the thickness or properties.

In many specimens, several necks were apparent on the surface. These necks were shallow grooves about 75 mm wide oriented diagonally across the specimen. Though several necks typically formed, eventually one began to dominate and initiate fracture. The onset of final necking occurs at the point of ultimate strength or uniform strain. In all specimens which failed in the base plate, the uniform strain was at least 6 percent.

Figure 3-23 shows the 70S-3 weld specimen in the 13 mm thickness. First, as noted in the previous section, the total elongation of these 70S-3 welds was limited, i.e. about 1.2 percent. This is significantly less than the 120S-1 overmatched welds and the moderately undermatched 100S-1 welds in the first series of tests (which were welded at low heat input). Figure 3-23 shows that the weld strain clearly exceeded the base plate strain at all locations, and eventually fractured at about six percent weld strain. This strain is comparable to the weld strain at failure of the 100S-1 specimens from the first series of tests which also failed in the weld (such as Specimen 3). These data suggest that: 1) for these materials; 2) with this low-heat-input welding process; and, 3) in the absence of significant weld discontinuities; the weld fracture strain can be treated as a material property and it has a minimum value of at least six percent.

The behavior of this 70S-3 weld specimen is similar to the behavior of the specimens in the second and third series of tests welded width the 100S-1 weld metal at very high heat-input levels. These welds in the second and third series of tests were undermatched 18 percent or more. The behavior of specimens with these significantly undermatched welds is clearly different than the moderately undermatched welds, i.e. the 100S-1 welds made at low heat-input levels. The behavior of these significantly undermatched welds suggests that plastic constraint develops which is sufficient for the weld to achieve full base-plate strength, but that the development of this constraint requires significant strains in the weld metal. The strain required for the development of this constraint is so large that there is little residual ductility in the weld after the overall yield point is finally attained.

Actually, the elongation achieved by the 70S-3 specimens was slightly greater than less undermatched tests in the second and third series. This may be due to the degraded toughness of the high-heat-input welds in the second and third series, weld discontinuities in the high-heat-input welds, or a lower Y/T in the 70S-3 weld metal.

Figure 3-24 summarizes the weld metal strain data previously presented. The data are for the three weld metals and are the averages of the weld crown and root gages. As discussed previously, the minimum weld fracture strain was six percent and the minimum nominal elongation before necking in the base plate was also six percent. When the "critical weld-strain" is plotted on the Figure, the minimum ductility for each type of specimen can be shown. The criteria for determining the minimum ductility of the overall weldments are: six percent nominal elongation in the base plate or six percent local strain in the weld, whichever is achieved first. These criteria can be used in finite-element analyses of weldments to conservatively predict failure.

3.4.3.3 Comparison of Wide-Plate Tests to Flat Strap Specimens

Figure 3-25 shows the overmatched weld (120S-1 weld metal) wide-plate test result compared to two 38 mm wide flat-strap cross-weld tension tests. The normalized load-displacement curve (essentially, a stress-strain curve) is similar up to 8.5 percent nominal elongation, i.e. uniform strain at ultimate strength. Following uniform strain, the localization or necking occurs and results in different elongation in the two types of specimens. In the wide-plate tests, there is only about 0.2 percent additional elongation. The additional elongation after uniform strain in the small specimens is about 1.5 percent, or about seven times greater than the wide-plate test. Actually, the displacements after uniform strain are the same for the two types of specimens. For example, there was about 3 mm additional displacement after uniform strain in both types of specimens. The displacement results in less elongation when divided by the large gage length of the wide-plate test (1520 mm vs. 203 mm). As shown in Table 3-11, all the 120S-1 specimens failed in the base plate. The strain gage data for the small specimens was essentially the same as the strain gage data from the wide-plate tests.

Figure 3-26 shows the severely undermatched weld (70S-3 weld metal) wide-plate test result compared to two 38 mm wide flat-strap cross-weld tension tests. In contrast to the overmatched case, the stress-strain behavior of the small specimens is quite different from the wide-plate test. The stress at yield and ultimate is 5 and 9 percent lower, respectively, than the wide-plate test. This is significant because the wide-plate tests indicated the 70S-3 joint could achieve full base plate yield strength. In contrast, the small specimens lead to the conclusion that base-metal yield strength could not be reached. Both types of specimens reach ultimate strength at a uniform strain of about 1 percent. The elongation after necking is comparable to the overmatched weldment. The strain gage data for the small specimens was essentially the same as the strain gage data from the wide-plate tests.

The wide-plate test of a slightly undermatched joint (100S-1 weld metal) is compared to two 38 mm wide flat-strap cross-weld tensile tests in Figure 3-27. One of the small specimens exhibits the same stress-strain behavior as the wide-plate tests, although strength is slightly lower. However, one of the specimens begins to neck prematurely at about 2.5 percent elongation. Visual inspection of this specimen revealed a significant notch at the weld toe. This shows that small specimens are more sensitive to defects, which constitute a greater relative percentage of the cross section in the smaller specimens.

The load-displacement behavior of the 9 mm thick specimens is shown in Figure 3-28. The small-scale 9 mm thick specimens exhibit premature necking compared to the wide-plates. This is due to strain localization in the weld as indicated by the strain gage data in Figure 3-29. In fact, the small specimens fractured in the weld compared to the wide-plate test which fractured in the base plate. The 9 mm specimens were more undermatched relative to the 13 mm specimens in the first series (12 percent vs. 8 percent). Therefore, it can not be discovered whether the difference in performance is related to the level of undermatch or thickness. It is clear, however, that these results would lead to the finding that undermatched welds performed poorly compared to overmatched welds. This finding is only valid for the limited width of the small strap specimens and is not applicable to either the wide-plate test specimens or continuous ship-hull plating. The results from small specimens overstate the significance of the problem with undermatched welds.

The differences in behavior between specimen types are due to constraint. The wide-plate tests have greater constraint in the width direction, leading to higher hydrostatic stresses and higher apparent weld metal strength. The behavior of undermatched welds in structures should be assessed on the basis of full-scale tests since small-scale specimens do not behave in a manner consistent with the structure. In Section 4.1.1, it is shown through finite-element analysis that there is a zone near the edge of test specimens approximately 4 times the thickness in width where the stress and strain distributions are different from typical distributions through the core of the specimens. Clearly, these atypical edge regions comprise too large a portion of the 38 mm wide specimens.

Plate Chemistry									
Element	HSLA-100 ≤ 25 mm							HSLA-80	
	Thickness	9 mm	13 mm	13 mm	13mm	13mm	25mm		13 mm
	Specified	R9541 /2G	R9541 /2H	R7762 /39B	R7779 /5AA	new plate	R8126 /2D	Specified	307K 4000 0
Carbon	0.062	0.04	0.04	0.04	0.04	0.05	0.04	0.07	0.05
Manganese	0.75-1.25	0.89	0.89	0.84	0.88	0.98	0.90	0.40 -0.70	0.64
Phosphorus	0.020	0.004	0.004	0.006	0.007	0.012	0.007	0.025	0.016
Sulfur	0.006	0.003	0.003	0.005	0.002	0.003	0.002	0.010	0.001
Silicon	0.40	0.26	0.26	0.27	0.28	0.25	0.27	0.40	0.280
Nickel	1.50 -2.00	1.61	1.61	1.64	1.68	1.76	1.66	0.70 -1.00	0.92
Chromium	0.45 -0.75	0.56	0.56	0.62	0.60	0.55	0.57	0.60 -0.90	0.69
Molybdenum	0.30 -0.55	0.41	0.41	0.40	0.40	0.36	0.40	0.15 -0.25	0.200
Copper	1.00 -1.30	1.15	1.15	1.09	1.16	1.07	1.22	1.00 -1.30	1.08
Columbium	0.02 -0.06	0.031	0.031	0.039	0.030	0.022	0.030	0.02 -0.06	0.043
Aluminum		0.031	0.031	0.021	0.022	0.030	0.023		0.049
Titanium	0.02	0.003	0.003	0.002	0.002		0.002		
Arsenic	0.025	0.0060	0.0060	0.0060	0.0050		0.0050		
Antimony	0.025	0.0040	0.0040	0.0040	0.0040		0.0030		
Vanadium	0.03	0.003	0.003	0.005	0.004	0.009	0.003		
Tin	0.030	0.015	0.015	0.013	0.012		0.014		
Nitrogen		0.0068	0.0068	0.0085	0.0053		0.0082		
C_{eq}		0.61	0.61	0.61	0.62	0.63	0.62		0.51
P_{cm}		0.23	0.23	0.23	0.24	0.24	0.24		0.21

Table 3-1 Base Metal Chemistry

Filler Metal Chemistry						
Element	Type Mil-120S-1		Type Mil-100S-1		Type Mil-70S-3	
	Specified	120027	Specified	248B	Specified	182968
Carbon	0.10	0.07	0.08	0.047	0.07 -0.19	0.09
Manganese	1.40 -1.80	1.58	1.25 -1.80	1.65	0.90 -1.40	1.17
Silicon	0.25 -0.60	0.35	0.20 -0.55	0.47	0.40 -0.70	0.60
Phosphorus	0.01	0.008	0.01	0.009	0.025	0.016
Sulfur	0.01	0.004	0.01	0.003	0.035	0.013
Nickel	2.00 -2.80	2.40	1.40 -2.10	1.89		
Molybdenum	0.30 -0.65	0.48	0.25 -0.55	0.43		
Chromium	0.60	0.32	0.30	0.08		
Vanadium	0.03	0.01	0.05	0.001		
Aluminum	0.10	0.01	0.10	0.01		
Titanium	0.10	0.01	0.10	0.036		
Zirconium	0.10	0.02	0.10	0.004		
Copper					0.30	0.26
C_{eq}		0.17		0.14		0.02
P_{cm}		0.25		0.21		0.18

Table 3-2 Filler Metal Chemistry

Material	Yield Strength (MPa)			Tensile Strength (MPa)		
	min.	avg.	max.	min.	avg.	max.
original 13 mm plate	750	779	813	827	837	855
100S-1, <1.2kJ/mm	670	717	750	750	765	780
new 13 mm plate	712	740	784	738	760	809
100S-1, 2.2 kJ/mm	570	580	610	655	695	731
100S-1, 1.8 kJ/mm	589	603	611	672	705	744

Table 3-3 Range and Averages of Strength for 13 mm thick base plate and 100S-1 Weld Metal with Varying Heat Input

Base Metal	Filler Material (MIL - Type)		
Thickness	120S-1	100S-1	70S-3
13 mm HSLA 100	1 - STD	1 - STD 1 - WGAP 1 - MOD	1 - STD

KEY: STD - Standard Specimen, Reinforcement Ground Flush
WGAP - Two Plates with Buildup Applied to Each Edge
MOD - Standard Specimen, Perpendicular Stiffener

Table 3-4 Shear Specimen Test Matrix

Welding Process	GMAW-P, semi-automatic (pulsed- arc, spray transfer) (Third series of tension test specimens were not pulsed)
Base Material	MIL-S-24645, grades HSLA-80 and 100
Weldment Class	Mil-Std-1689, Hull Structure
Base Material Thickness	9 mm, 13 mm, and 25 mm
Position	Flat, 1G
Joint Design	9 mm and 13 mm ; single v-groove 25 mm ; double v-groove
Filler Metal	MIL-120S-1 of MIL-E-23765/2C MIL-100S-1 of MIL-E-23765/2C MIL-70S-3 of MIL-E-23765/1E
Shielding Gas	Argon/Carbon Dioxide (95/5) @ 40-60 cfh
Electrical Characteristics	Tip to cup: 0 mm -3 mm recess Cup to Work: 13 mm nominal Current: DCEP-pulsed, electrode positive
Preheat, Minimum	First series: 16°C less than 13 mm 52°C 13 mm or greater Second series: 175°C Third series: 150°C
Interpass,	First series: Maximum 150°C Second series: 175°C Third series: 150°C
Postweld Thermal Treatment	None Allowed
Additional Parameters	Torch Work Angle: 80° Torch Travel Angle: 10°-20° push

Table 3-5 Welding Procedure Specification for Shear and Tension Specimens.

Spec #	Type	Wire	Layer	Pass	Amp	Volts	Travel Speed mm/s	Heat Input kJ/mm
19	Std	120S	root	1	202	22.0	3.81	1.1
			fill	3	214	22.9	6.73	0.73
			dress	2	211	23.6	5.00	1.00
20	Std	100S	root	1	192	20.6	3.64	1.09
			fill	3	220	20.9	6.31	0.73
			dress	2	212	22.2	5.84	0.81
21	Std	100S	root	1	196	22.2	3.64	1.20
			fill	2	204	23.1	4.57	1.03
			dress	2	209	22.8	6.05	0.79
22	WGap	100S	buildup	14	190	22.6	5.59	0.77
			root	1	190	22.7	4.15	1.04
			fill	3	208	23.0	6.18	0.77
			dress	3	212	22.0	4.87	0.96
23	Mod	100S	root	1	196	22.2	3.64	1.20
			fill	2	204	23.1	4.49	1.05
			dress	2	207	23.1	5.84	0.82
24	Std	70S	root	1	199	19.4	5.50	0.70
			fill	2	206	22.7	4.91	0.95
			dress	2	213	22.0	5.50	0.85

Table 3-6 Shear Specimen Welding Parameters

Spec #	Butt Weld	Type	τ_u (MPa)	σ_u (MPa)	τ_u/σ_u
19	120S-1	STD	549	871	0.63
20	100S-1	STD	520	751	0.69
21	100S-1	STD	514	751	0.68
23	100S-1	MOD	479	751	0.64
22	100S-1	WGAP	465	796	0.58
24	70S-3	STD	467	597	0.78
	Fillet Weld				
FW5	120S-1	2.17 kJ/mm	594	871†	0.68
FW1	100S-1	2.17 kJ/mm	591	751†	0.79
FW2	100S-1	2.17 kJ/mm	570	751†	0.76
FW3	100S-1	0.91 kJ/mm	700	751†	0.93
FW4	70S-3	2.17 kJ/mm	302	597†	0.51

The design shear strength for fillet welds given in MIL-STD 1628 for the 120S-1 and 100S-1 filler metal is 600 and 572 MPa, respectively. The expected minimum base plate shear yield strength is 0.6 * F_y = 414 MPa, where F_y is the MSYS.

†Values from groove weld specimens with different heat inputs. The accuracy of this approximation can not be estimated.

Table 3-7 Comparison of Ultimate Strengths and τ_u/σ_u for Butt-Weld and Fillet Weld Shear Tests

Base Material	Filler Material (MIL - type)		
Thickness	120S-1	100S-1	70S-3
9 mm HSLA 100		1 - STD	
13 mm HSLA 100 (first series)	1 - STD 1 - IP 1 - MISAL 1 - UC	3 - STD 1 - IP 1 - MISAL 1 - UC 2 - WGAP	1 - STD 1 - 3 mm REINF
13 mm HSLA 100 (new plate) (second and third series)		5 - VHHI 3 - HHI	
13 mm HSLA 100/80		1 - STD	1 - STD
25 mm HSLA 100		1 - STD	

KEY:
STD - Standard Specimen, Reinforcement Ground Flush
IP - Standard with Intentional Incomplete Penetration or Lack-of-Fusion
MISAL -Two Plates with Maximum Allowable Misalignment
UC - Standard Specimen with Intentional Undercut (Ground In)
WGAP - Two Plates with Buildup Applied to Each Edge
REINF - Standard Specimen, Reinforcement Not Ground
VHHI - Very High Heat Input (second series of tests)
HHI - High Heat Input (third series of tests)

Table 3-8 Tensile Specimen Test Matrix.

Spec #	Description	Wire	Layer	Passe	Amps	Volts	Travel Speed (mm/s)	Heat Input kJ/mm
1	9 mm HSLA100	100S-1	root	1	187	20.6	4.28	0.90
	Std		fill	1	204	21.7	5.80	0.76
			dress	2	204	22.2	6.35	0.71
2	13 mm HSLA100	120S-1	root	1	190	20.4		??
	Std		fill	3	206	22.2	5.08	0.90
			dress	2	205	22.1	5.46	0.83
3	13 mm HSLA100	100S-1	root	1	196	21	3.81	1.08
	Std		fill	3	200	22	5.93	0.74
			dress	2	199	22.8	5.42	0.84
4	13 mm HSLA100	100S-1	root	1	193	20.1	3.39	1.14
	Std		fill	3	203	21.3	6.39	0.68
			dress	2	198	23.2	6.43	0.71
5	13 mm HSLA100	100S-1	root	1	189	20.8	3.60	1.09
	Std		fill	3	202	21.9	5.63	0.79
			dress	2	198	22.5	5.63	0.79
6	13 mm HSLA100	70S-3	root	1	205	18.3	4.53	0.83
	Std		fill	3	225	23	6.77	0.76
			dress	2	225	23	5.72	0.90
7	13 mm HSLA100	120S-1	root	1	196	20.8	3.81	1.07
	IP		fill	3	205	22.6	5.55	0.83
			dress	2	208	23	5.50	0.87
			dress2/	2	208	23		??
8	13 mm HSLA100	100S-1	root	1	196	20.8	3.81	1.07
	IP		fill	3	208	22.7	6.05	0.78
			dress	2	198	23.7	5.93	0.79
			dress2/	2	201	23.4		
9	13 mm HSLA100	120S-1	root	1	181	19.9	2.46	1.46*
	Misal		fill	3	205	22.7	5.50	0.85
			dress	2	215	22.2	5.72	0.83
10	13 mm HSLA100	100S-1	root	1	174	20.7	2.24	1.61
	Misal		fill	3	218	22.1	5.80	0.83
			dress	3	210	24	5.59	0.90

Spec #	Description	Wire	Layer	Passe	Amps	Volts	Travel Speed (mm/s)	Heat Input kJ/mm
11	13 mm HSLA100	120S-1	root	1	199	20.8	3.73	1.11
	UC		fill	3	203	22.7	6.14	0.75
			dress	2	196	23.7	5.08	0.91
12	13 mm HSLA100	100S-1	root	1	201	20.3	3.89	1.05
	UC		fill	2	225	21.5	5.21	0.93
			dress	2	217	23.5	6.56	0.78
13	13 mm HSLA100	100S-1	buildup	6	205	22.5	6.18	0.75
	Wgap (9.5 mm)		root	1	221	22.7	6.05	0.83
	steel backing		fill	3	230	23.2	4.95	1.08
			dress	3	220	23.9	5.46	0.96
14	13 mm HSLA100	100S-1	buildup	10	193	22.7	6.43	0.68
	Wgap (13 mm)		root	1	233	22.5	5.16	1.02
	steel backing		fill	3	219	23.7	5.63	0.92
			dress	3	221	23.6	6.56	0.80
15	13 mm HSLA100	70S-3	root	1	185	21.9	3.51	1.15
	Rein		fill	3	224	23.4	5.84	0.90
			dress	2	222	23.7	5.29	0.99
16	13 mm HSLA100	100S-1	root	1	183	22	4.23	0.95
	13 mm HSLA-80		fill	3	214	21.2	6.39	0.71
	Std		dress	2	214	21.1	6.77	0.67
17	13 mm HSLA100	70S-3	root	1	201	19.9	4.15	0.96
	13 mm HSLA-80		fill	3	216	21.4	6.82	0.68
	Std		dress	2	193	24	5.72	0.81
18	25 mm HSLA100	100S-1	root	1	197	20.7	4.45	0.92
	Std		fill-1	4	224	22.5	5.12	0.98
			dress-1	3	215	23.4	4.91	1.02
			fill-2	1	215	22.4	4.32	1.11
			dress-2	2	203	24.0	6.31	0.77

Spec #	Description	Wire	Layer	Passe	Amps	Volts	Travel Speed (mm/s)	Heat Input kJ/mm
25-26	13 mm HSLA100	100S-1	root	1	290	30	4.02	2.16
second	Std		fill	1	290	30	4.02	2.16
series			dress	1	285	30	4.02	2.13
27-29	13 mm HSLA100	100S-1	root	1	290	30	4.02	2.16
second	Std		fill	1	285	30	4.02	2.13
series								
25R	13 mm HSLA100	100S-1	root	1	260	27	3.81	1.84
third	Std		fill	4	250	27	3.81	1.77
series			dress	2	230	27	5.5	1.13
26R,27R	13 mm HSLA100	100S-1	root	1	260	27	3.81	1.84
third	Std		fill	3	250	27	3.81	1.77
series			dress	2	245	27	5.5	1.2

Table 3-9 Tensile Specimen Welding Parameters.

Spec #	Thick ness (mm)	Weld Metal	Joint Type	P_y MN	σ_y MPa	P_u MN	σ_u MPa	Y/T	Unif Strain (%)	Nom. Elong (%)	Fail Loc
1	9	100	STD	4.6	785	4.9	891	0.88	6.7	7.2	BP
2	13	120	STD	6.1	781	6.4	843	0.93	6.5	8.7	BP
3	13	100	STD	6.0	776	6.4	836	0.93	5.7	6.7	W
4	13	100	STD	6.1	792	6.5	857	0.92	6.7	7.5	BP
5	13	100	STD	6.1	781	6.4	840	0.93	5.8	8.0	BP
6	13	70	STD	6.0	770	6.1	794	0.97	1.1	1.2	W
15	13	70	REI	6.1	781	6.2	812	0.96	1.3	1.3	W
13	13	100	WG	5.9	764	6.3	820	0.93	4.2	5.7	BP
14	13	100	WG	6.1	781	6.4	841	0.93	5.5	7.8	BP
18	25	100	STD	10.9	705	12.1	794	0.89	8.2	10.7	BP
25	13	100	VHH	6.0	766	6.0	766	1.0	0.4	0.4	W
26	13	100	VHH	6.0	765	6.0	765	1.0	0.4	0.4	W
27	13	100	VHH	6.0	771	6.0	771	1.0	0.4	0.4	W
28	13	100	VHH	6.1	783	6.1	785	0.99	0.8	0.8	W
29	13	100	VHH	6.2	797	6.2	798	0.99	0.5	0.5	W
25R	13	100	HHI	6.1	780	6.1	790	0.99	0.8	0.8	W
26R	13	100	HHI	6.2	790	6.2	800	0.99	1.1	1.1	W
27R	13	100	HHI	6.2	790	6.2	800	0.99	0.9	0.9	W
7	13	120	IP	5.9	776	6.0	786	0.99	0.7	0.8	W
8	13	100	IP	5.2	672	5.3	701	0.96	0.4	0.7	W
9	13	120	MIS	6.2	805	6.7	873	0.92	5.3	5.3	W
10	13	100	MIS	6.0	770	6.3	824	0.93	5.7	6.4	W
11	13	120	UC	6.0	770	6.1	799	0.96	1.1	1.2	HA
12	13	100	UC	6.1	781	6.5	849	0.92	4.3	5.9	HA
16	13	100	DIS	5.2	672	5.6	736	0.91	4.7	7.3	80
17	13	70	DIS	5.2	667	5.6	730	0.91	4.3	6.3	80

Notes:
In Failure Location, HA is for Heat-Affected Zone, 80 is for the HSLA-80 base plate. For Joint Type, refer to Table 3-8. DIS is for dissimilar base plates (HSLA-100/HSLA-80) Specimens 25R, 26R, and 27R are the third series of tests, which were rewelded from the plates in specimens 25-27 with a slightly lower heat input and preheat temperature.

Table 3-10 Results of Wide-Plate Tension Tests.

Spec #	Weld Metal	Joint	Thick mm	Spec Width mm	σ_y MPa	σ_u MPa	Y/T	Unif Strain (%)	Nom Elong (%)	Fail Loc
1	100S	STD	9	610	785	891	0.88	6.7	7.2	BP
1A			9	38	738	791	0.93	1.6	3.3	W
1B			9	38	735	792	0.93	1.8	3.9	W
BP			9	38	747	806	0.93			
AWM				6 DI	647	714	0.91			
UM %					13	11				
2	120S	STD	13	610	781	843	0.93	6.5	8.7	BP
2A			13	38	793	856	0.93	6.6	11.2	BP
2B			13	38	791	849	0.93	6.7	11.5	BP
BP			13	38	811	855	0.95			
AWM				6 DI	822	871	0.94			
UM %					-1	-2				
3	100S	STD	13	610	776	836	0.93	5.7	6.7	W
3A			13	38	741	812	0.91	5.0	10.0	BP
3B			13	38	782	847	0.92	2.8	6.2	W
BP			13	38	774	834	0.93			
AWM				6 DI	703	751	0.94			
UM %					9	10				
6	70S	STD	13	610	770	794	0.97	1.1	1.2	W
6A			13	38	700	748	0.94	1.2	2.1	W
6B			13	38	712	759	0.94	1.0	1.9	W
AWM			13	38	521	597	0.87			
UM %				6 DI	27	21				
29	100S	VHH	13	610	771	771	1.0	0.4	0.4	W
29A			13	38	592	655	0.90			W
29B			13	38	532	590	0.91			W
13	100S	WG	13	610	764	820	0.93	4.2	5.7	BP
13A			13	38	738	792	0.93	4.1	8.1	BP
13B			13	38	761	811	0.94	3.4	7.3	BP
BP			13	38	763	827	0.92			
AWM				6 DI	748	776	0.96			
UM %					2	6				
18	100S	STD	25	610	705	794	0.89	8.2	10.7	BP
18A			25	38	719	788	0.91	6.4	13.7	BP
18B			25	38	710	785	0.90	7.4	15.3	BP
BP			25	38	710	790	0.90			
AWM				6 DI	693	746	0.93			
UM %					2	6				

Table 3-11 Results of Selected Wide-Plate Tests Shown with Flat-Strap and Material Property Tests for Comparison.

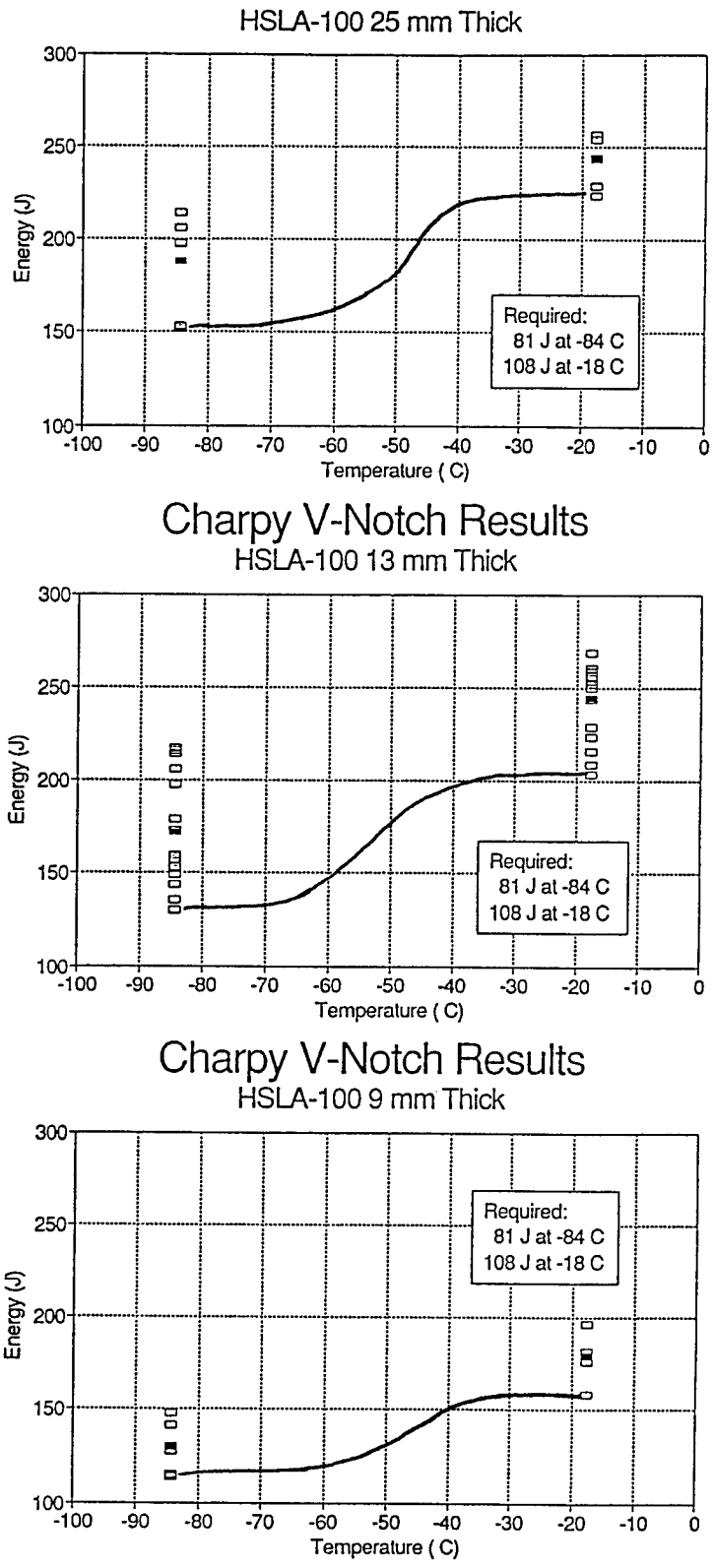

Figure 3-1 Charpy Toughness Data for HSLA-100 Plates in First Series of Tests.

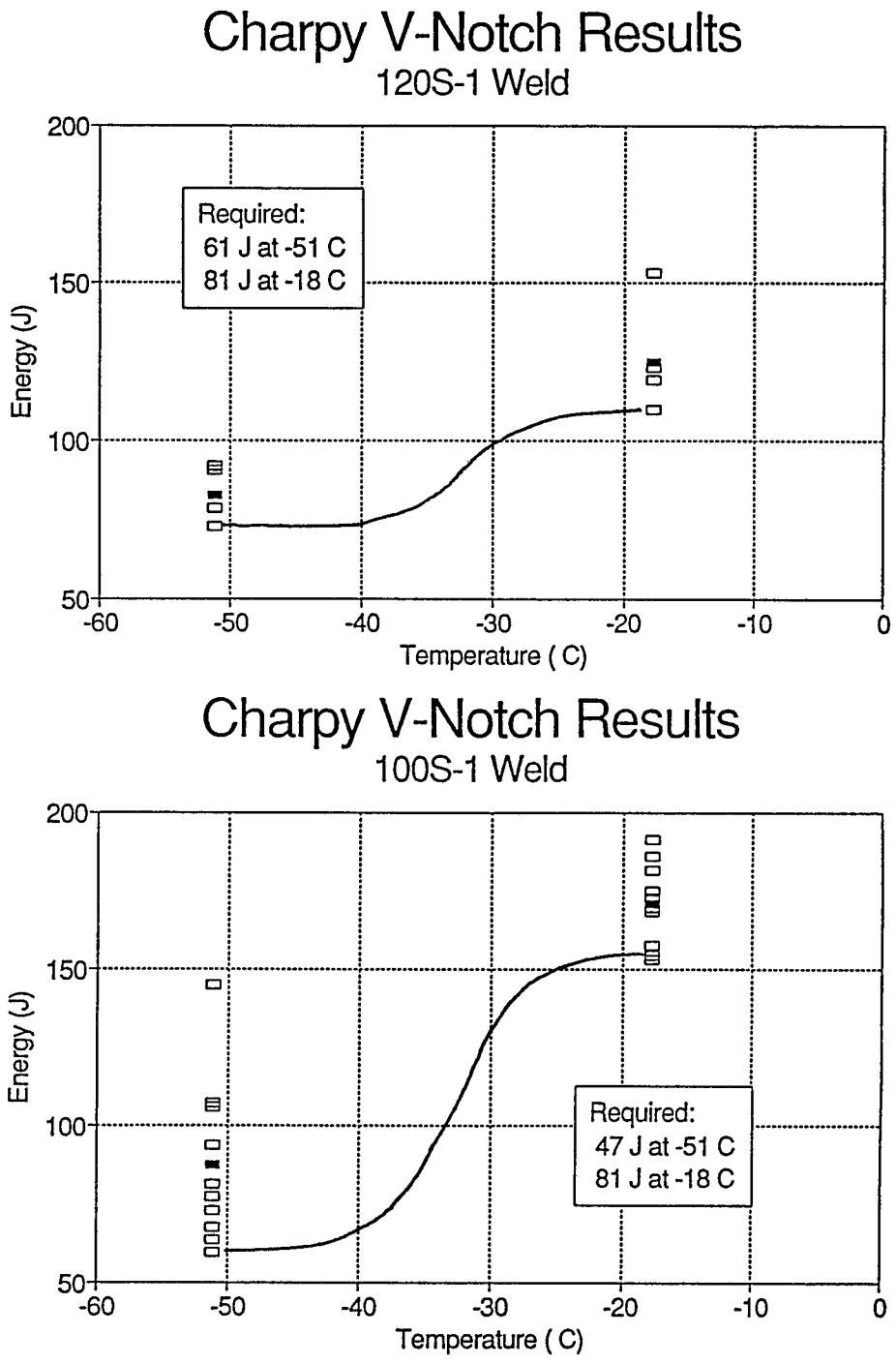

Figure 3-2 Comparison of Charpy Toughness Data for the 120S-1 and 100S-1 Welds Showing the Better Toughness of the 100S-1 Weld Metal.

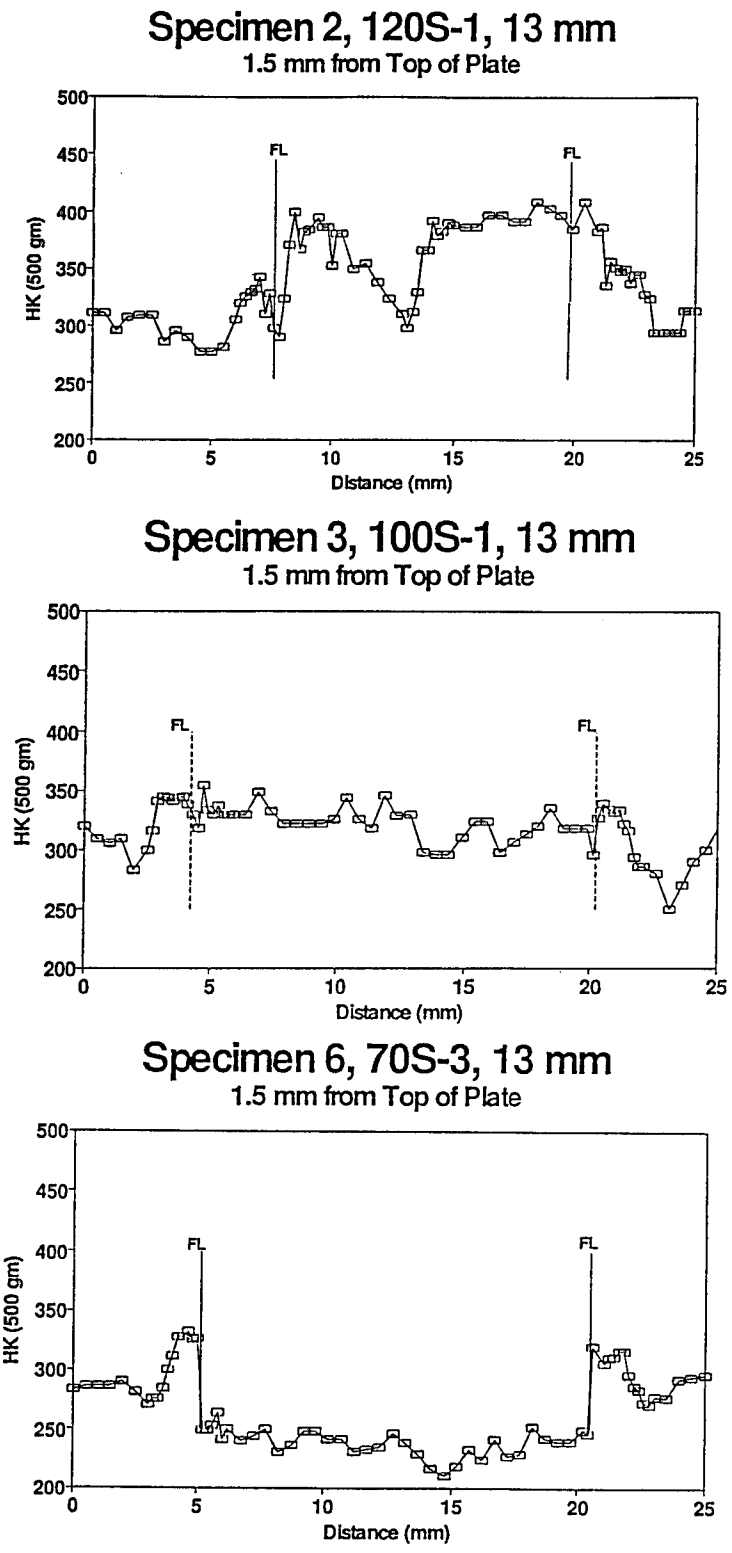

Figure 3-3 Comparison of Hardness data for Three Weld Metals Showing the Presence of Soft Zones Within the HAZ for All Three Weld Metals.

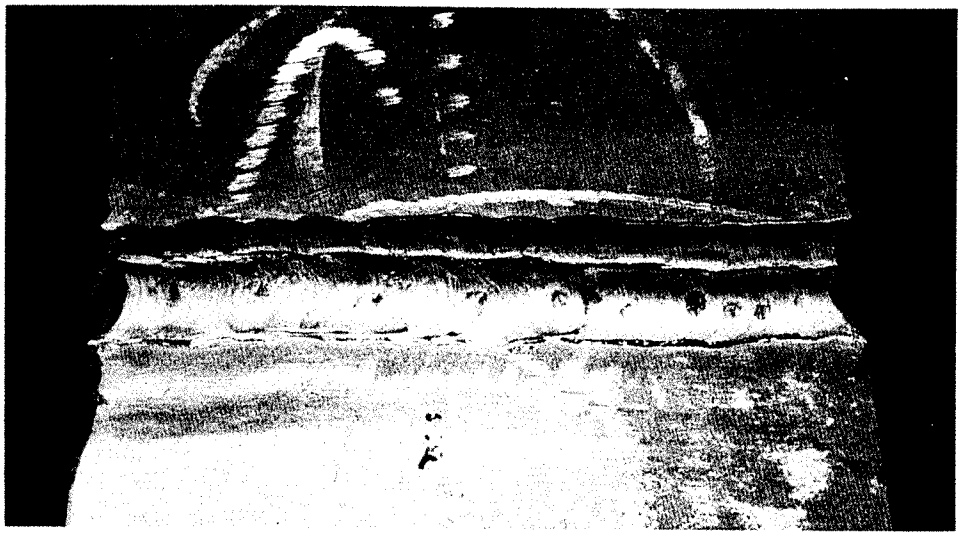

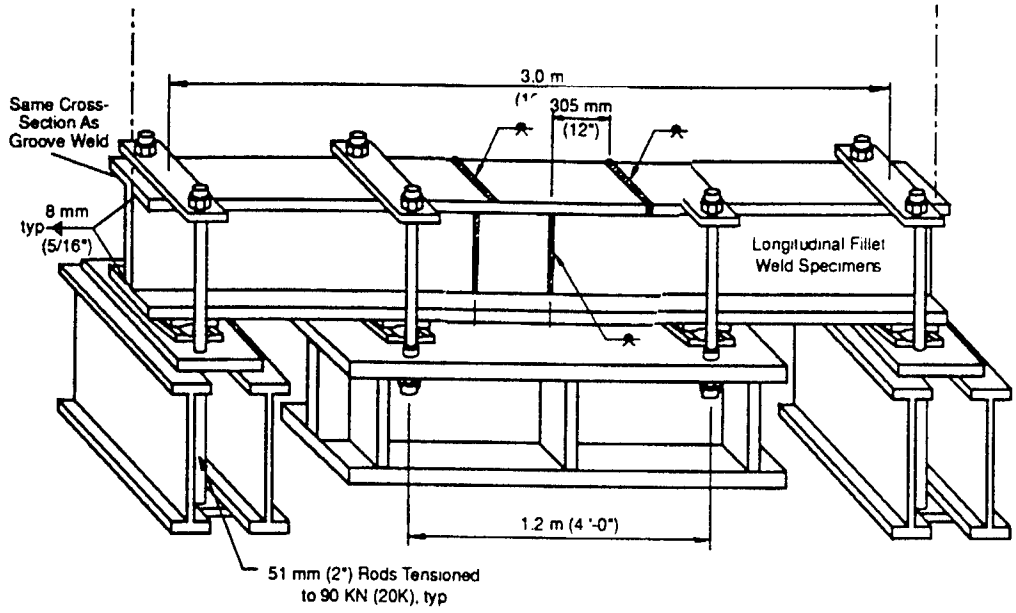

Figure 3-4 Fatigue Specimen and Test Set-Up.

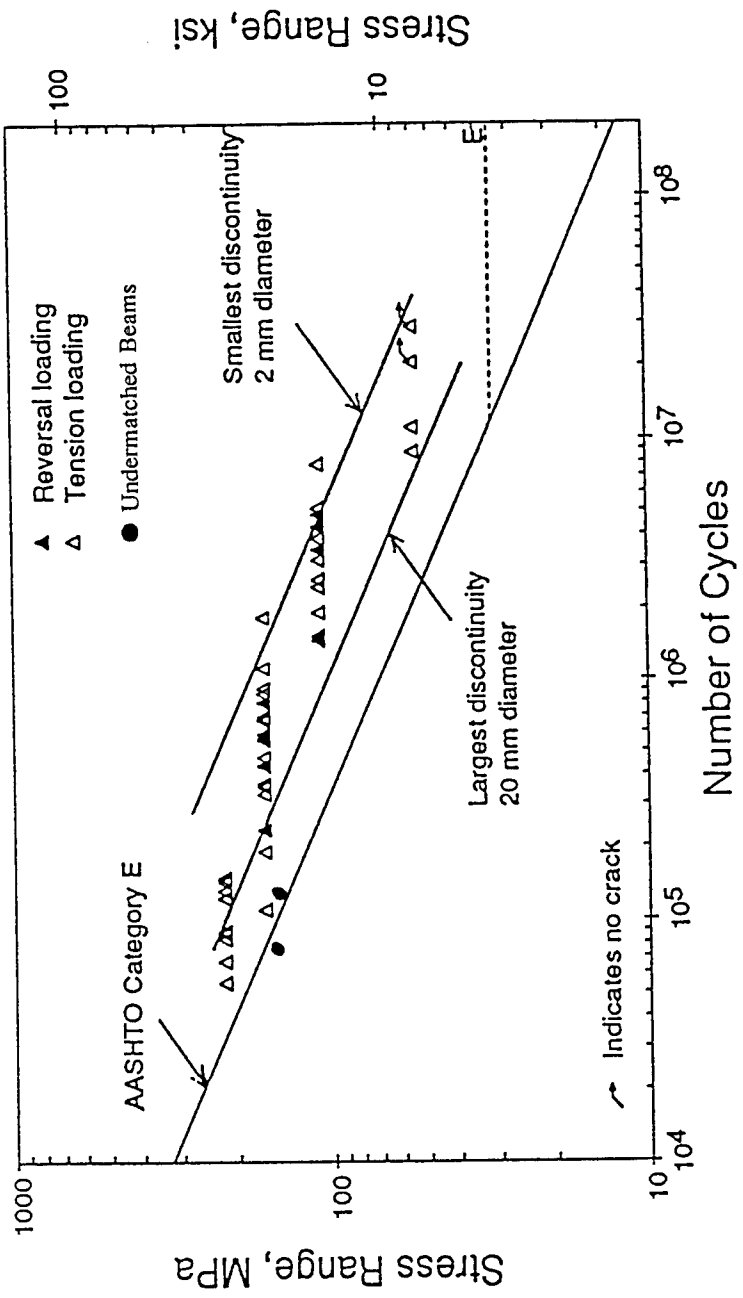

Figure 3-5 S-N Curve Comparing Undermatched Beams with Similar Overmatched Beams Showing Undermatched Beams Fall at the Lower End of Fatigue Life.

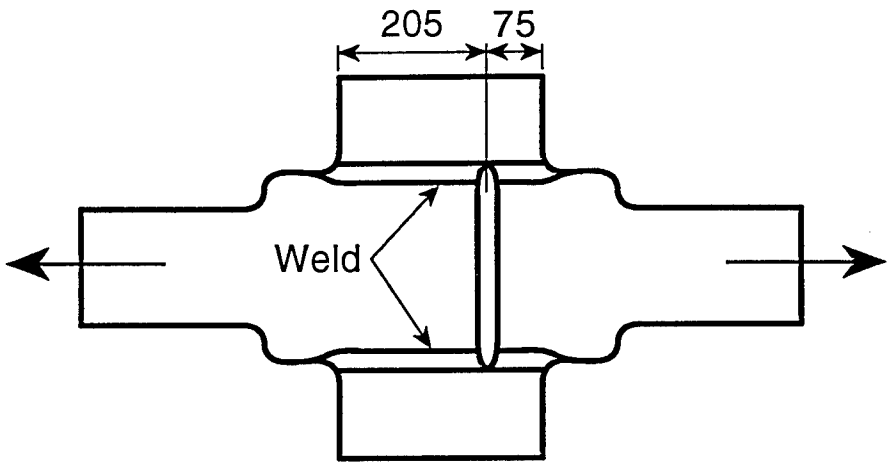

Figure 3-6 Shear Specimen Design.

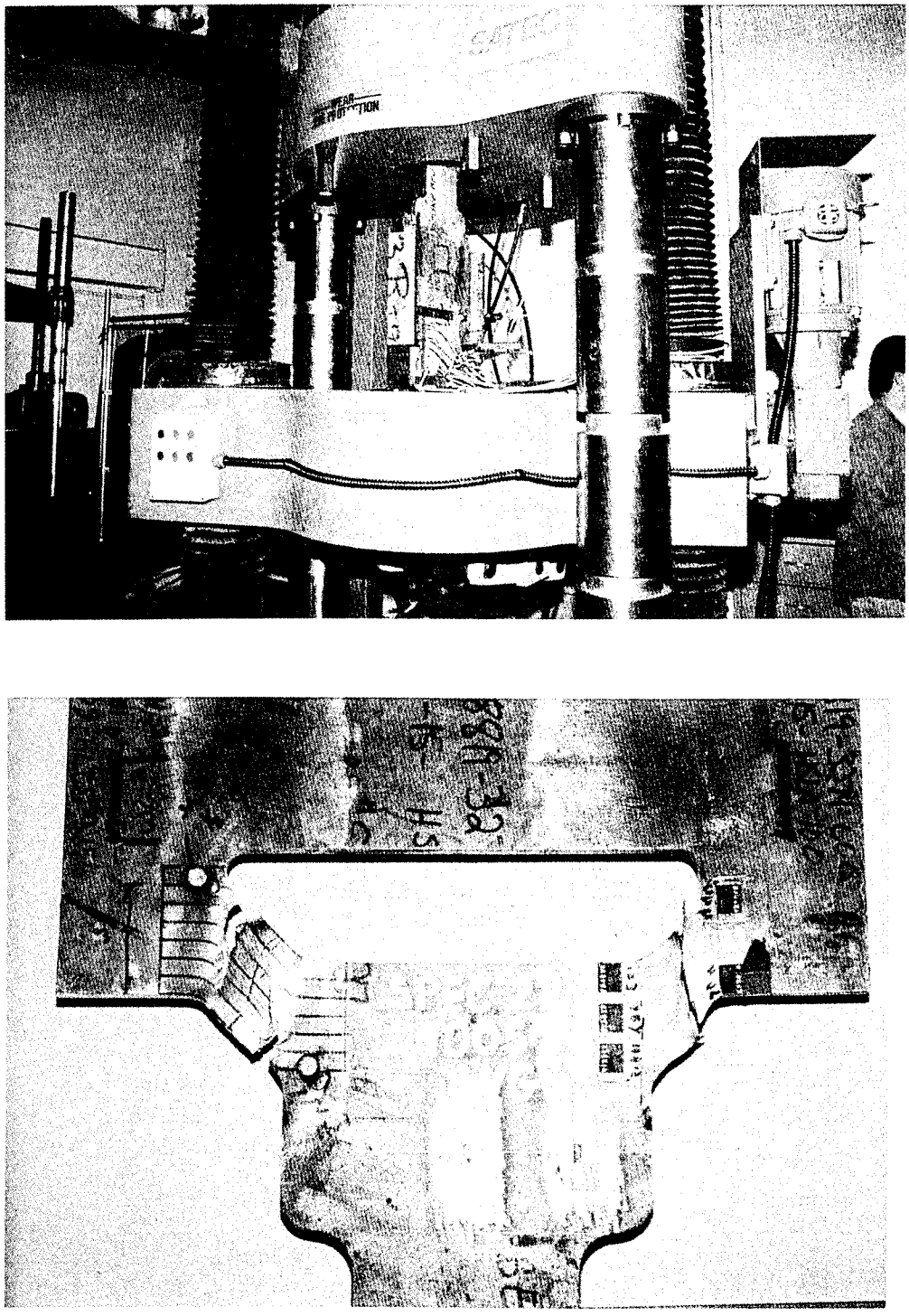

Figure 3-7 Photos of Shear Specimen Before and After Testing.

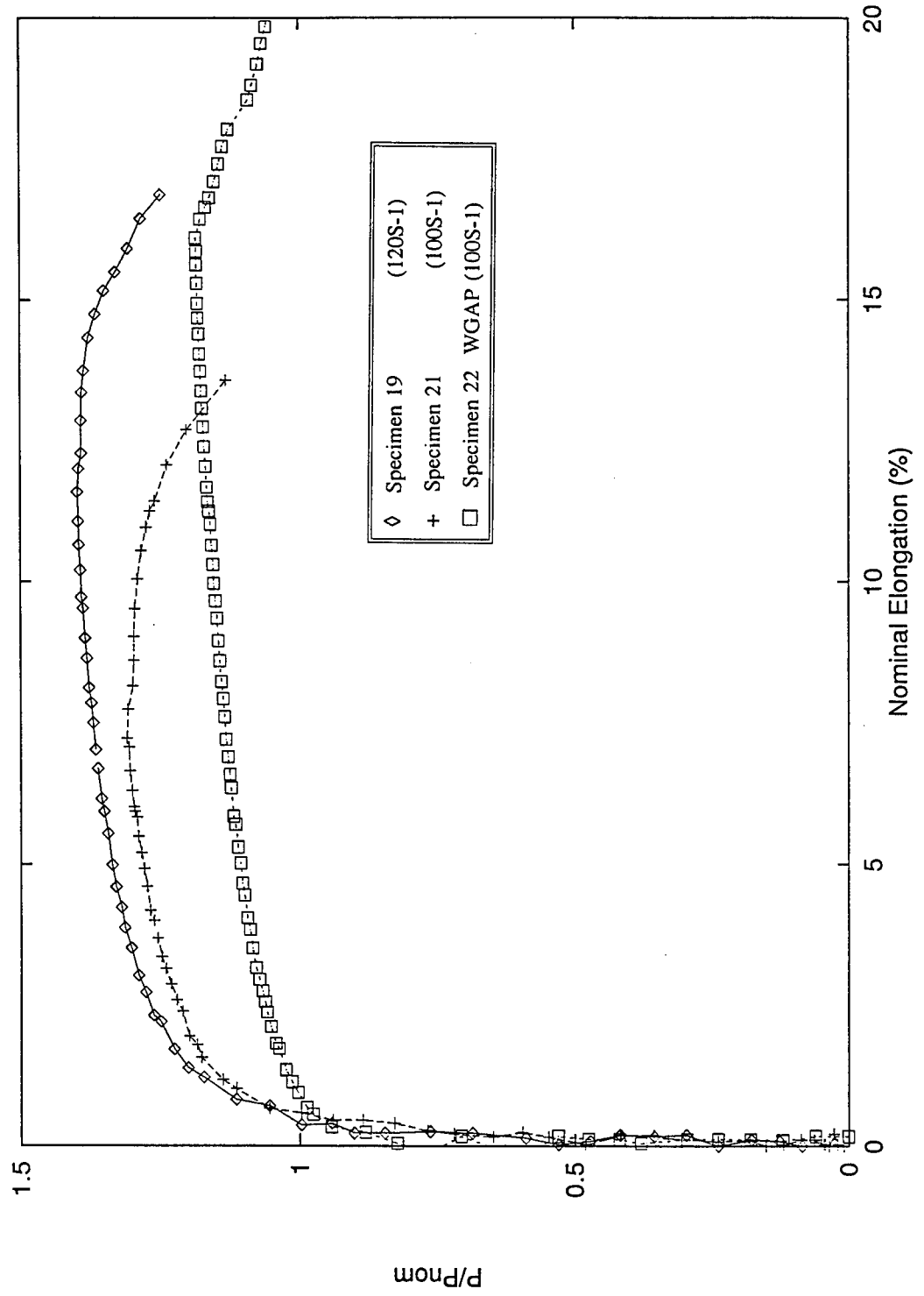

Figure 3-8 Normalized Load-Displacement Curves for Butt-Joint Shear Specimens.

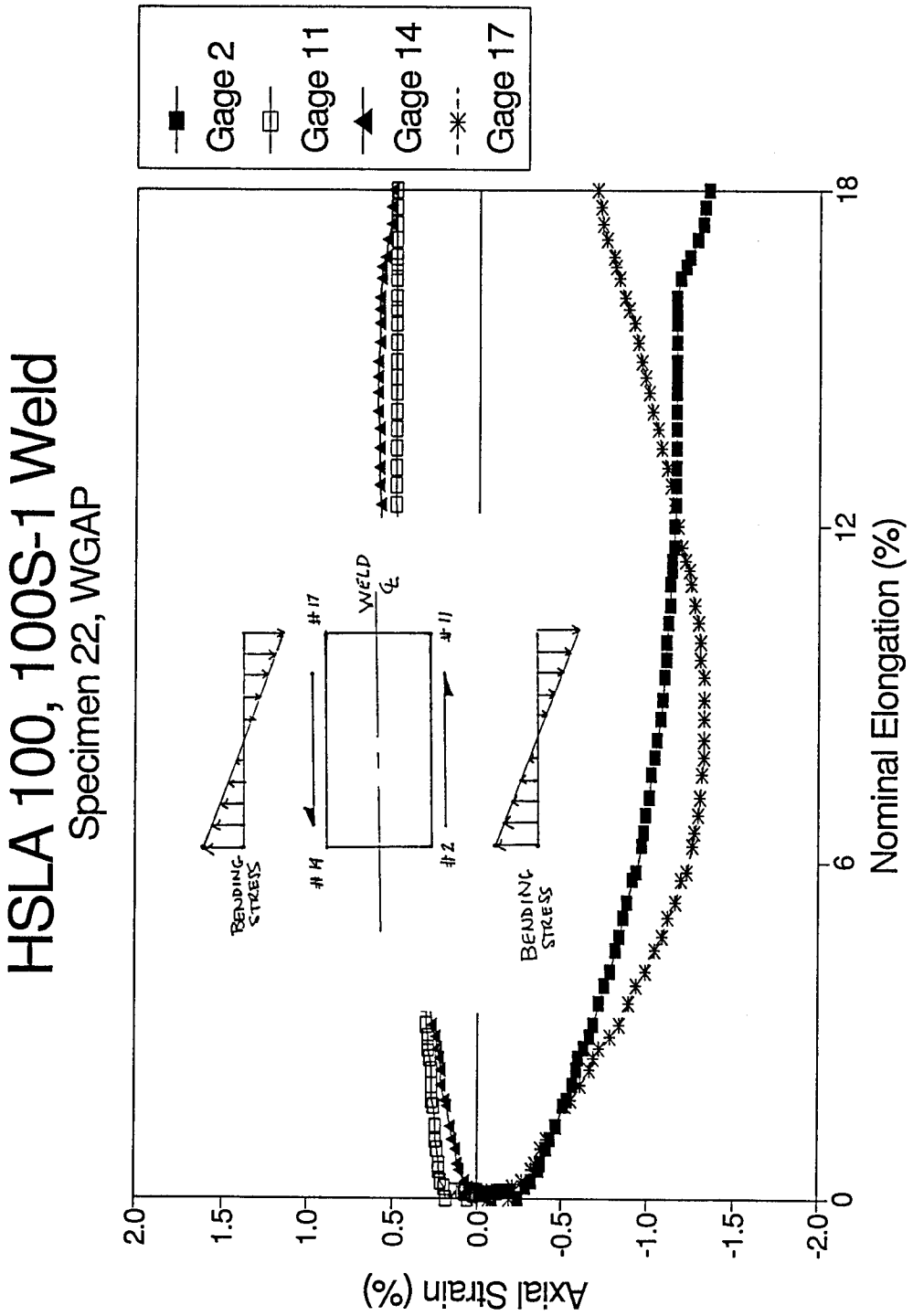

Figure 3-9 Axial Strain in the Base Plate Normal to Axis of the Widegap 100S-1 Groove Weld Showing the Bending Stresses Due to the Joint Eccentricity.

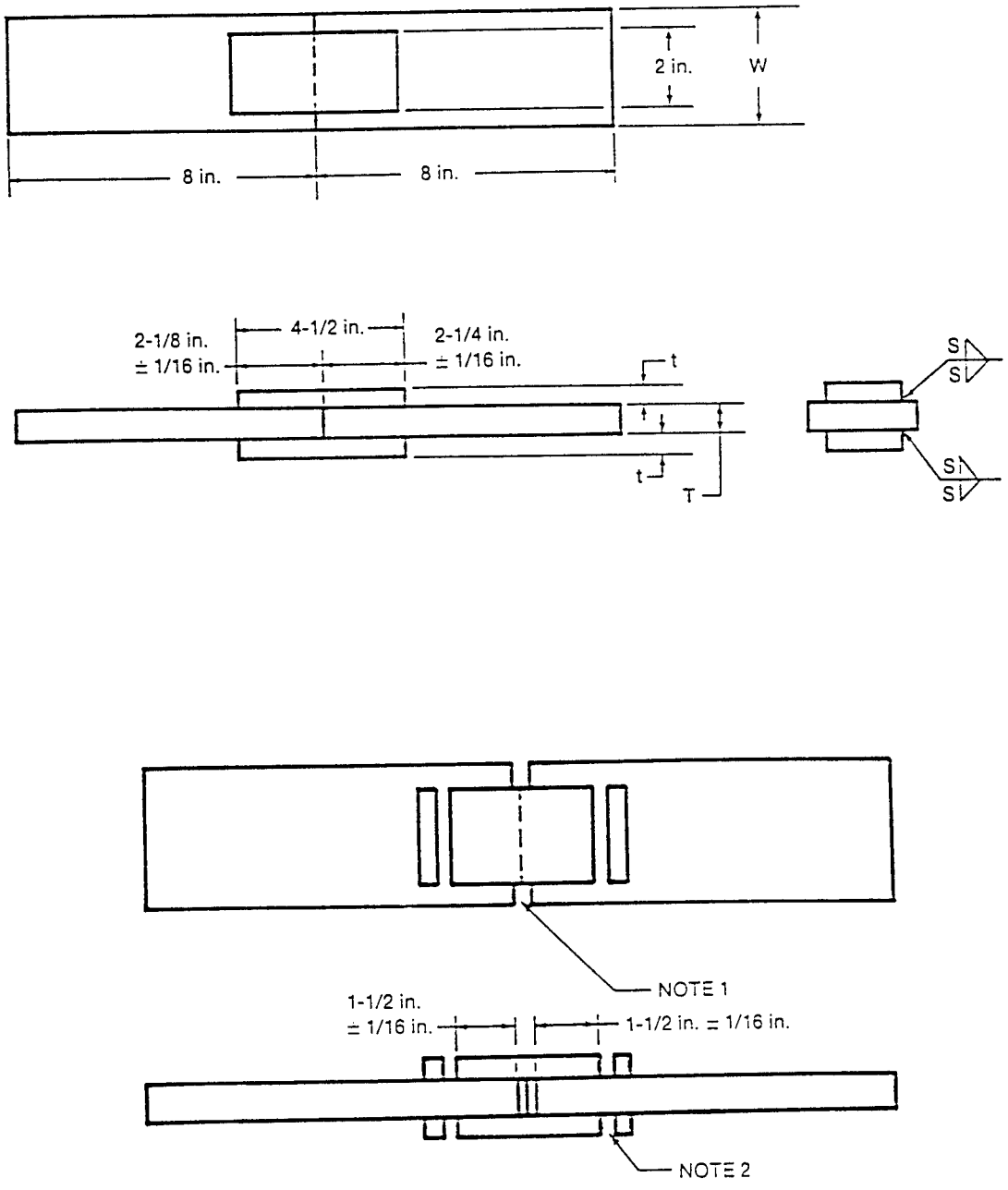

Notes:
1. Slot machined through root of test fillet weld.
2. Depth of machined notch shall extend through thickness of lap plate.

Figure 3-10 AWS Weld Qualification Fillet Weld Specimens.

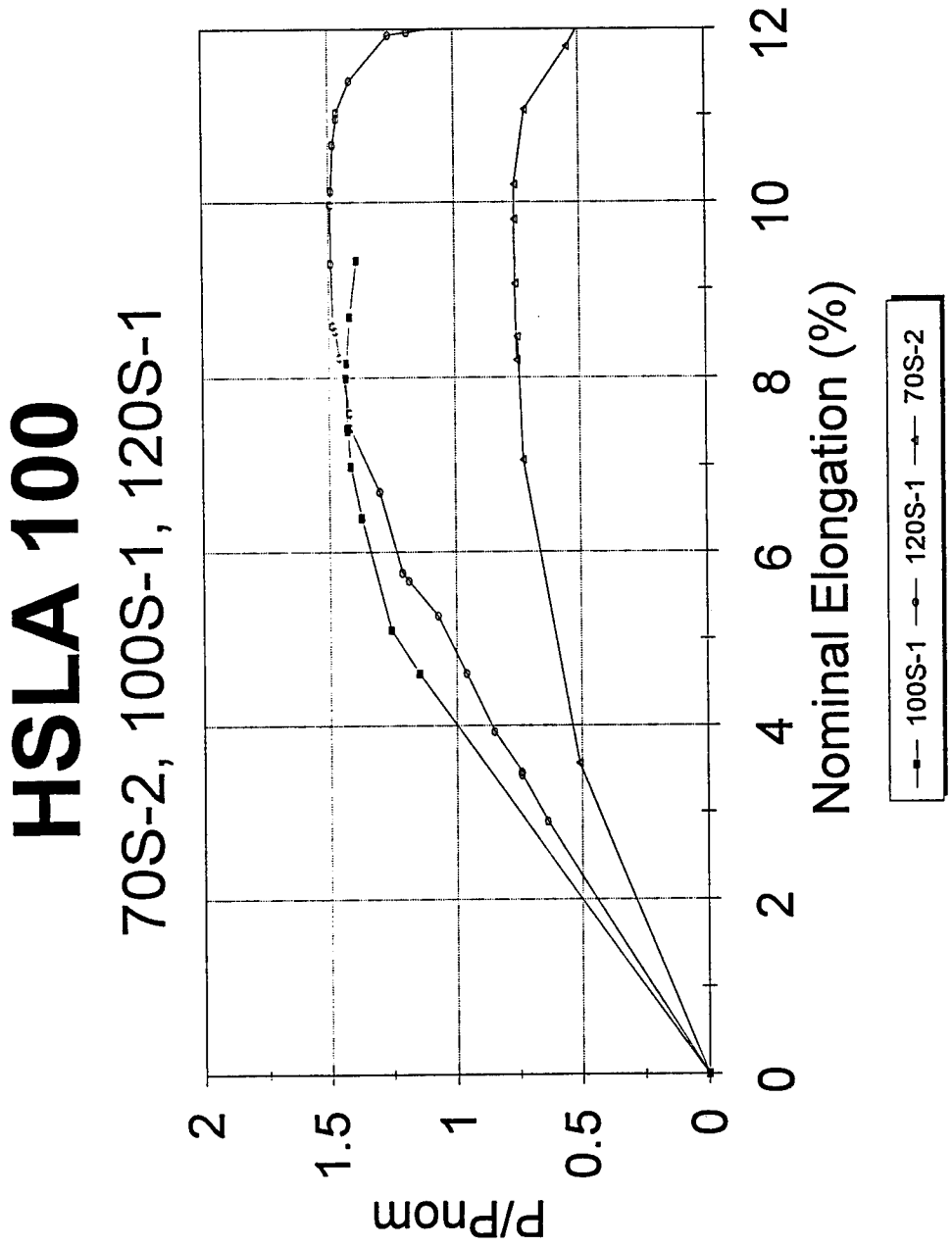

Figure 3-11 Results of Fillet Weld Tests for Three Weld Metals Showing the 120S-1 and 100S-1 Welds Achieve Base Plate Strength but the 70S-3 Does Not.

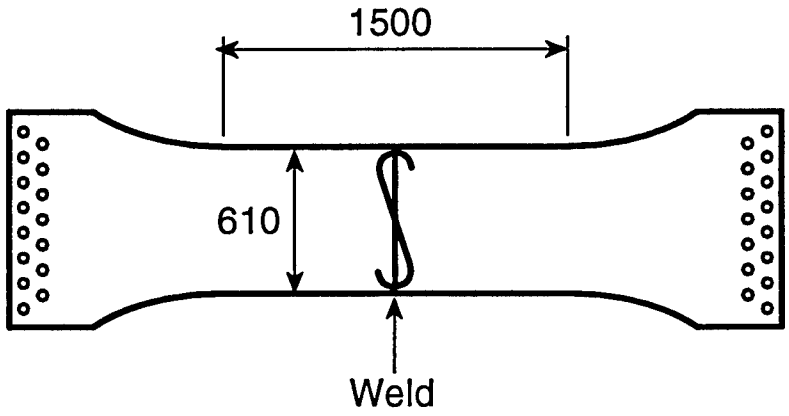

Figure 3-12 Tension Specimen Design.

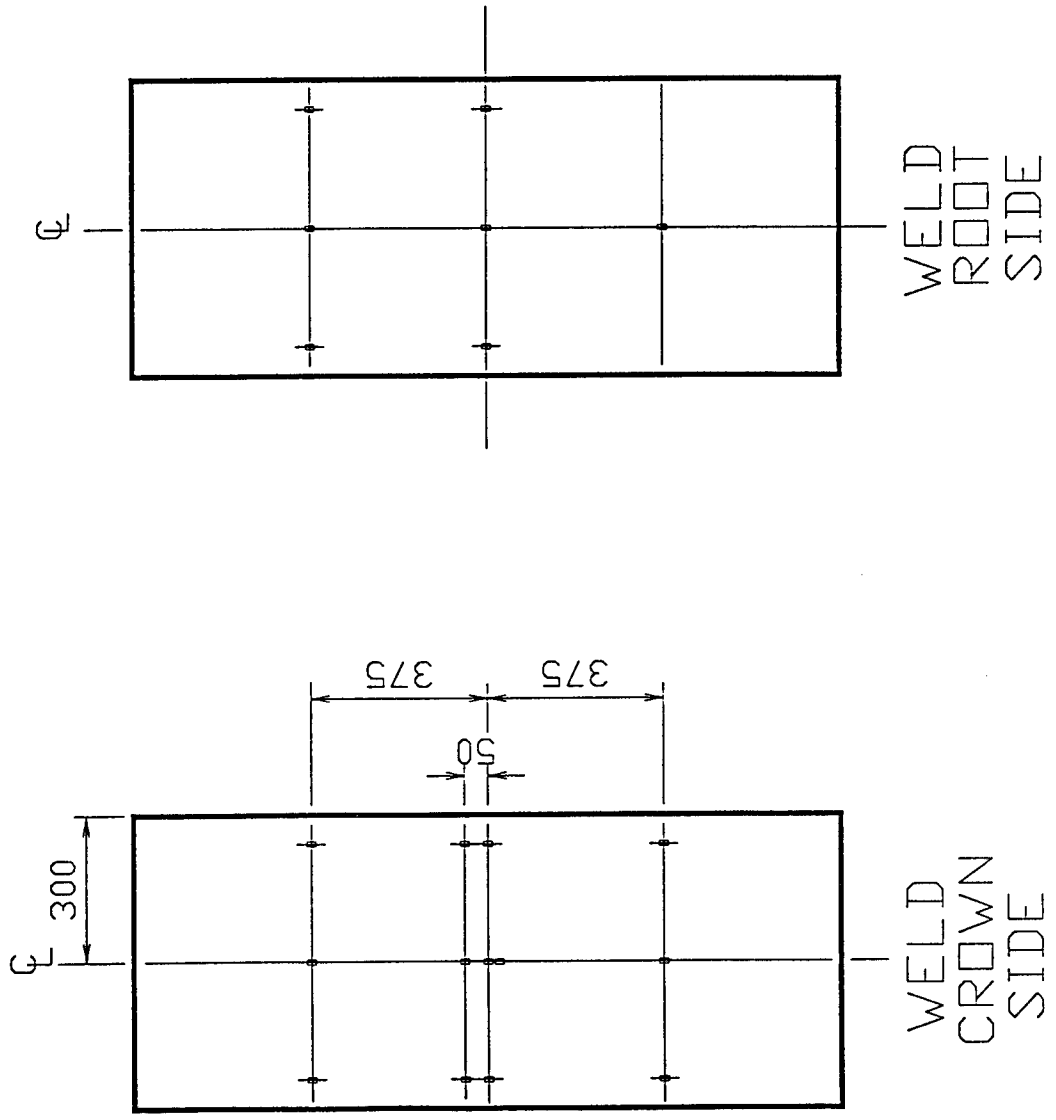

Figure 3-13 Instrumentation Plan for Tension Specimens.

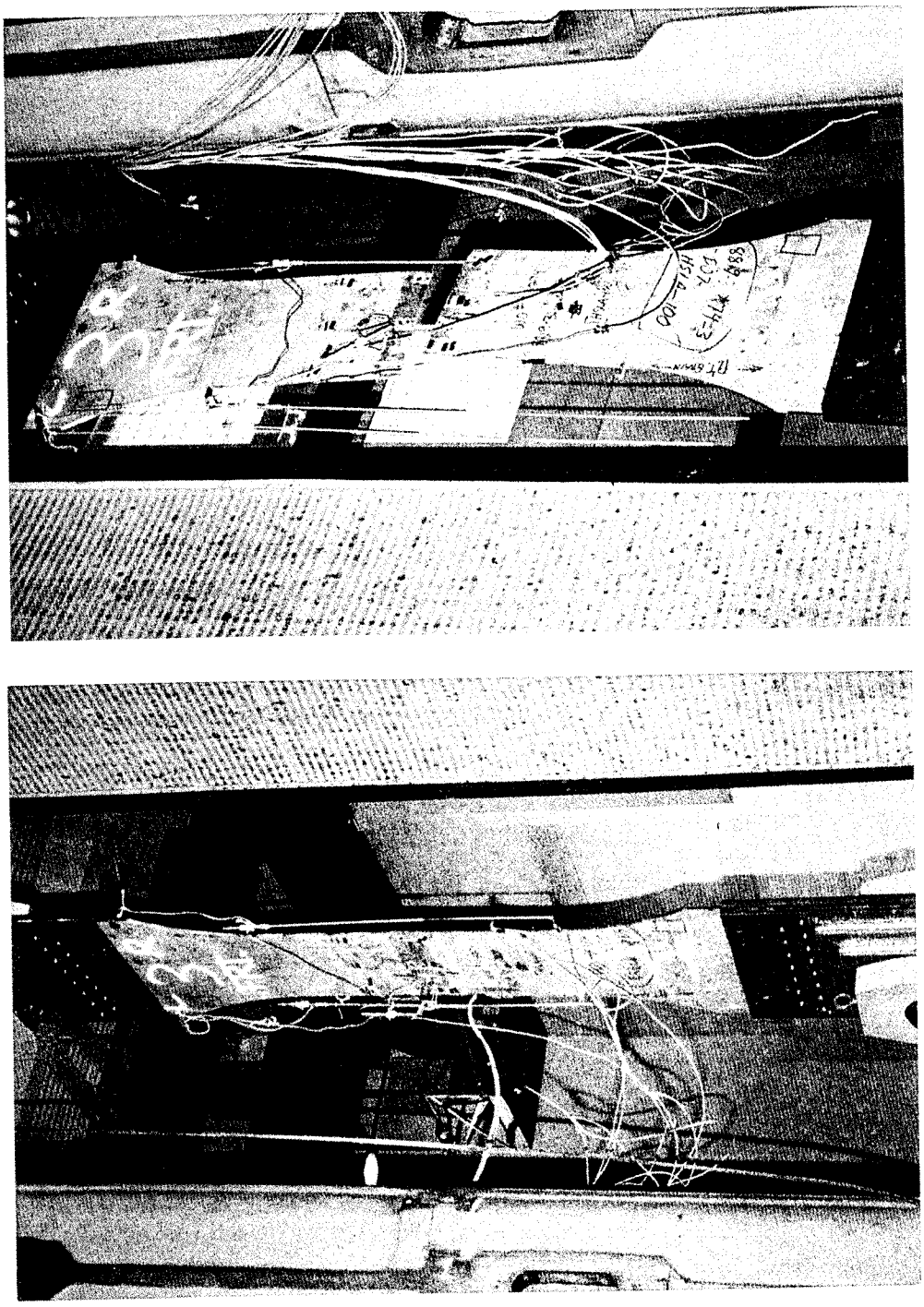

Figure 3-14 Photo of Tension Specimen Before and After Testing.

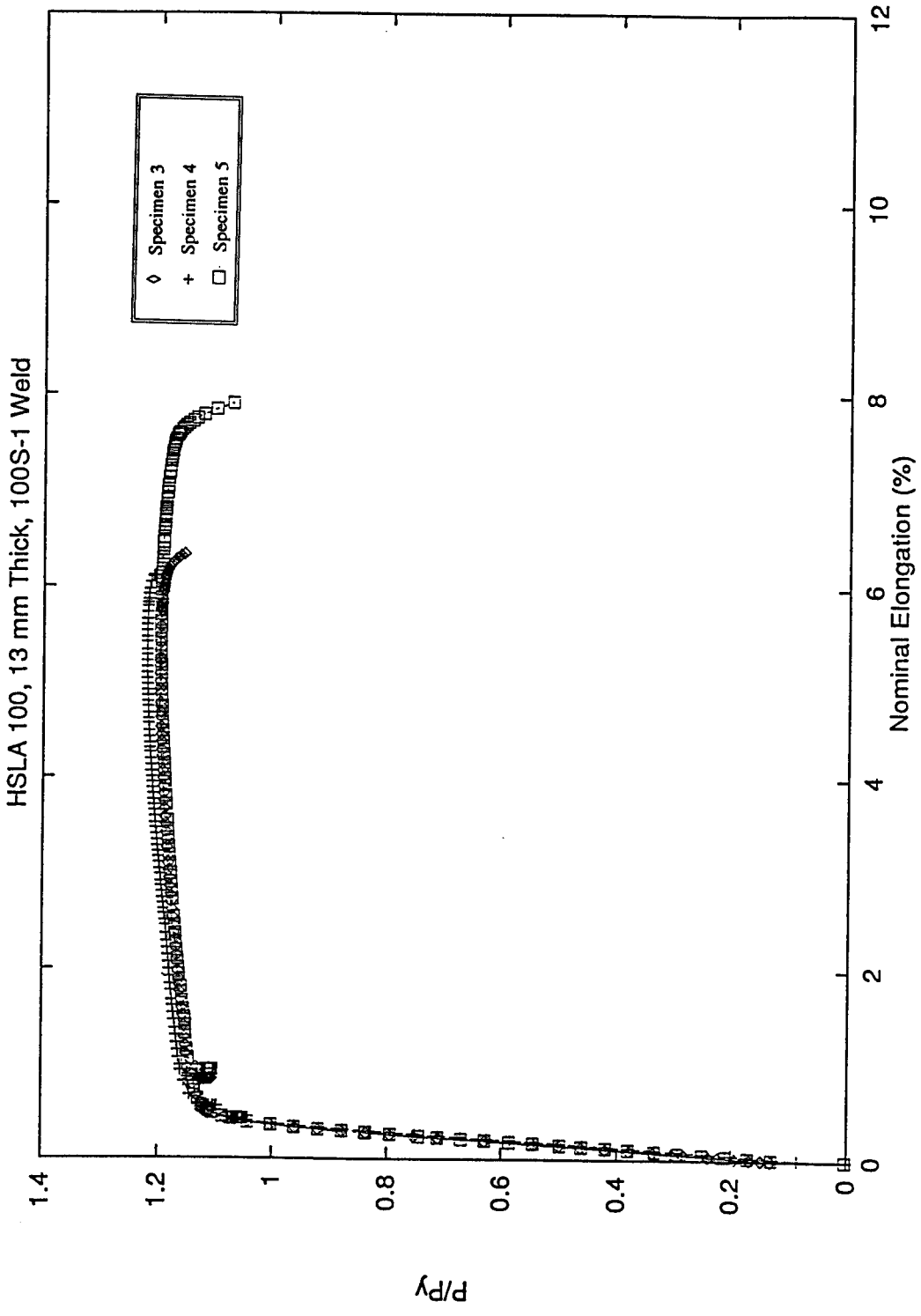

Figure 3-15 Normalized Load Displacement Curves for Three Replicate 100S-1 Weld Specimens.

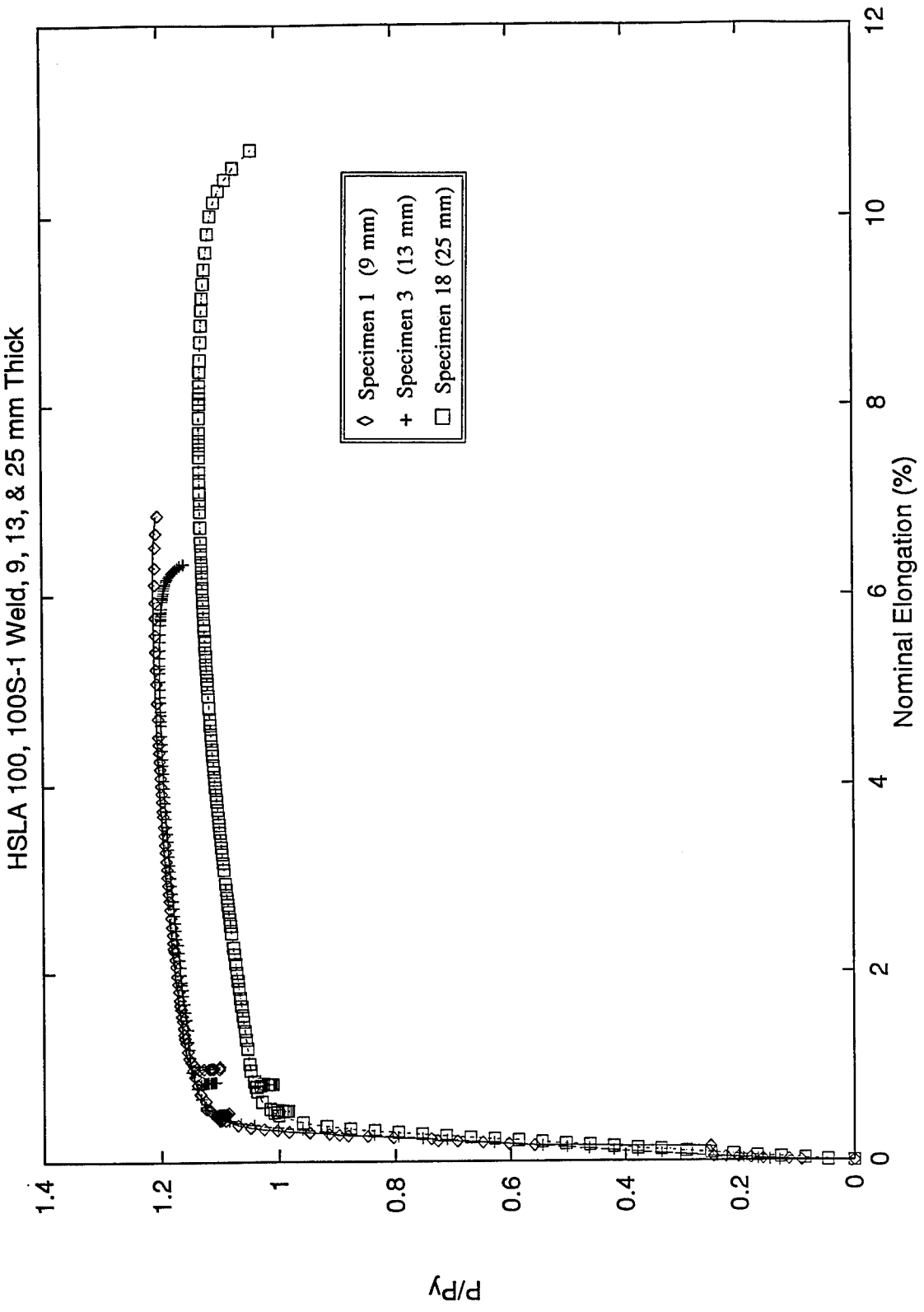

Figure 3-16 Normalized Load Displacement Curves for Three Different Thicknesses of the 100S-1 Weld Metal.

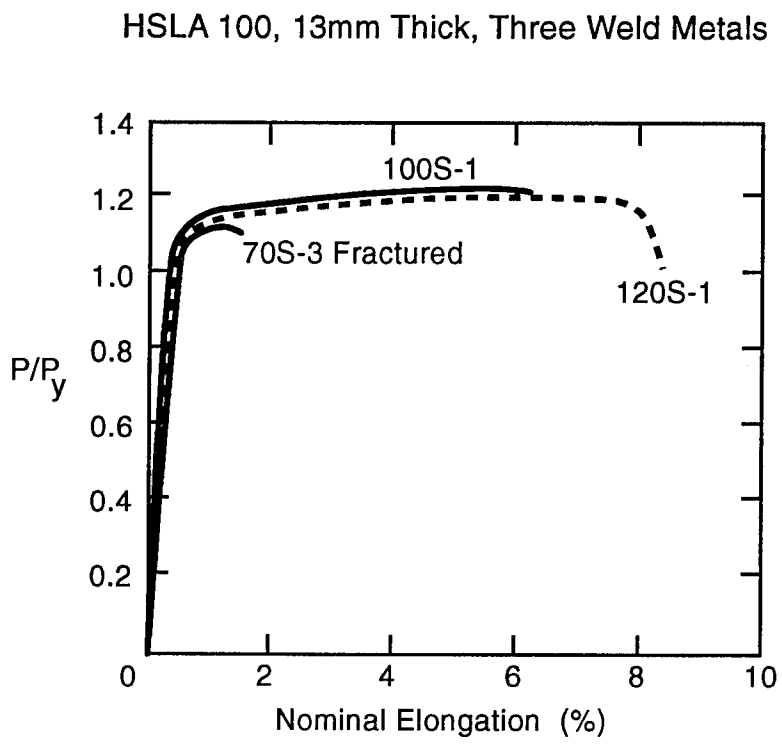

Figure 3-17 Normalized Load Displacement Curves for Three Different Weld Metal Specimens.

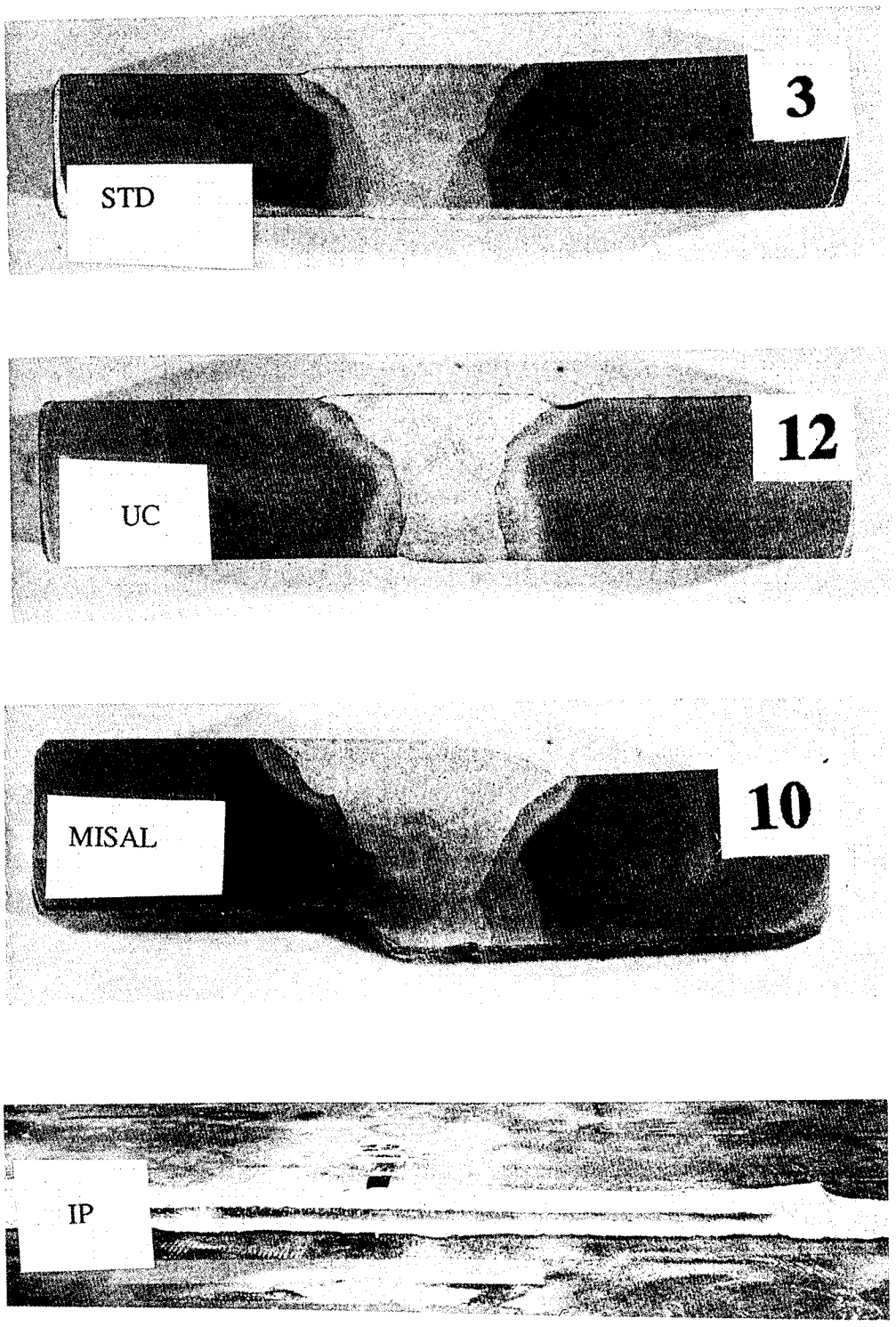

Figure 3-18 Photos Showing Intentional Defects with a Standard Specimen for Comparison.

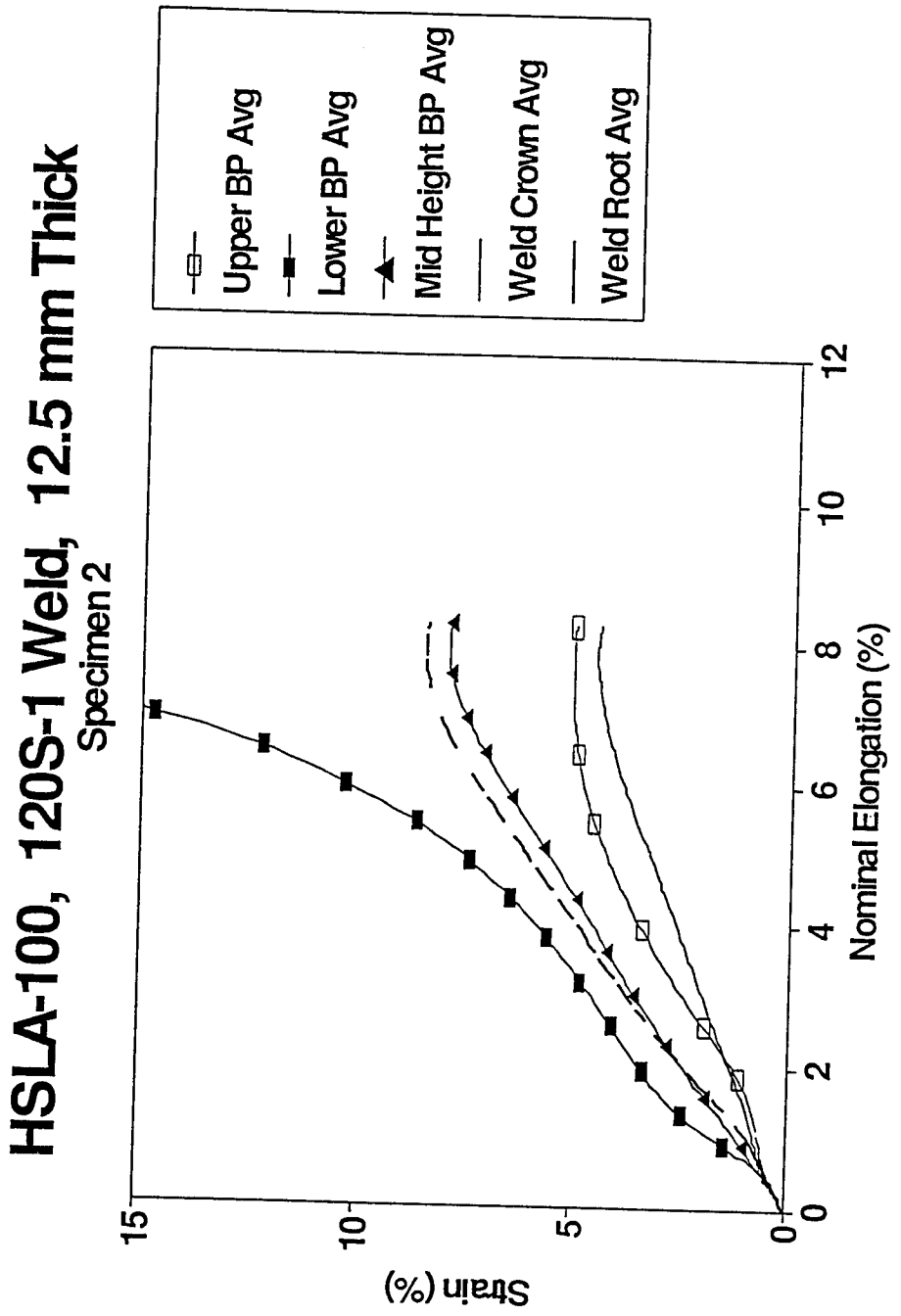

Figure 3-19 Strain Gage Results from 120S-1 Weld Specimen Showing Strain Localization in the Lower Base Plate.

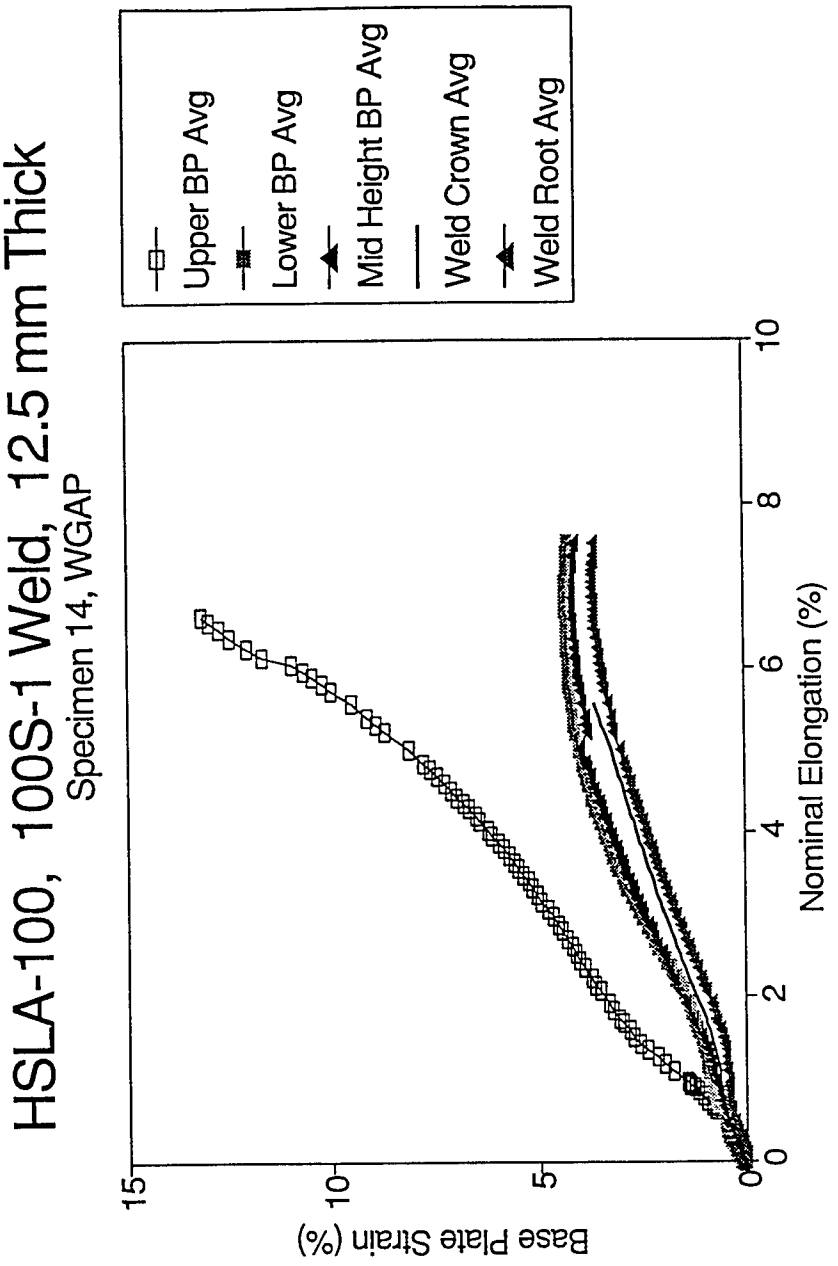

Figure 3-20 Strain Gage Results of the Normalmatched Widegap Specimen Showing Strain Localization in the Upper Base Plate.

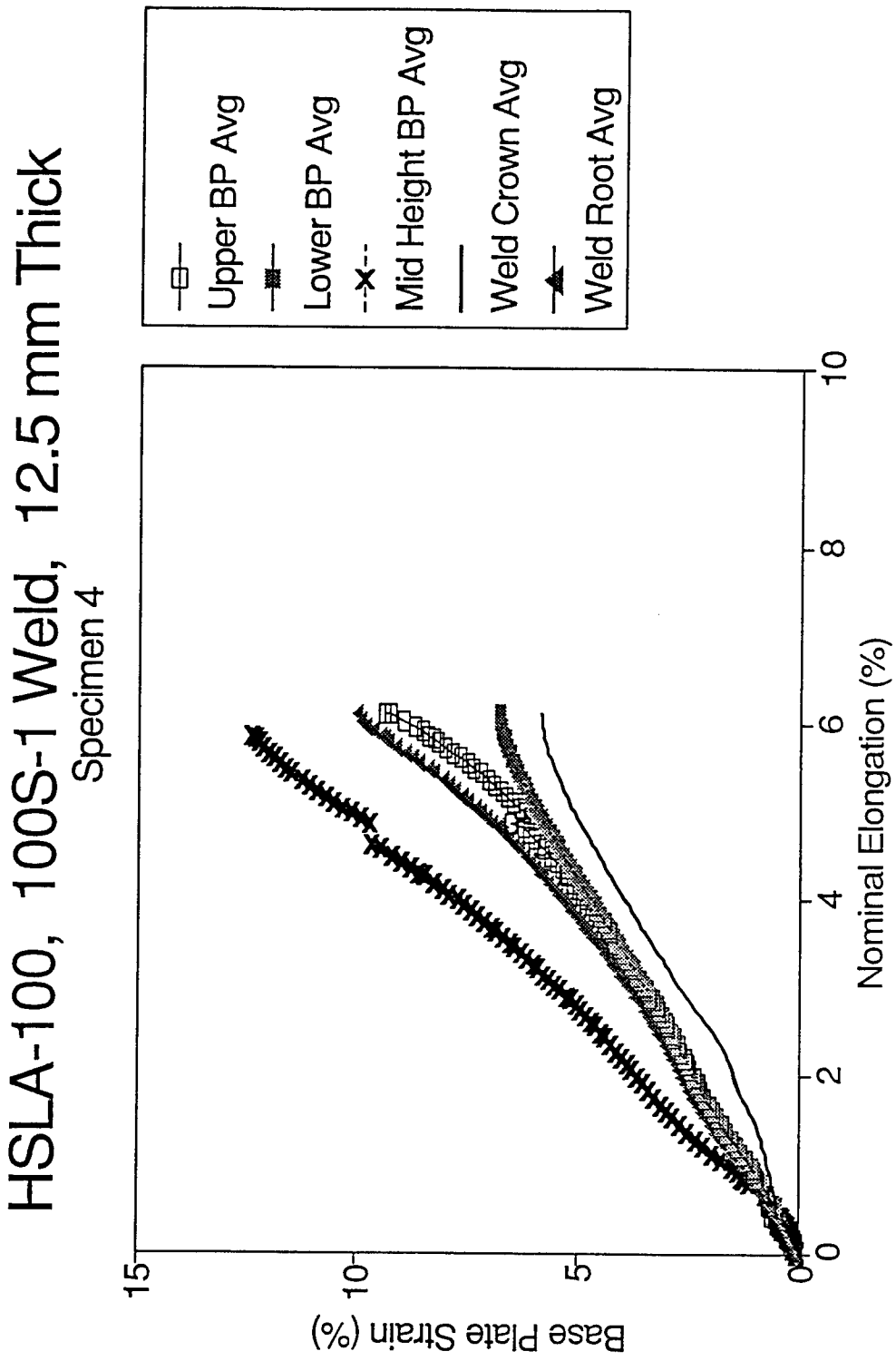

Figure 3-21 Strain Gage Data from the 100S-1 Weld Specimen Showing Localization in the Mid-Height Gages Near the HAZ.

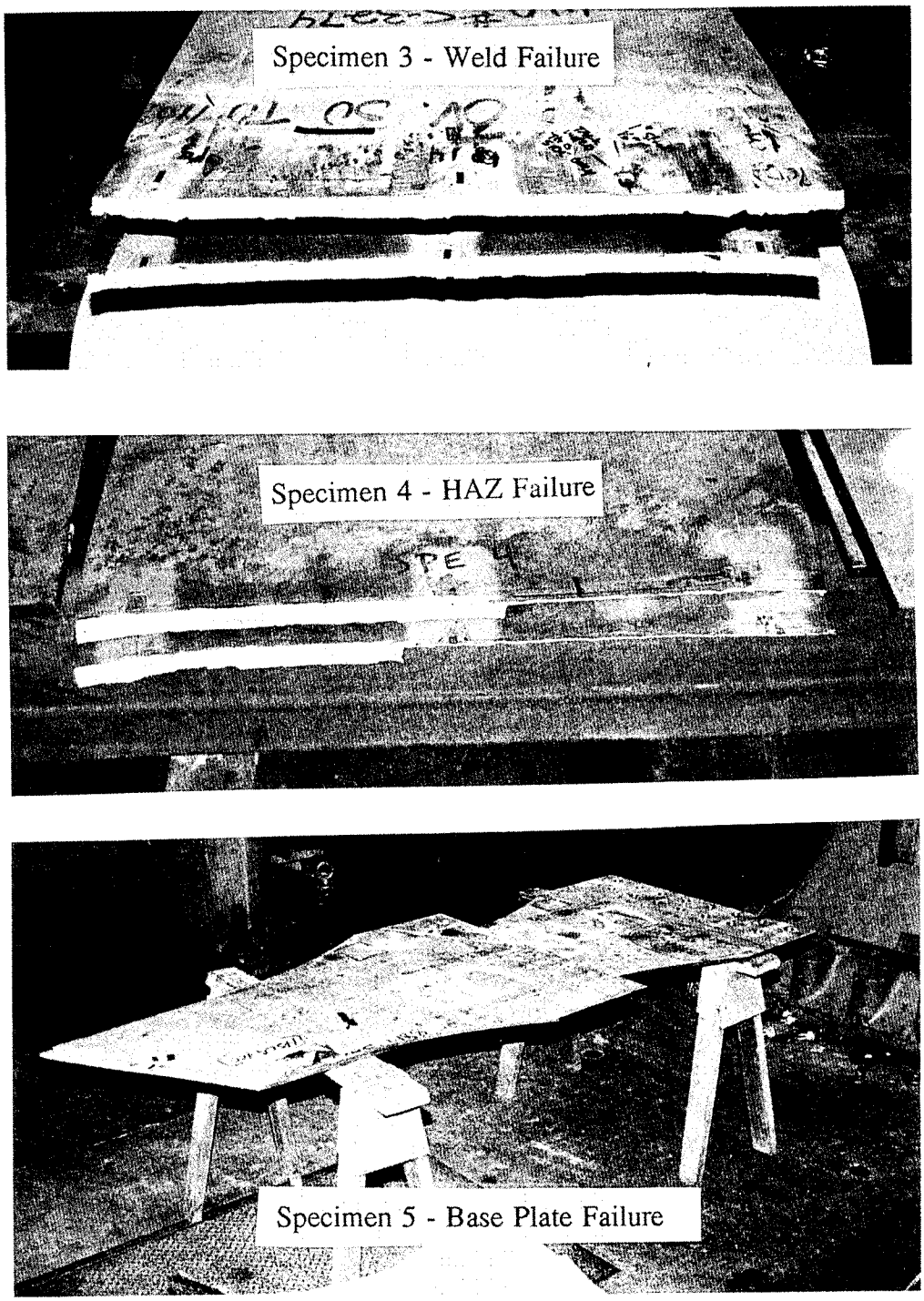

Figure 3-22 Photos Show the Various Fracture Locations for the Replicate 100S-1 Weld Specimens.

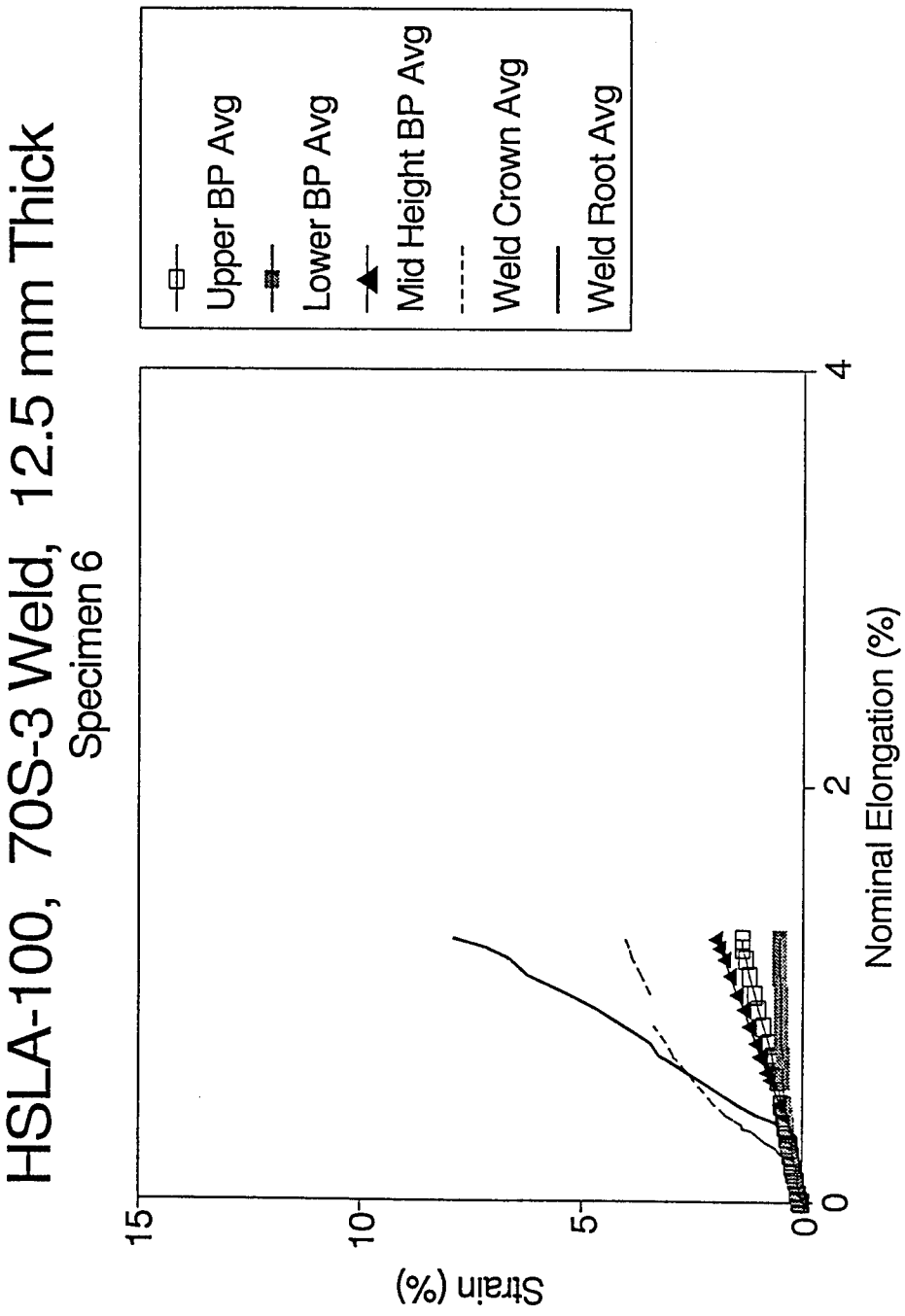

Figure 3-23 Strain Gage Results from the 70S-3 Weld Specimen Showing Strain Localization in the Severely Undermatched Weld.

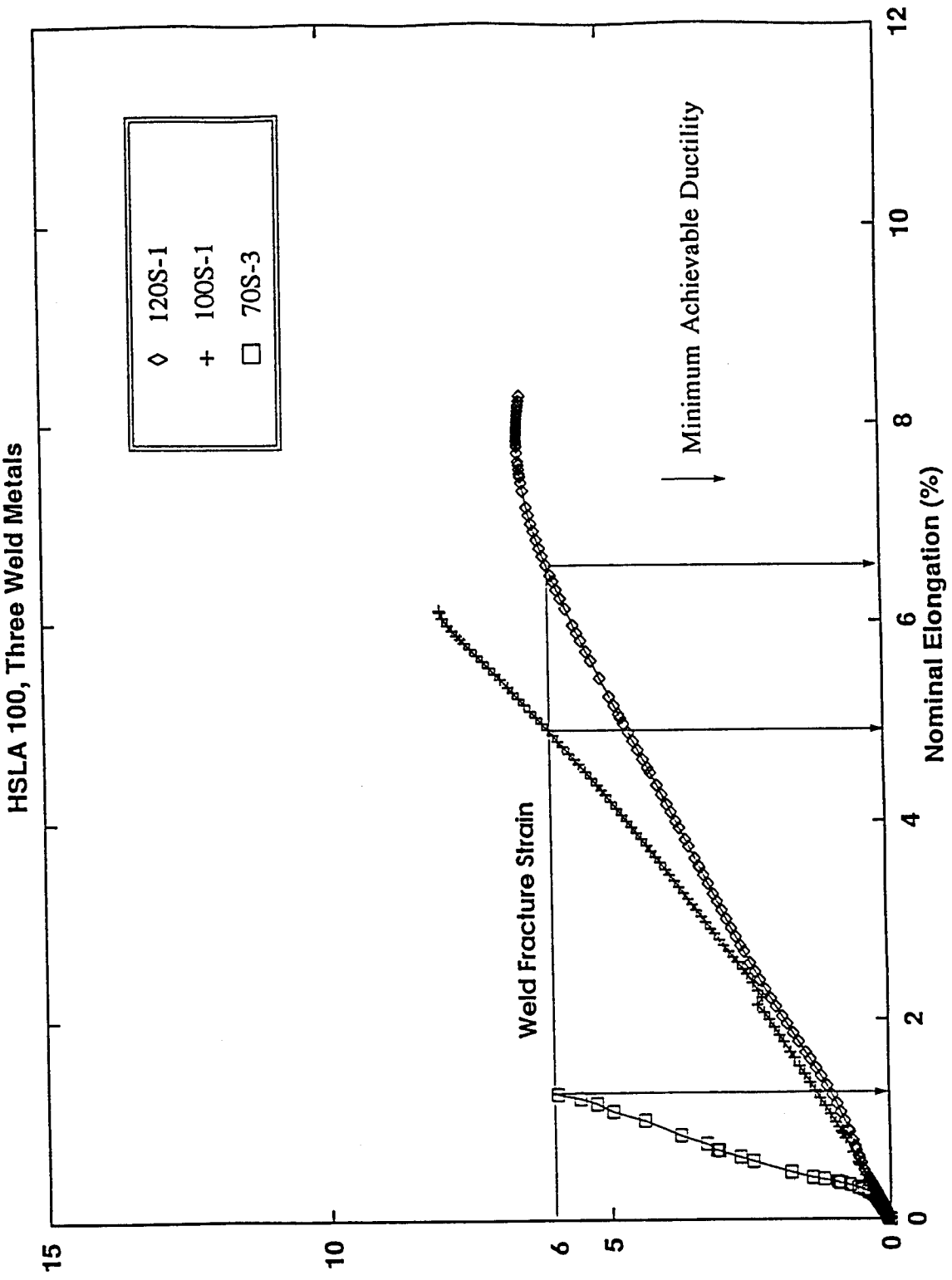

Figure 3-24 Strain Data for the Three Weld Metals and Developed Failure Criterion which Indicates Minimum Achievable Ductility.

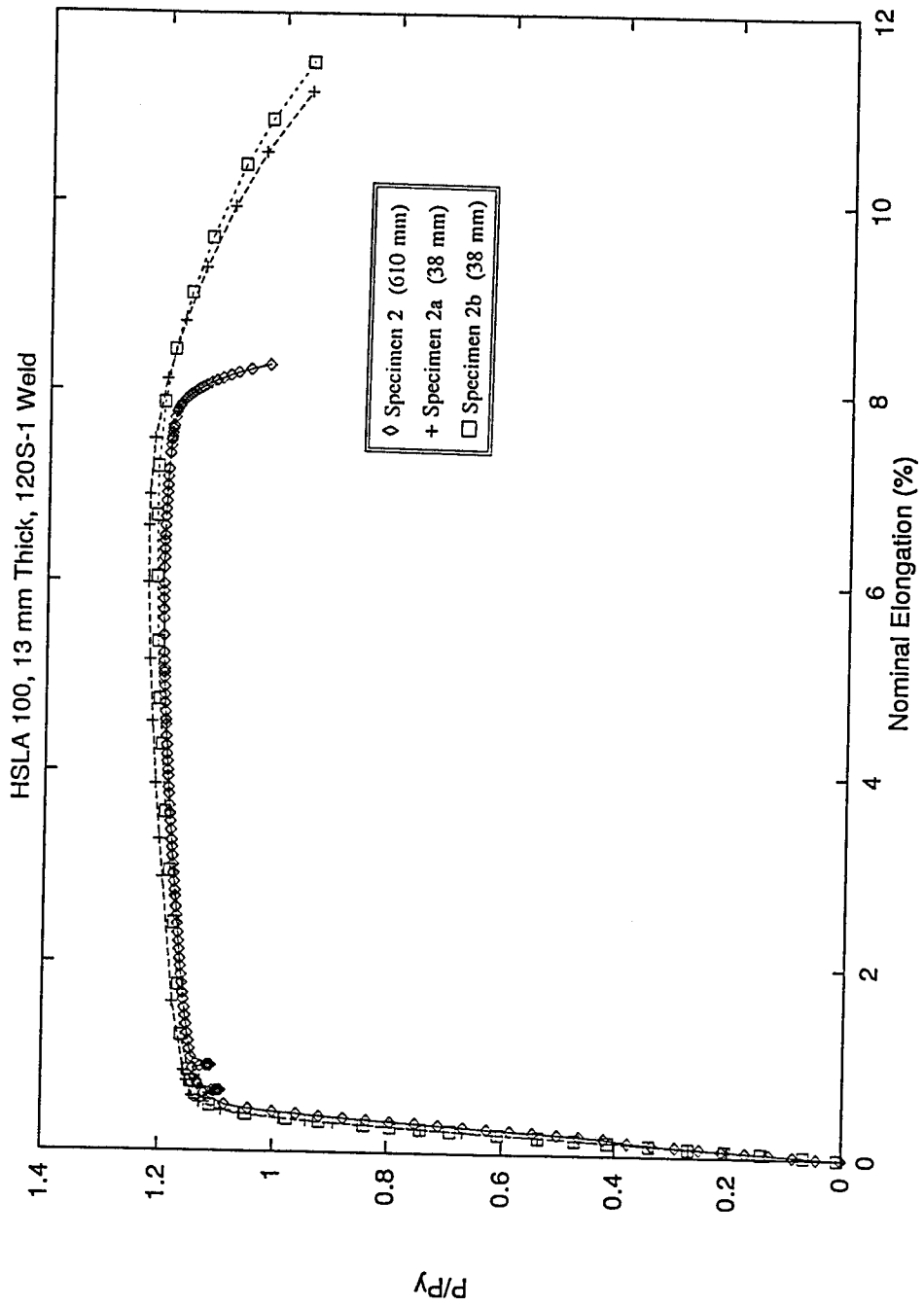

Figure 3-25 Comparison of Wide-Plate and Flat-Strap Load-Displacement Results for the 120S-1 Weld Metal Showing Similar Strength Behavior, but a Apparent Increase in Ductility for the Flat-Strap Specimens.

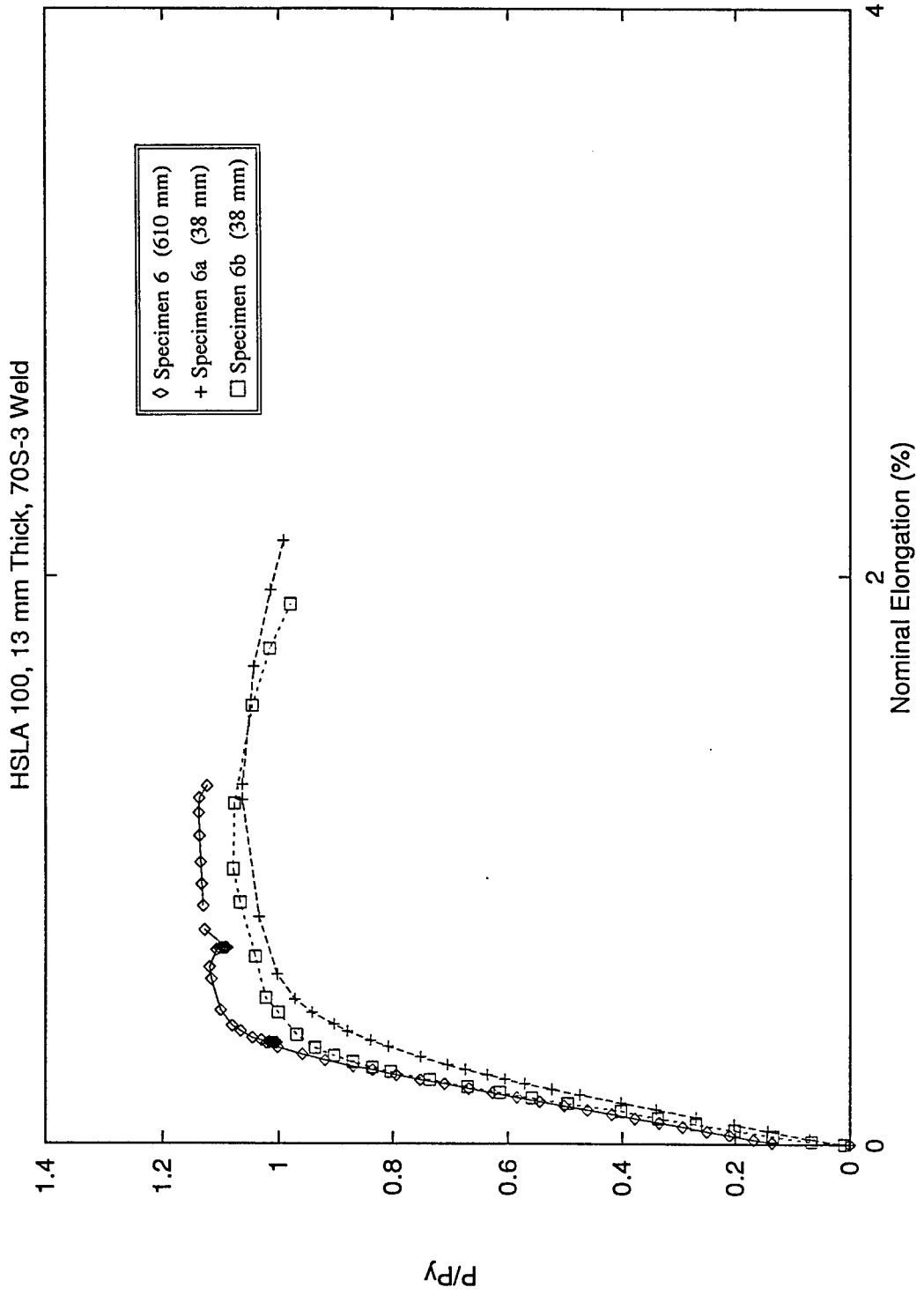

Figure 3-26 Comparison of Wide-Plate and Flat-Strap Load-Displacement Results for the 70S-3 Weld Metal Showing Both Lower Strength and Less Ductility for the Flat-Strap Specimens.

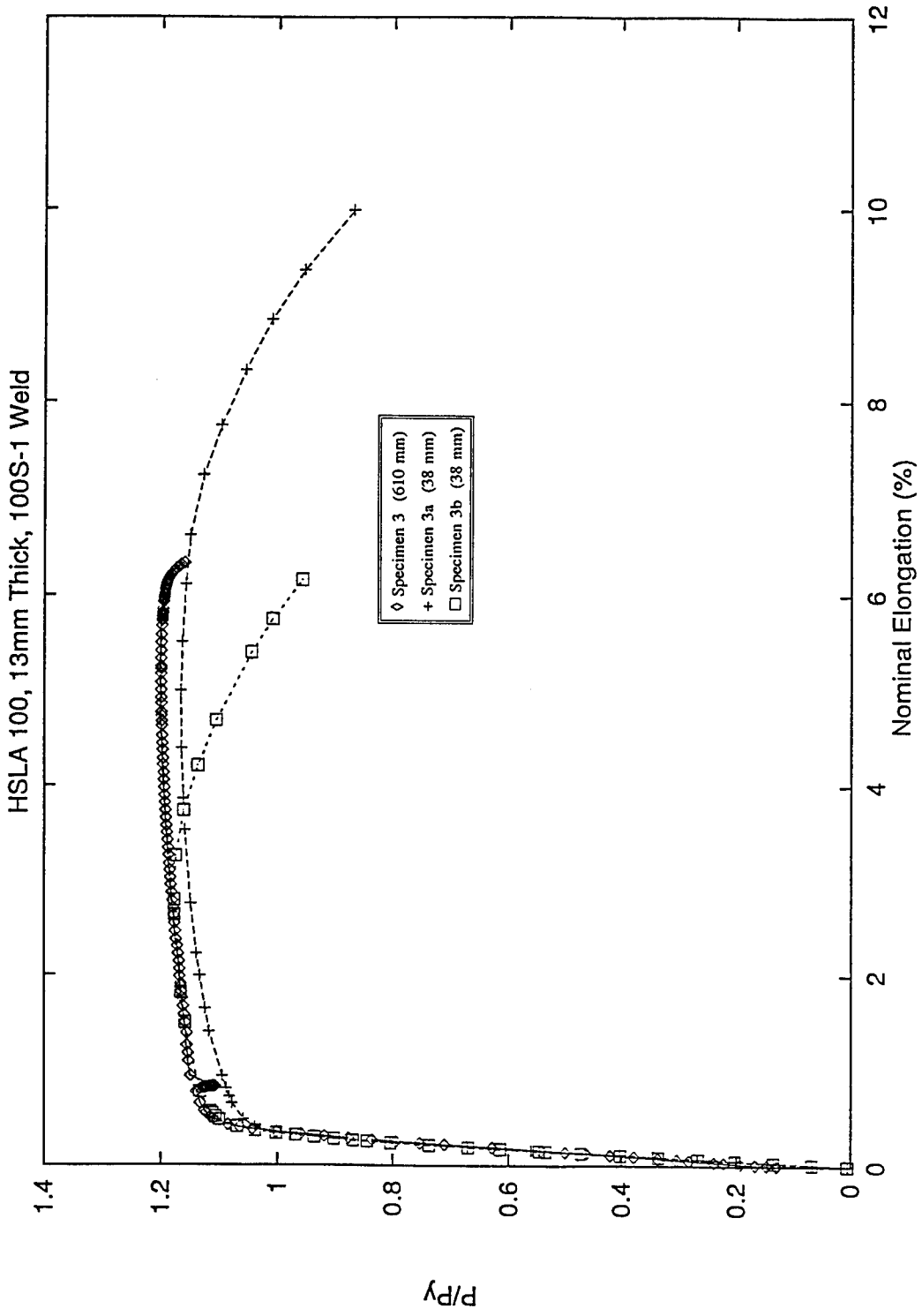

Figure 3-27 Comparison of Wide-Plate and Flat-Strap Load-Displacement Results for the 100S-1 Weld Metal Showing One Specimen with Lower Strength and One with Less Ductility for the Flat-Strap Specimens.

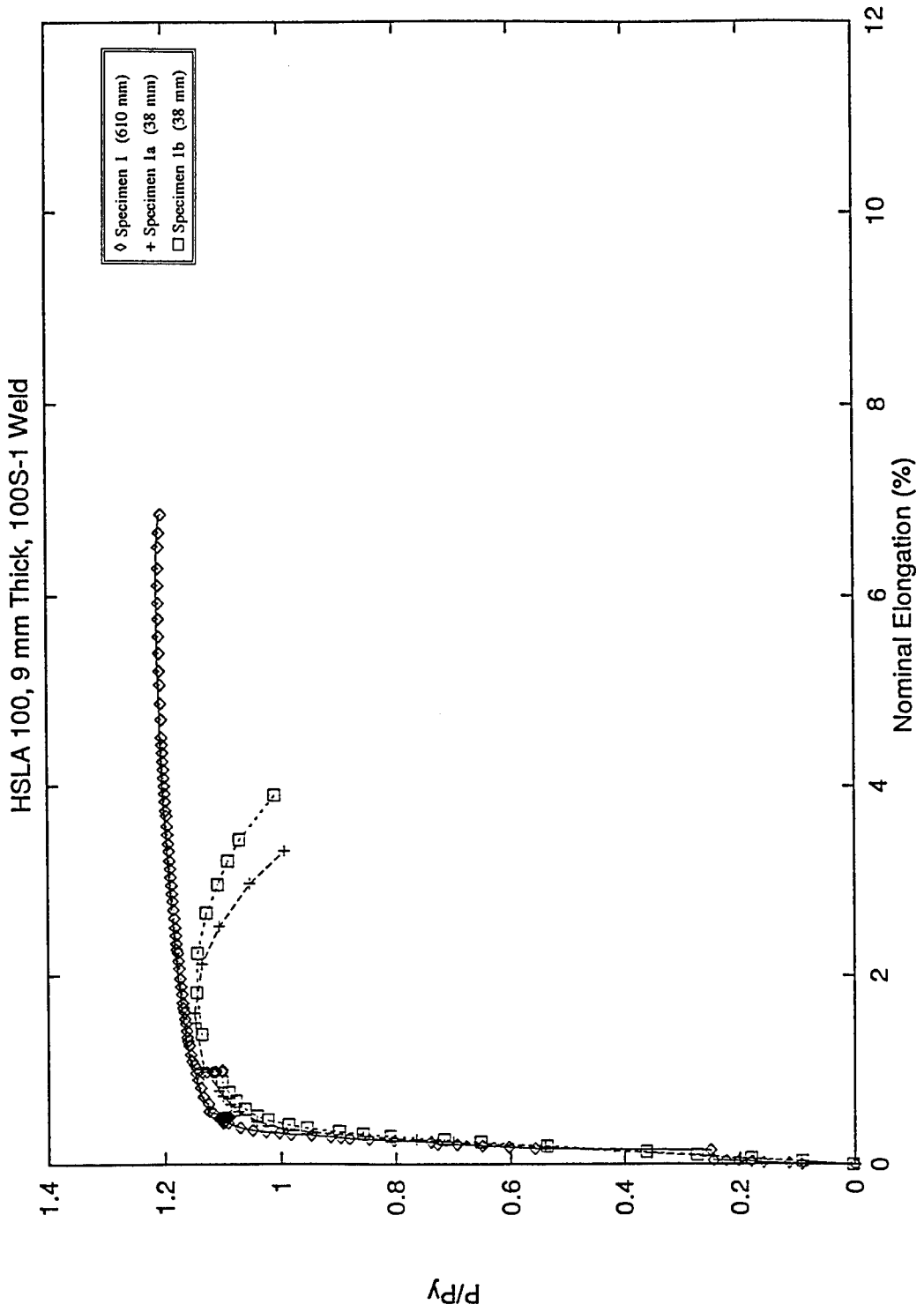

Figure 3-28 Comparison of Wide-Plate and Flat-Strap Load-Displacement Results for the 100S-1 Weld Metal, 9 mm Thickness, Showing Both Lower Strength and Less Ductility for the Flat-Strap Specimens.

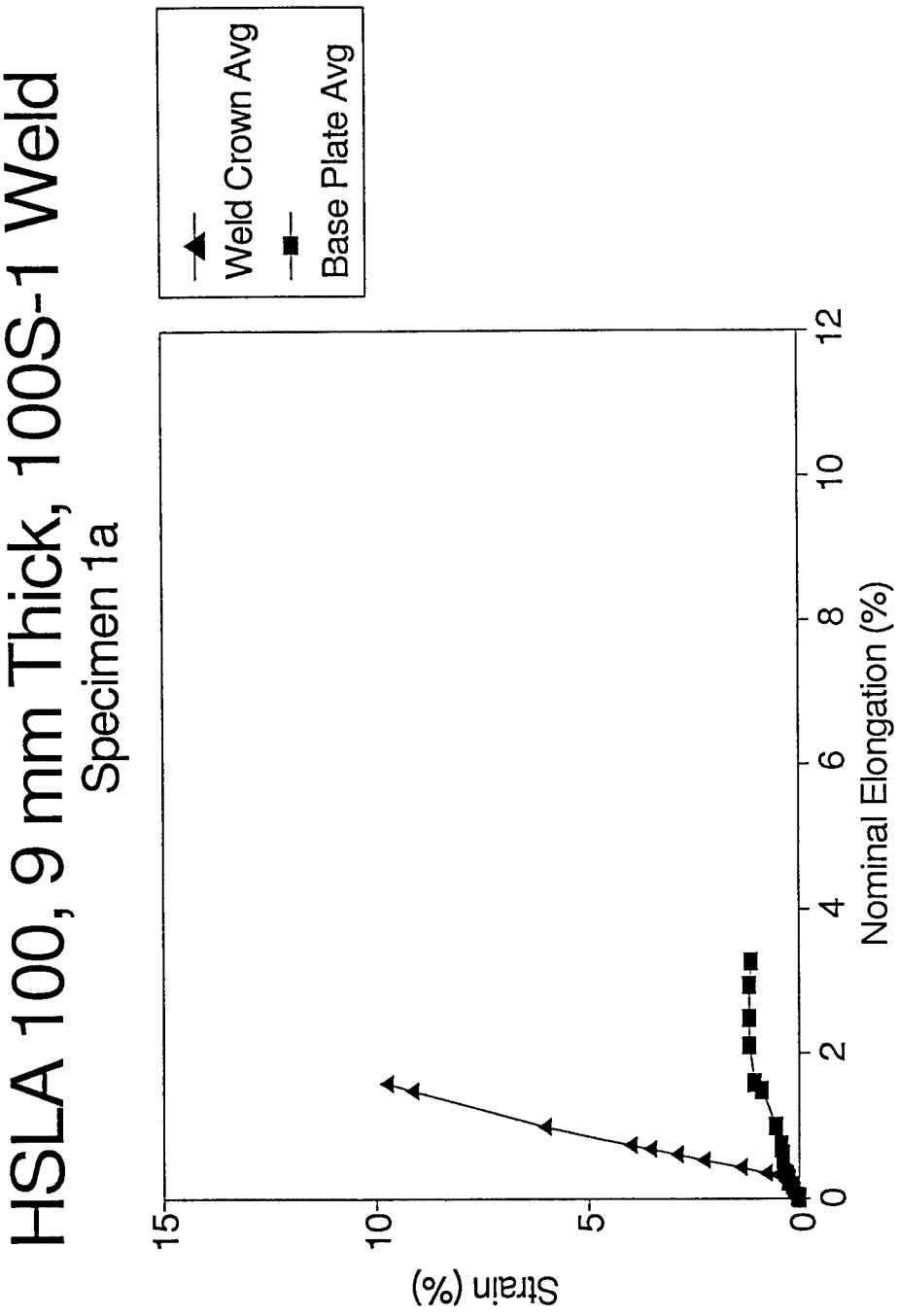

Figure 3-29 Strain Gage Data for the 100S-1 Weld, 9 mm Thickness, Flat-Strap Specimen Showing Strain Localization in the Weld Not Seen in the Wide-Plate Test.

4.0 FINITE-ELEMENT ANALYSIS

The experiments described in the previous chapter revealed the global load-deformation behavior of specific test specimens as well as the strain at selected locations on the surface of these specimens. Finite-element analyses were conducted for several reasons, i.e.: 1) to simulate the experiments and obtain a more complete estimate of the strain distribution, including internal strains, as well as the resulting stresses; 2) to establish guidelines for proper modelling including element type, mesh refinement, selection of boundary conditions, and selection of material plasticity models; and, 3) to analyze hypothetical joint geometries and material combinations in a systematic way to examine the effect of variation of selected parameters. Once the accuracy of the finite-element analysis is established by comparison to the experiments, it becomes a powerful and efficient tool for exploring many more cases than could have been tested in this program. As the guidelines for proper modelling are turned over to practicing engineers, they will have a tool which enables them to examine a variety of joints and materials that were not specifically addressed in this project. The simulation of the experiments is discussed first to establish the validity of the finite-element analysis. The results of a parametric studies are then presented.

4.1 Numerical Simulation of Experiments

The behavior of the welds is dependent on the development of constraint which is obviously a three-dimensional phenomenon. Therefore, the finite-element models were built using three dimensional solid elements. However, two-dimensional analyses are much more cost effective. A series of two dimensional cross-sectional analyses were performed and contrasted to the experiments and the three-dimensional analyses in order to see which aspects of the undermatched weld deformation behavior could be adequately represented in the two-dimensional analyses.

4.1.1 Three-Dimensional Analysis

Most of the finite-element simulations of the experiments were performed using three-dimensional models. The primary model, shown in Figure 4-1, consisted of 540, 20-node, quadratic, reduced-integration, isoparametric-formulation solid brick elements. Also, a finer mesh, shown in Figure 4-2, of 2850 similar elements was analyzed to assess the effect of mesh refinement on the results. These models used two planes of symmetry as shown in the figures. The entire gage length was not modelled since at some distance from the weld the base plate strains are predicted to be relatively uniform. The model included a length of 20 thicknesses (260 mm). The results indicate the strains were relatively uniform at this distance from the weld. The actual geometry of the weld cross-section was used and independent properties were prescribed for the weld and HAZ.

The steel was assumed to be isotropic and elastoplastic. The Von-Mises yield criterion was used with isotropic hardening. The constitutive properties for the base plate and weld materials was input as piecewise-linear, "effective" stress-strain curves obtained from uniaxial tension tests. The HAZ properties were estimated from hardness traverses across the weld and regions of the HAZ. The HAZ was assumed to consist of three distinct regions, a coarse-grained region which generally has higher strength than the original base metal, a grain-refined region which often experiences softening or a lower strength than the base metal, and an intercritical region which is typically similar to the base metal. These three regions were assigned constitutive properties that were proportional to the base metal stress-strain curve by the relative hardness of the specific HAZ region.

All of the tests were conducted at quasi-static strain rates so there was no need to account for viscoplasticity or strain-rate effects. It is anticipated that strain rate would increase the yield strength and ultimate strength of all the materials approximately the same proportion, e.g. high strain rates associated with impact might increase the strength by about 30 percent. Because all the strength levels would be increased proportionally, and it is the relative strength level (i.e. percentage of undermatching) that is the key variable that determines performance, it is not expected that strain rate would alter the conclusions of these tests on the relative performance of undermatched welds.

The analyses used small-strain theory, which is sufficient to simulate the load-deformation curves up to the point of ultimate strength. In order to simulate the localization and necking which occurs after ultimate strength and the descending branch of the load-deformation curve, large-deformation analyses would have to be used. Based on a review of the literature and prior experience, it was noted that large-deformation analysis to predict necking is extremely resource intensive and in the end, not very accurate. This is believed to be due to the somewhat random occurrence of thickness variations and low-strength regions in the plate, which are important in initiation of necking and failure. For example, as previously noted in the discussion of the experiments, in those experiments where there was good ductility, several necks often occurred in seemingly random locations, and failure occurred eventually in one of these necks. Because of these complexities, it was not attempted to predict necking and failure. The meshes were loaded in displacement control (as shown) and stopped at five percent nominal elongation. Failure could be inferred from the results by monitoring the average strains in the base metal and the weld metal and applying the "critical strain" failure criterion as explained in Section 3.4.3.2.

The first runs were made with the coarse-grid three-dimensional mesh using constitutive properties determined from mechanical testing for a 100S-1 weld specimen (Specimen 3). Initially, the results did not compare favorably to the experiment. It was noted that in the model the weld was considered flush with the base plate surfaces, while in reality there was always a small amount of reinforcement left on the specimens after grinding. The reinforcement could not be completely removed due to angular distortion or "winging" of the specimens. When the slight reinforcement was included in the model, very good

results were obtained. The load-displacement curves from the finite-element analysis and the experiment are compared in Figure 4-3. The computed load-displacement behavior is in very good agreement with the experimental data. Figure 4-4 compares computed weld strain data from the model and the experimental data. The experimental data were the average of three strain gages on both the weld crown and weld root. The computed weld strain is obtained from the average of the integration points in a typical element within the weld. This element was at mid-thickness at the quarter point of the specimen (mid-width between the free edge and plane of symmetry). All subsequent discussion of computed strains refer to this element. The magnitudes of the computed strain show good agreement with the experimental data. The computed results also show the change in the rate of strain accumulation in the weld as the constraint takes effect.

The same mesh was used with the constitutive properties for other specimens and the results were then compared to other experimental data. For example, Figure 4-5 shows the results from the severely undermatched (70S-3 weld) case. Not only does the model adequately describe the magnitudes of the strain, the point of initial strain localization is quite clear as well. Finite-element analyses of other thicknesses and weld strengths were similarly successful.

In order to verify adequate refinement, the fine mesh was run with identical constitutive properties. Comparison of the load-displacement behavior of the two meshes (Figure 4-6) indicates good agreement between the two models. Figures 4-7 and 4-8 compare contours of the longitudinal strain for the coarse and fine meshes, respectively. The comparison shows the same general patterns and magnitudes of axial strain, though the resolution and level of detail provided by the fine mesh are slightly greater. For the purposes of these analyses, it was judged that the coarse mesh is adequately refined. Since the solution time for the coarse mesh was five percent of the solution time for the fine mesh, the coarse mesh was used in following analyses for computational efficiency.

4.1.1 Two Dimensional Analyses

Previous work [6] analyzing E6010 undermatched welds in wide-plate tests found that plane stress and plane strain analysis provided narrow bounds about the measured average weld strains. However, these cross-sectional analyses did not produce realistic results for these experiments with HSLA-100 and 100S-1 weld metal.

The reason these cross-sectional analyses were unsuccessful is believed to be the high yield-to-tensile (Y/T) ratio for the 100S-1 weld metal. The Y/T for the 100S-1 weld metal was in the range of 0.90 to 0.97 compared to the 0.80 to 0.85 for the E6010 weld metal used in the previous research. Since there is very little strain hardening in the 100S-1 weld metal, plastic strain accumulates very rapidly in these analyses. In contrast, the E60 welds had sufficient strain hardening to force some yielding into the base metal. This was seen in both the plane-stress analysis where very little constraint develops, and in the plane-strain analysis where the constraint is applied to the base metal as well as the

weld metal and artificially raises the axial stress level. It was concluded that bounding the solutions with plane-stress and plane-strain analyses is not possible for weld metals with a high Y/T (>0.85) ratio.

Another two-dimensional approach is the use of generalized plane strain analysis. In generalized plane-strain there can be an out-of-strain component. In effect, the planes on the edges of the plate may displace or rotate but remain plane. Generalized plane strain is intermediate between plane-strain and plane-stress analyses, because the rotational capacity of the bounding planes allows some reduction in width of the weld zone relative to the base plate.

Generalized plane-strain analysis was compared to the coarse and fine three-dimensional analyses for the case of the 100S-1 weld metal in a 13 mm thick plate. The weld strains for typical elements from the three-dimensional models are compared to a mid-height element for the two-dimensional model (shown in Figure 4-9) in Figure 4-10. Only minor differences in strain are observed, but these are not significant in view of the total weld strains. Therefore, for 100S-1 weld metal (about nine percent undermatch), the generalized plane strain model adequately represents the experimental behavior. The use of the two-dimensional analysis is beneficial in terms of computational efficiency. The solution time for the two-dimensional analysis was only 0.2 percent of the solution time for the fine analysis and four percent of the solution time for the coarse three-dimensional analysis.

However, the applicability of the two-dimensional generalized plane strain analysis has limits. For example, the strains predicted by the generalized plane-strain analysis for the case with 70S-3 weld metal (28 percent undermatch) in a 13 mm thick plate localized instantly and were significantly higher than both the three-dimensional analysis and the experimental data. It seems that at moderate levels of undermatch, where strain localization is not extreme, generalized plane-strain analysis adequately describes the behavior of the undermatched welds. Severely undermatched welds, however, are more sensitive to constraint, and therefore can not be adequately represented with two-dimensional analysis procedures.

In cases where the generalized plane-strain analyses provided a good approximation of the global load and elongation, a good approximation of the strain in the core region of the wide-plate specimens was also provided. However, the generalized plane-strain analyses do not capture the changes that occur near the free edges. For example, Figures 4-7 and 4-8 indicate that there is a region near the edge of the plate where three-dimensional effects are significant. This is expected near the edge since the constraining stress in the width (z) direction must go to zero at the free surface since no tractions are applied. Both finite-element results show that the loss of constraint at the free edge causes axial strains at least twice as high at the free edge compared to the axial strains of the typical element (i.e. an element at mid-width). The width of these "plane-stress" zones near the edges is about 50 mm, i.e. about 4 times the thickness or about 16 percent

of the width of the wide-plate specimen. The width of this zone can be used to estimate the width of smaller specimens necessary to develop true constraint at least near the center of the specimen. To develop constraint over one third the width, as in the wide plate specimens, a specimen would have to be at least 150 mm wide. Clearly, the small flat-strap specimens (38 mm wide) are inadequate, which was shown by the differences in the experimental results for these specimens compared to the wide-plate tests.

The two-dimensional generalized plane strain model yields results comparable to the three-dimensional meshes at the symmetry axis, as shown in Figure 4-11. Clearly, the results of the two-dimensional mesh are not representative of the behavior near the free edge. This zone of plane stress near the edge can not be modelled with plane analysis. However, for structural joints which are sufficiently wide (> 150 mm) (and only moderately undermatched), the generalized plane-strain analyses should give adequate results.

In the parametric studies described in the following section, two-dimensional generalized plane-strain analysis was used where the level of undermatch was not severe (>20 percent) and the variation of strains through the width was not expected to have an effect. Three-dimensional analysis was used for cases anticipated to have significant three-dimensional effects, e.g. severe undermatch which the generalized plane-strain model would be unable to describe.

4.1.3 Analyses of Specimens with Defects

Finite-element simulations of the experiments with intentional undercut and misalignment defects were also performed using generalized plane-strain two-dimensional models. Loading was displacement controlled and stopped at five percent nominal elongation.

Figure 4-12 shows a weld macrosection for the misaligned joint and the strain contours resulting from the analysis of the undermatched misaligned weld joint when the base plate achieves a nominal elongation of 5 percent.. Note that the slip plane develops across the weld in the misaligned joint and that a maximum strain level of just over 20 percent strain is predicted in that slip plane The load deformation curves from the two misaligned specimens as well as the overmatched specimen without misalignment are shown in Figure 4-13. As predicted by the finite-element analyses, the misaligned joints attained full base plate strength with only minor decreases in ductility relative to the specimens which were not intentionally misaligned. The elongation was reduced to 5.5 percent on average versus 7.7 percent on average for the joints without intentional misalignment. Considering the yield strain is about 0.36 percent, at 5.5 percent overall elongation, the plates achieved a ductility factor greater than 15. Therefore it can be concluded that misalignment up to 3 mm (25 percent of the thickness) can be tolerated with no appreciable effect on strength and ductility.

Figure 4-14 shows a weld macrosections for the joint with the simulated undercut and the strain contours resulting from a two-dimensional analysis of the undermatched joint with simulated undercut when the base plate achieves a nominal elongation of 5 percent.. Note that the strain is just over 20 percent in a small area at the tip of the notch. Figure 4-15 compares the load deformation curves for the standard undermatched weld joint to the undermatched weld joint with the simulated undercut. The undercut does not cause an appreciable decrease in the strength or ductility of the weld. Therefore, the specimens with the simulated undercut developed the yield strength of the base plate material based on the gross cross-sectional area, despite the notch equal to 12 percent of the thickness in depth. Both the overmatched and undermatched specimens fractured at the notch, though the nominal elongation of the 120S-1 specimen was significantly reduced while the ductility of the 100S-1 specimen was not affected. The undermatched weld was apparently beneficial in this case, though the result may be random.

4.2 Parametric Studies

A number of parametric variations were analyzed to examine variables outside the test matrix that were of interest. These analyses were carried out with the two-dimensional generalized plane-strain model as most of the studies examined geometric variations at moderate levels of undermatch (typically 10 percent).

The effect of bevel angle was examined at both 10 and 18 percent undermatch. The actual bevel in the specimens (60° nominal included angle) was compared with an equivalent weld metal volume with no bevel, i.e. straight sided weld preparation. As shown in Table 4-1, no significant difference in typical element strains was observed for either level of undermatch. Local variations in strain contours were present, but it was concluded that the bevel angle had no effect on the overall behavior.

Another study was conducted on the effect of root opening. Five different root openings were compared at 10 percent undermatch. As shown in Table 4-2, small, but insignificant, increases in strain were developed as the root opening increases. These findings are in agreement with previous work [7] in the analysis of pipeline girth welds. The pipeline research found that neither root opening or bevel angle had any significant effect on the average weld strains.

In addition to the geometric variations, the effect of alternate HAZ material properties were examined. The HAZ properties were estimated from hardness traverses across the weld and regions of the HAZ. The regions of the HAZ were assigned constitutive properties that were proportional to the base metal stress-strain curve by the relative hardness of the specific HAZ region. These analyses predicted local variation in strain behavior in the HAZ, but the weld strains were relatively unaffected, as shown in Table 4-3.

The efforts to characterize the undermatched weld in two dimensions clearly indicated the sensitivity of undermatched welds to yield-to-tensile (Y/T) ratio. Therefore, a parametric study of undermatch and Y/T ratio was conducted. Over 35 three-dimensional finite-element analyses were run, varying the percentage undermatch from 2 to 28 percent, and Y/T ratios from 0.9 to 0.7. Three-dimensional analyses were used due to the limitations of the two-dimensional mesh as the level of undermatch becomes large.

The results of the study are shown in Figure 4-16. The results are expressed as a weld strain concentration factor; the computed weld strain of the typical element at five percent nominal elongation normalized by the nominal elongation. The study confirms that as the level of undermatch approaches zero, the strain concentration approaches 1.0 for all Y/T ratios, which is expected. It is also clear that for low Y/T ratios, the level of undermatch can be increased significantly, without severe strain concentration in the weld. Typical Y/T ratios for realistic weld metals (Y/T of 0.85 to 0.90) are of more practical interest.

The fracture criterion which was derived from the experimental data in Section 3.4.3.2 can be stated as follows. The weldment will fracture when the average strain in either the weld or base metal exceeds six percent. If the welded components are intended to achieve five percent elongation, this criteria amounts to an allowable strain concentration of about 1.2. Figure 4-16 indicates the for practical Y/T from 0.85 to 0.90, if the strain concentration is to be limited to about 1.2, the maximum tolerable undermatch is from eight to 12 percent. This is consistent with the findings of the wide-plate tests, which showed poor performance when the undermatch exceeded 18 percent. Although not verified by experiments, the results show that the maximum tolerable undermatch could be greater if the weld metal had a lower Y/T ratio.

Wide-plate test results are also shown in Figure 4-16. The 13 mm thick 100S-1 weld specimens (Y/T=0.93, UM=9 percent) and 9 mm and 25 mm thick 100S-1 specimens (Y/T=0.88, UM=12 percent and Y/T=0.89, UM=1 percent, respectively) show reasonably good agreement with the finite-element analysis. The strain concentration was greater than 4 for the second and third series of wide-plate tests (undermatched in excess of 18 percent) and the 70S-3 tests.

It was concluded that small-strain finite-element analysis can adequately predict the plastic behavior of heterogeneous welds. Generalized plane strain analysis can model the core region of full-scale experimental testing up to about 20 percent undermatch. More significant undermatch requires the use of three-dimensional models to adequately characterize the performance of the joint.

	Strain Concentration (at 5 % Nominal Elongation)	
Model	8 percent UM	18 percent UM
Actual Bevel (60°)	1.44	1.55
No Bevel (0°)	2.28	2.33

Table 4-1 Comparison of Computed Weld Strain Data at a Typical Element for Two Bevel Angles at Two Levels of Undermatch.

Root Opening (mm)	4	8	12	16
Strain Concentration (at 5 % Nominal Elongation)	1.31	1.36	1.39	1.39

Table 4-2 Comparison of Computed Weld Strain Data at a Typical Element for Several Root Openings.

	Strain Concentration (at 5 % Nominal Elongation)	
Model	Without HAZ Properties	With HAZ Properties
120S-1 Weld	0.84	0.81
100S-1 Weld	1.55	1.62

Table 4-3 Comparison of Computed Weld Strain Data at a Typical Element for Different Welds Assessing the Effect of Including HAZ Properties.

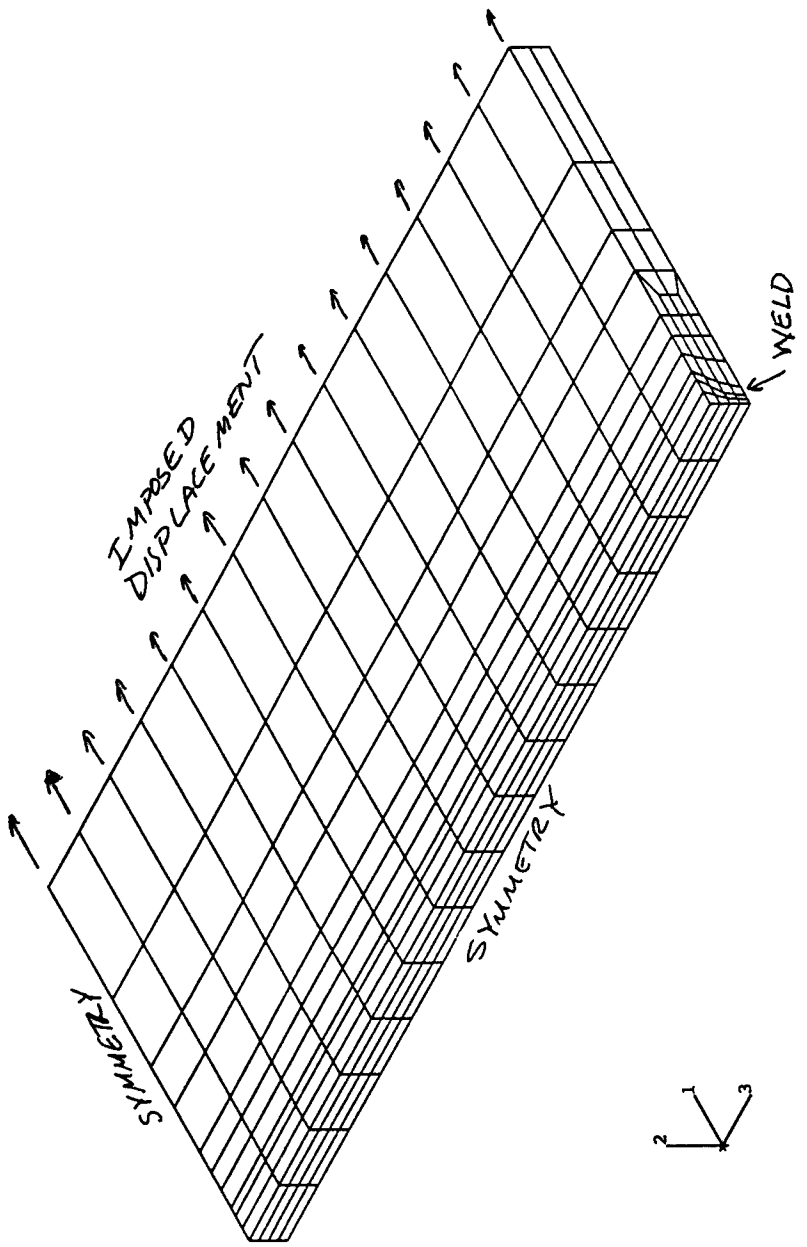

Figure 4-1 Three-dimensional Finite Element Model of 540, 20-Node, Reduced Integration Solid Brick Elements

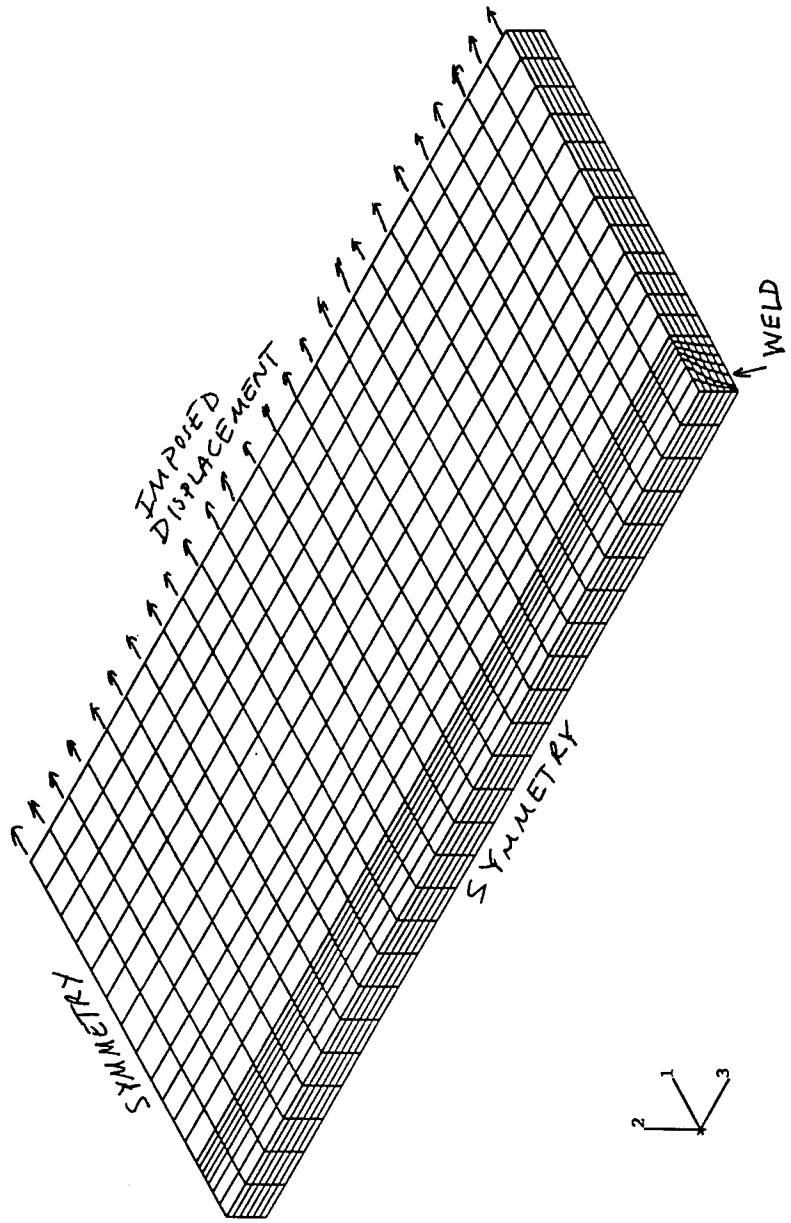

Figure 4-2 Three-dimensional Finite-Element Model of 2850, 20-Node, Reduced Integration Solid Elements

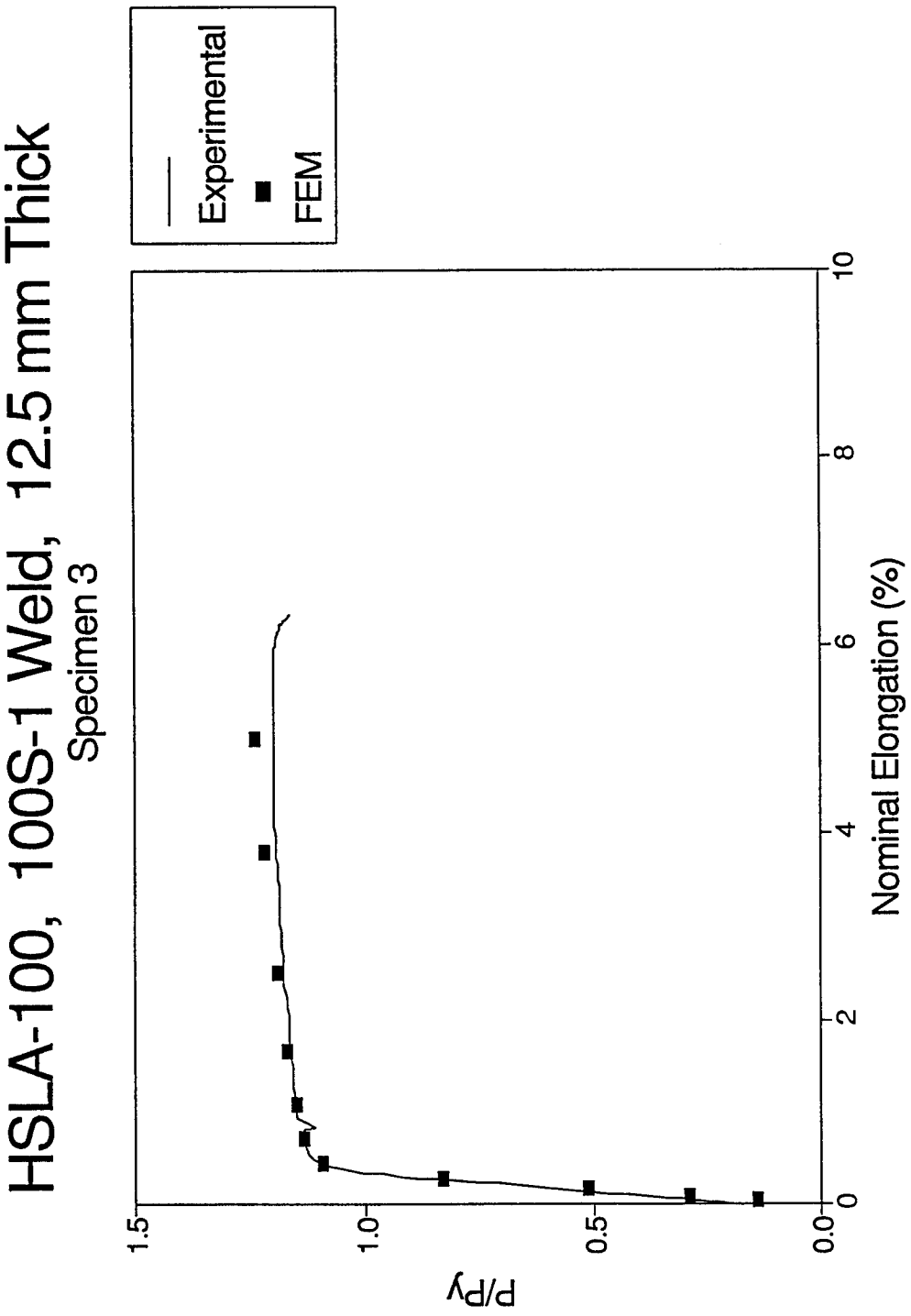

Figure 4-3 Comparison of Computed Load-Displacement Curve with the Experimental Data for the 100S-1 Weld Specimen Showing Good Agreement.

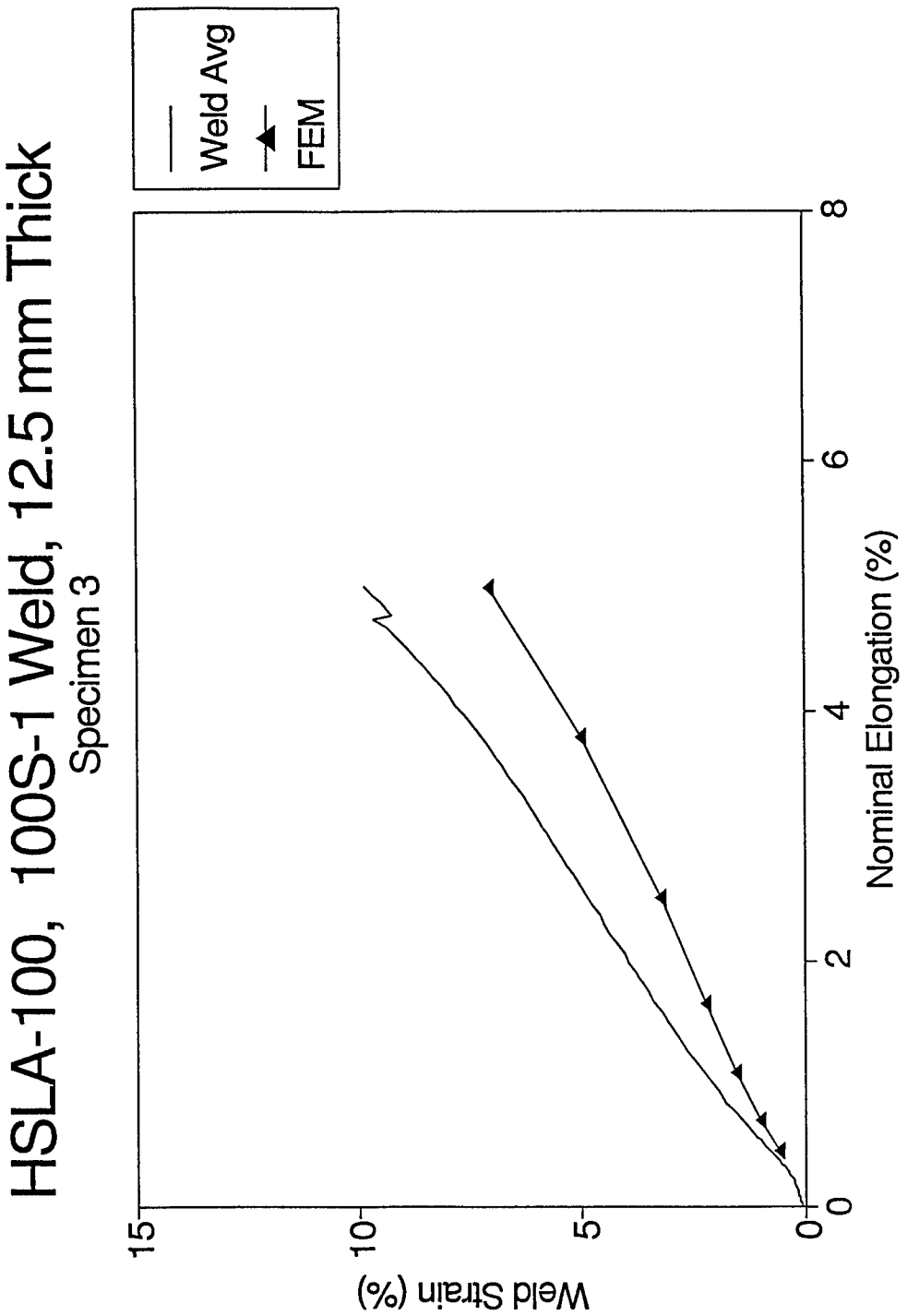

Figure 4-4 Comparison of Computed Weld Strain with the Experimental Data for the 100S-1 Weld Specimen Showing Good Agreement.

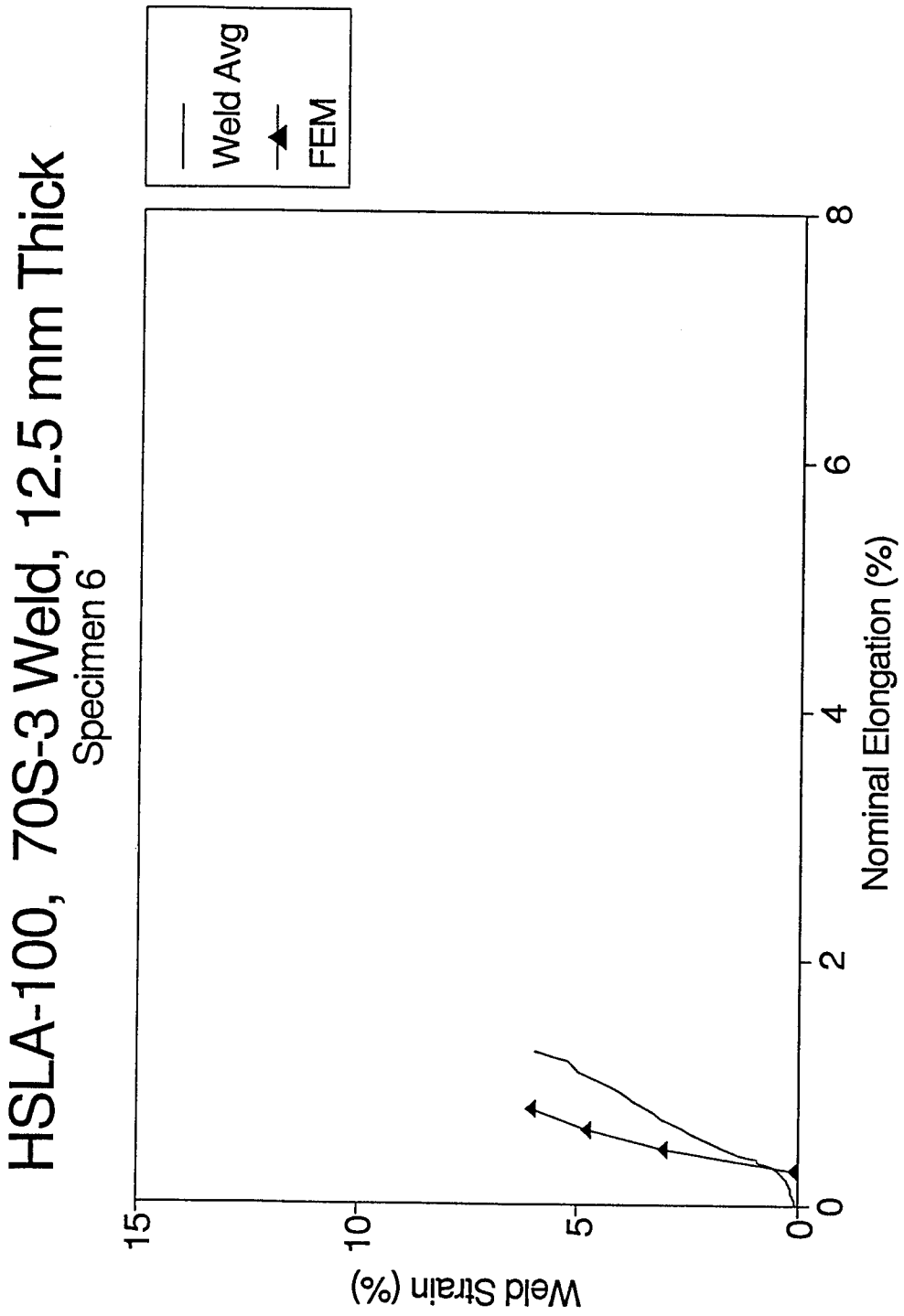

Figure 4-5 Comparison of Computed Weld Strain with the Experimental Data for the 70S-3 Weld Specimen Showing Good Agreement.

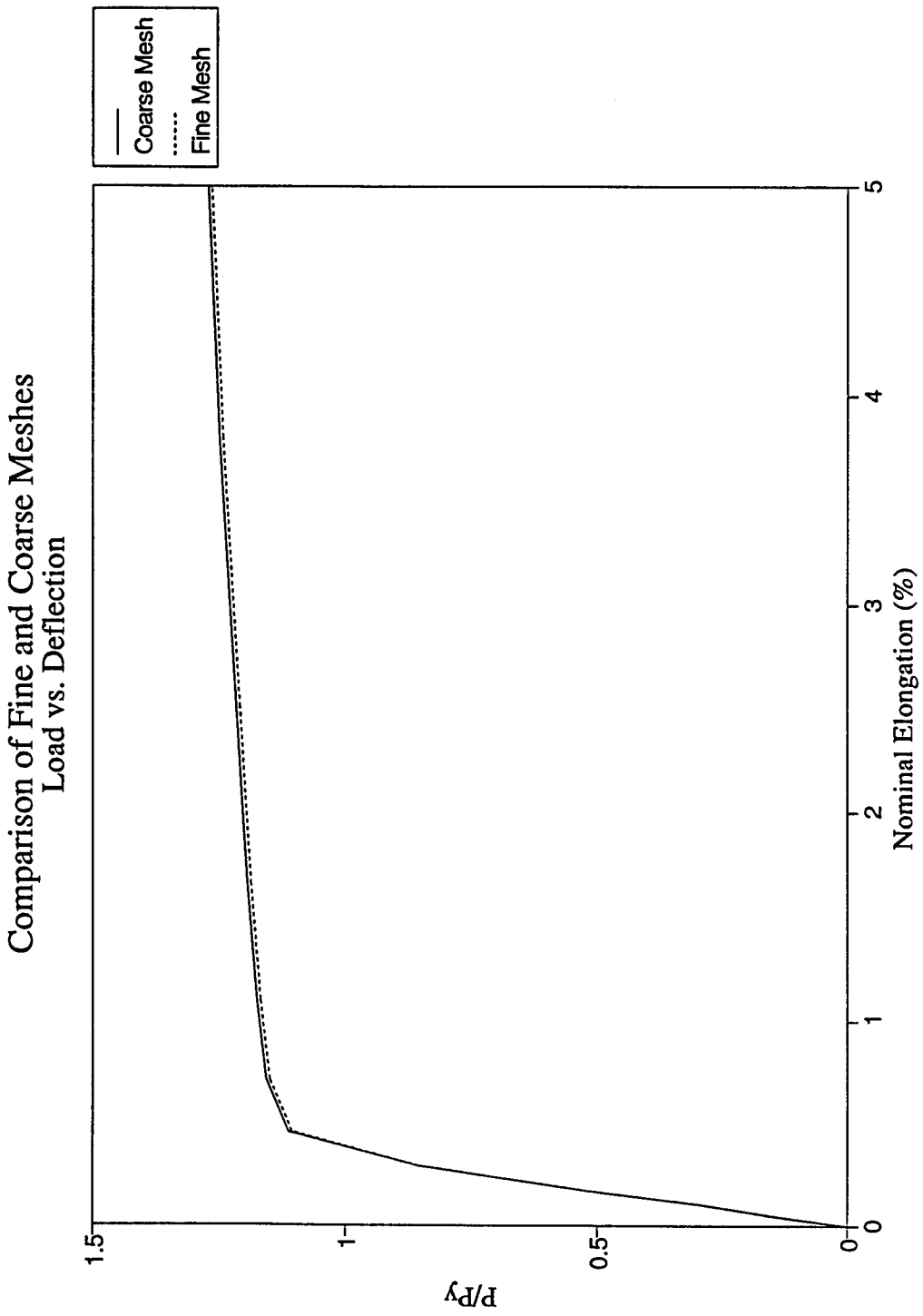

Figure 4-6 Comparison of Computed Load-Displacement Data for the Coarse and Fine Meshes Showing Good Agreement.

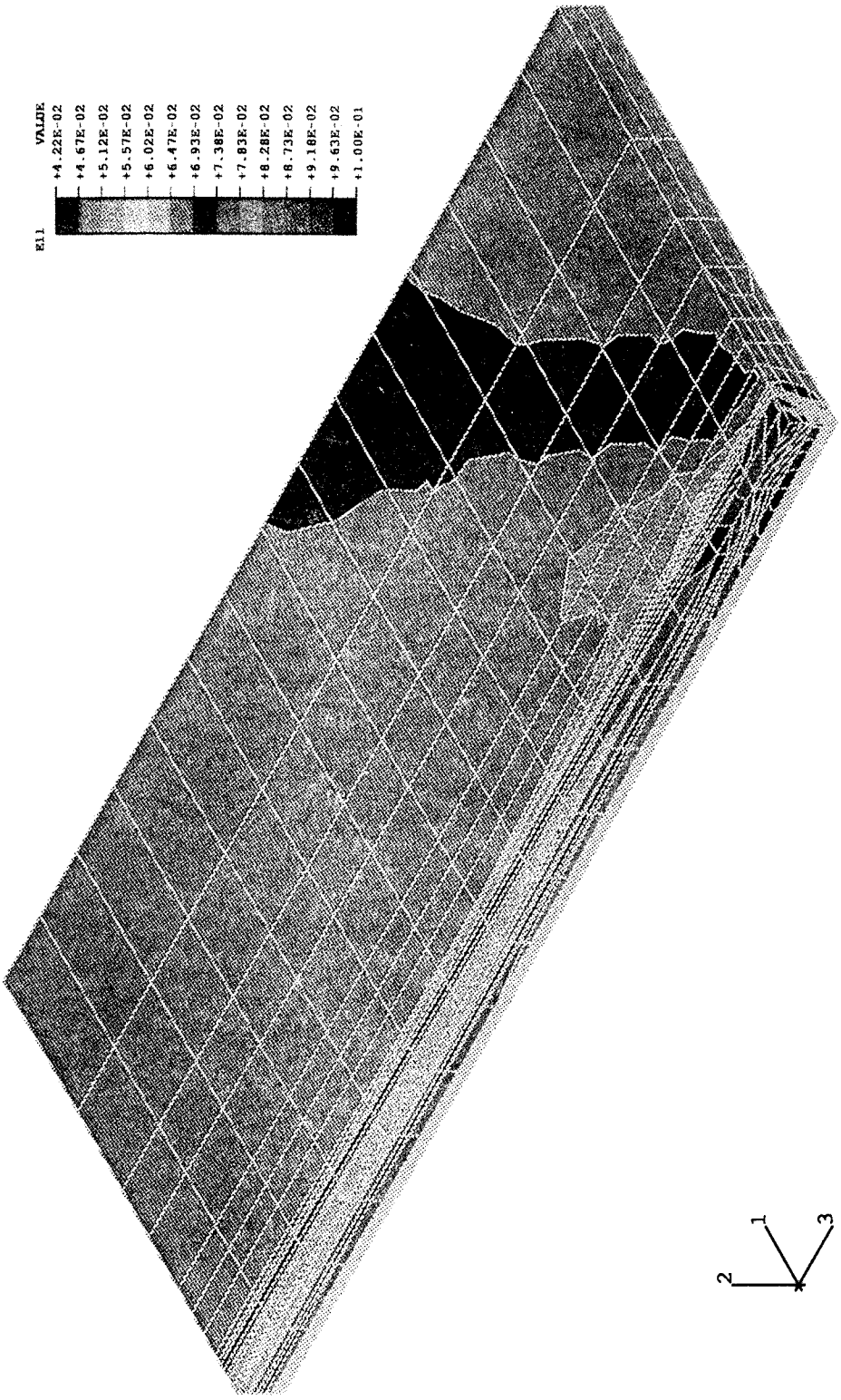

Figure 4-7 Contour Plot of Longitudinal Strain for the Coarse Three-Dimensional Finite-Element Model.

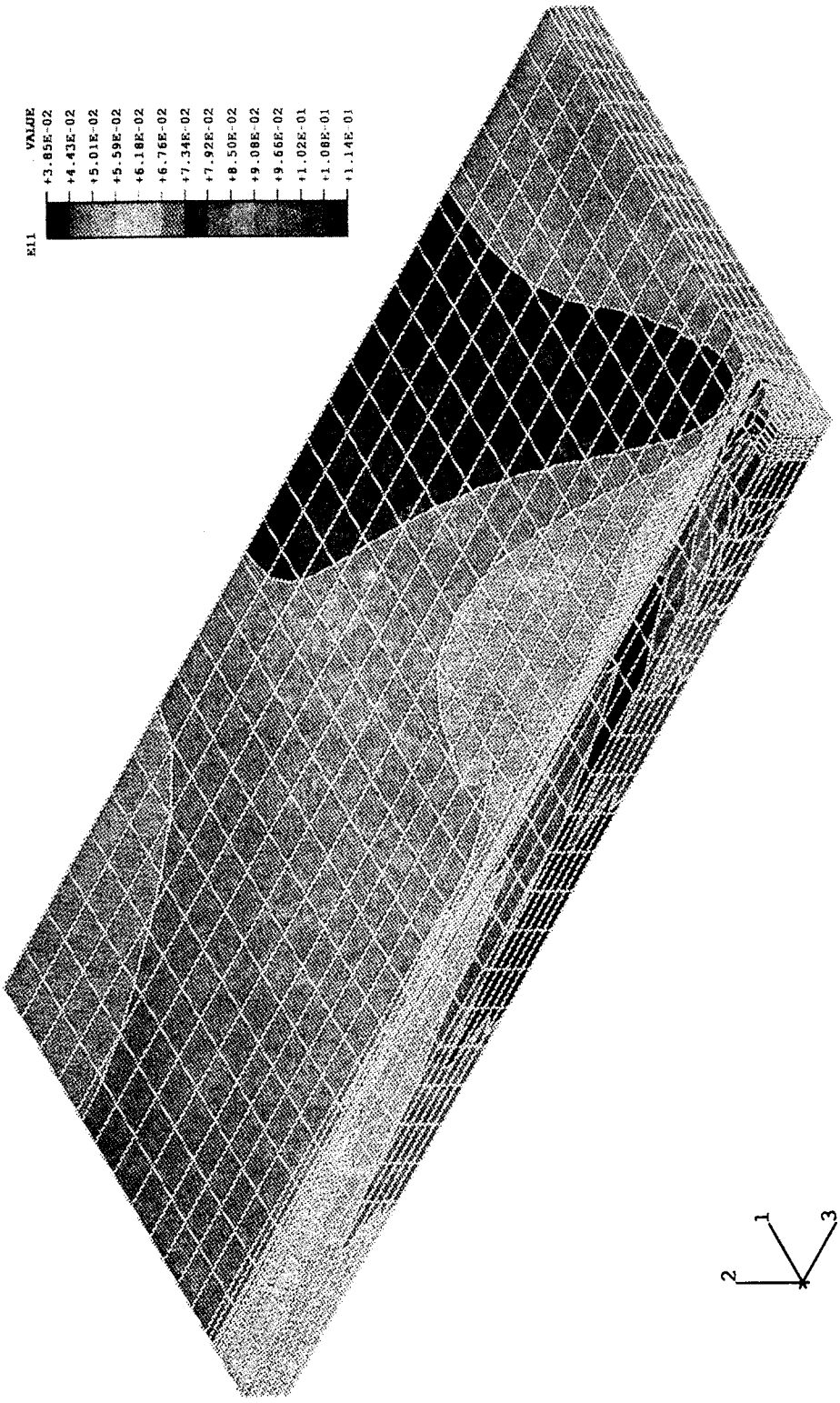

Figure 4-8 Contour Plot of Longitudinal Strain for the Fine Three-Dimensional Finite-Element Model.

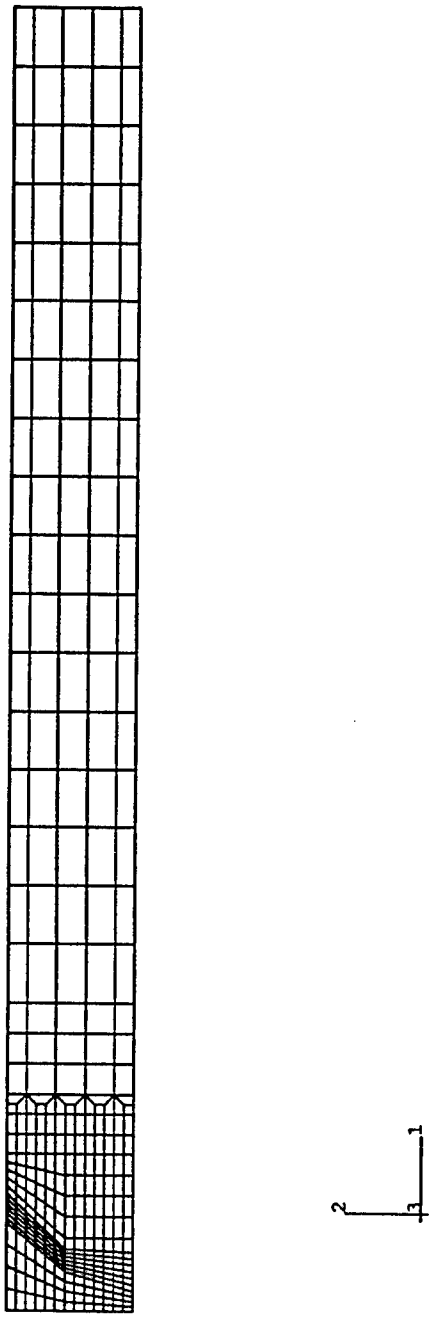

Figure 4-9 Two-Dimensional finite-Element Model of 339, 8-Noded, Reduced Integration, Generalized Plane-Strain Elements.

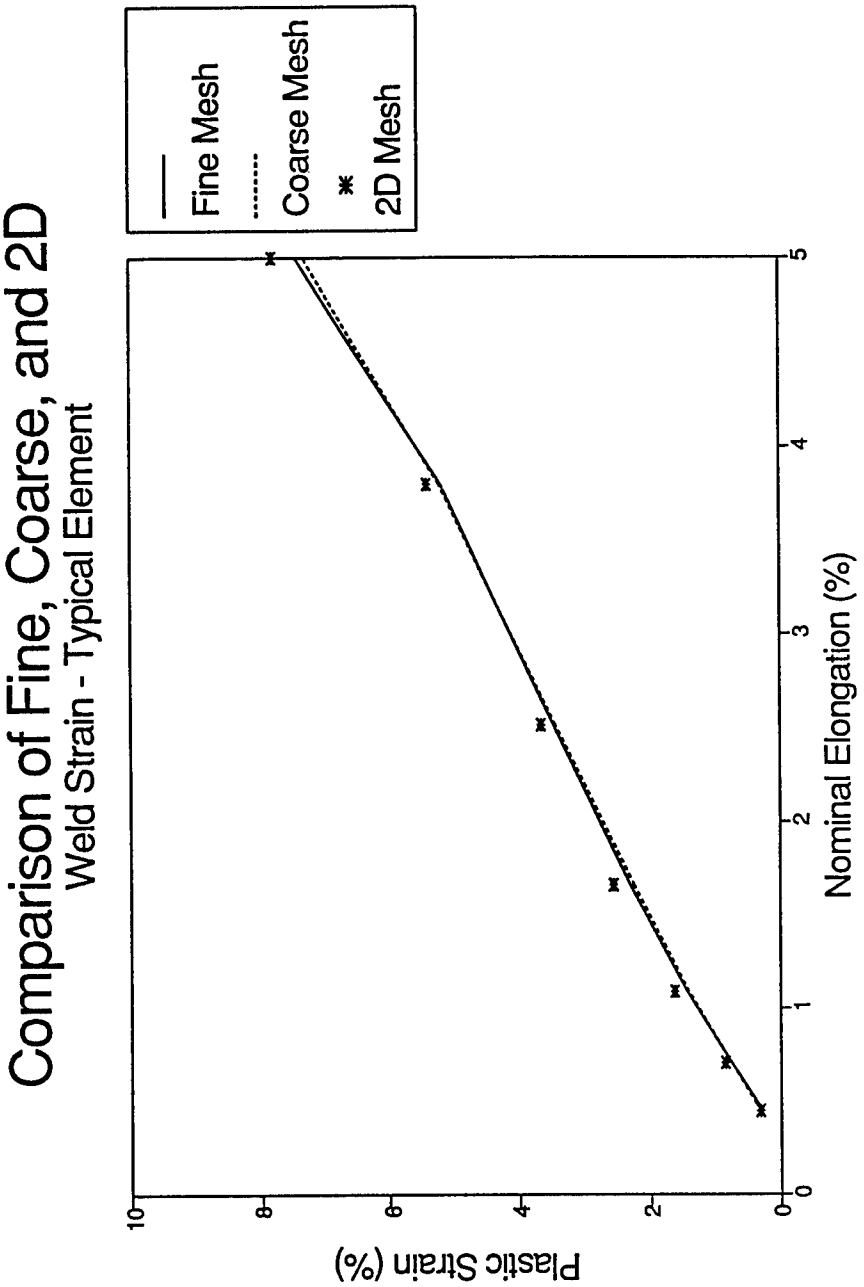

Figure 4-10 Comparison of Computed Weld Strains for the Three-dimensional Models and the Two-Dimensional Model Showing Good Agreement.

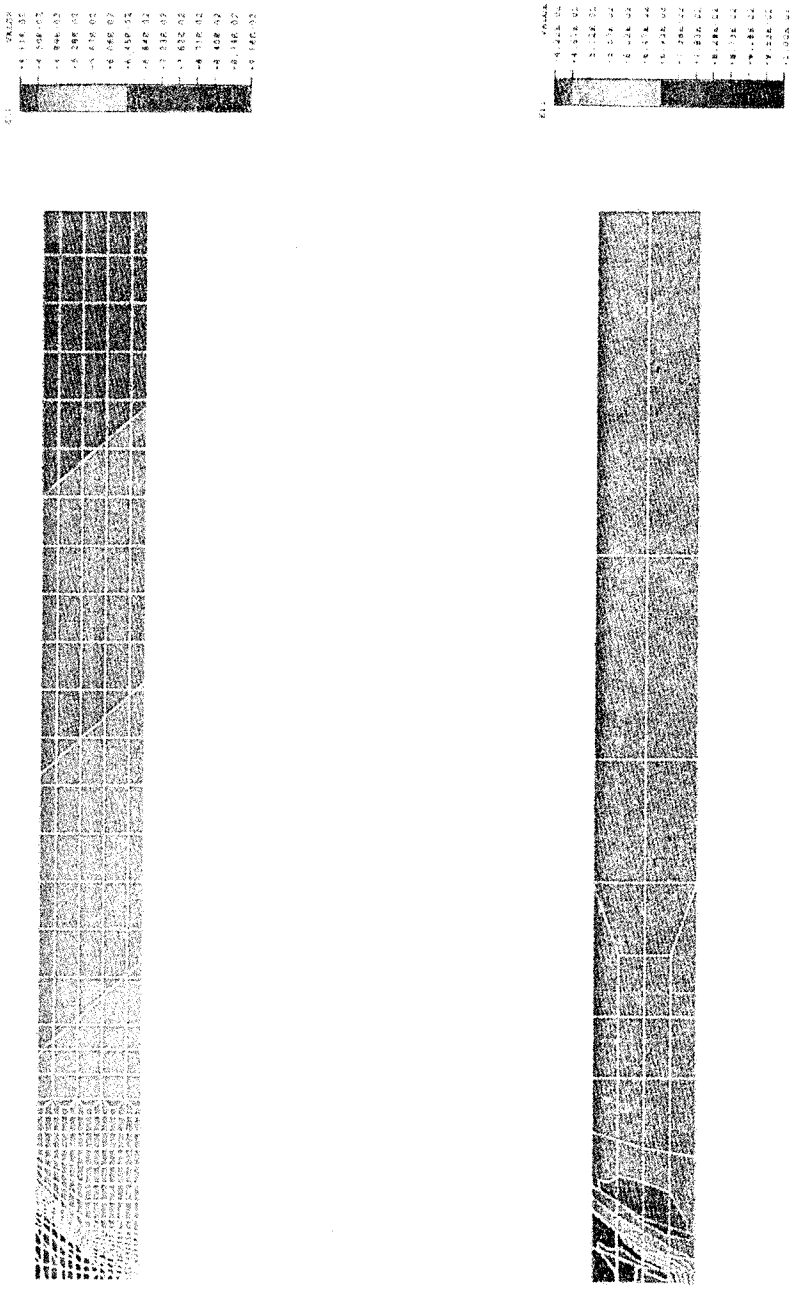

Figure 4-11 Comparison of Longitudinal Strain Contours for the Two-Dimensional Model and the Plane-Strain Region of the Three-Dimensional Model.

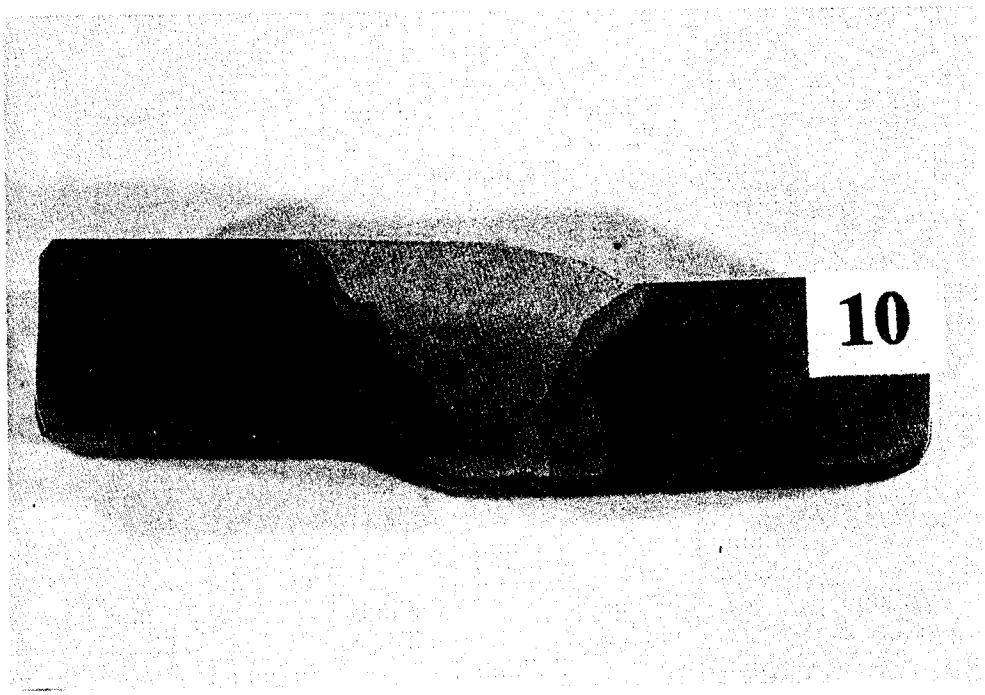

Misaligned Welded Joint
HSLA-100, 100S-1 Weld
3 mm Offset

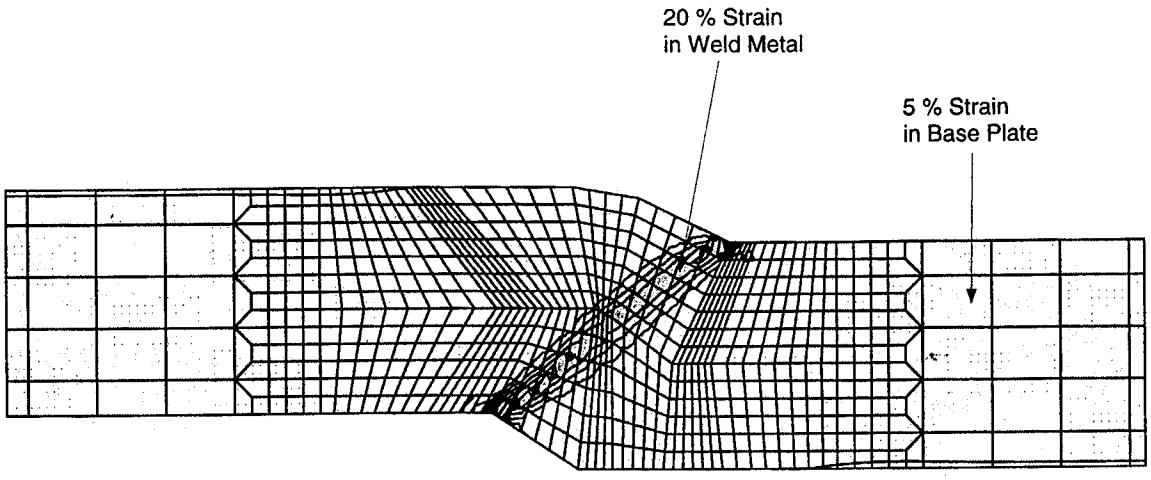

Figure 4-12 Weld Macrosection and Strain Contours from a Generalized Plane-Strain Finite Element Analysis of a Misaligned Welded Joint.

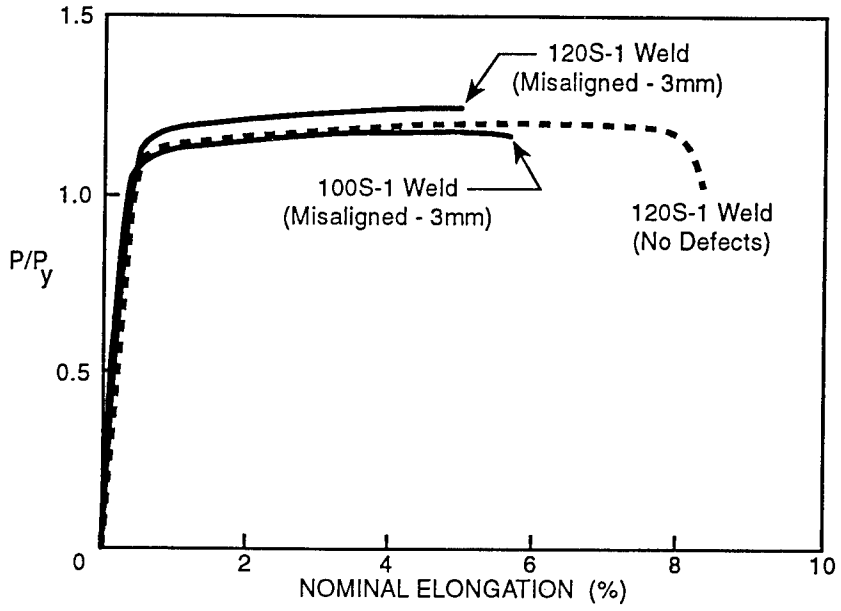

Figure 4-13 Comparison of the Load-Deformation Behavior of Misaligned Over- and Undermatched Welded Joints with Overmatched Welded Joint Showing the Misalignment has no Effect on Strength and Only Slightly Decreases Ductility.

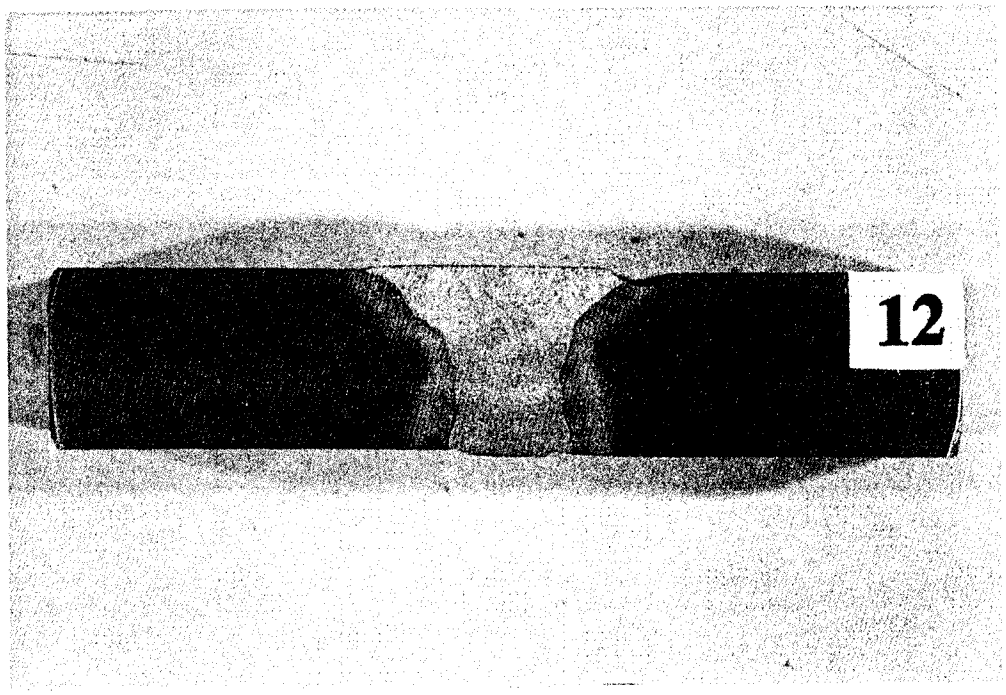

Undercut Welded Joint
HSLA-100, 100S-1 Weld
3 mm Notch

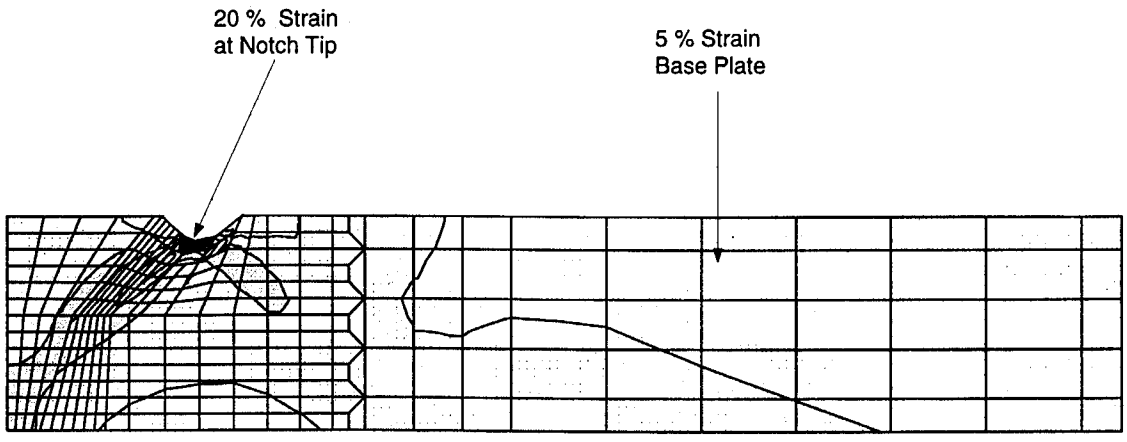

Figure 4-14 Weld Macrosection and Finite-Element Strain Contours for a Welded Joint with Simulated Undercut.

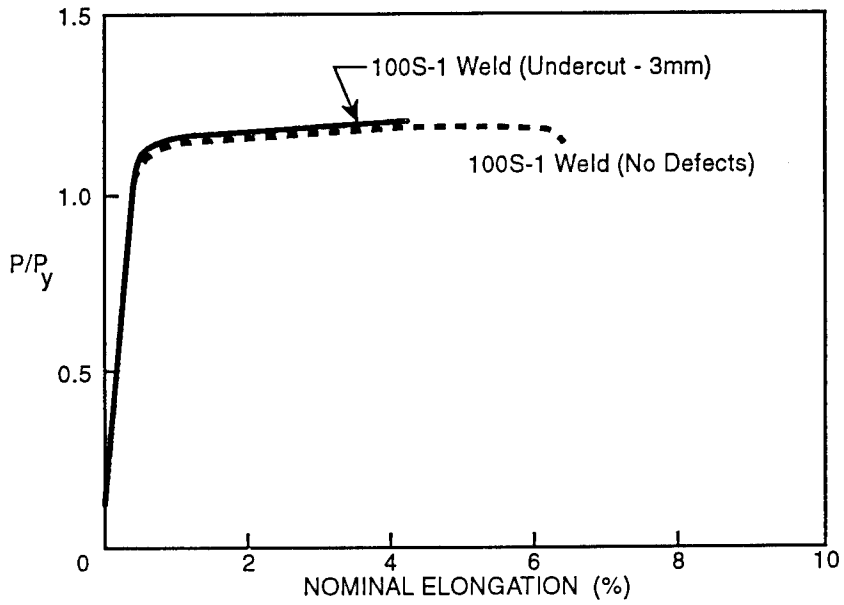

Figure 4-15 Comparison of the Load Deformation Curves of an Undermatched Welded Joint with Simulated Undercut to an Undermatched Welded Joint Without Defects Showing the Undercut Does Not Cause a Significant Reduction of Strength or Ductility.

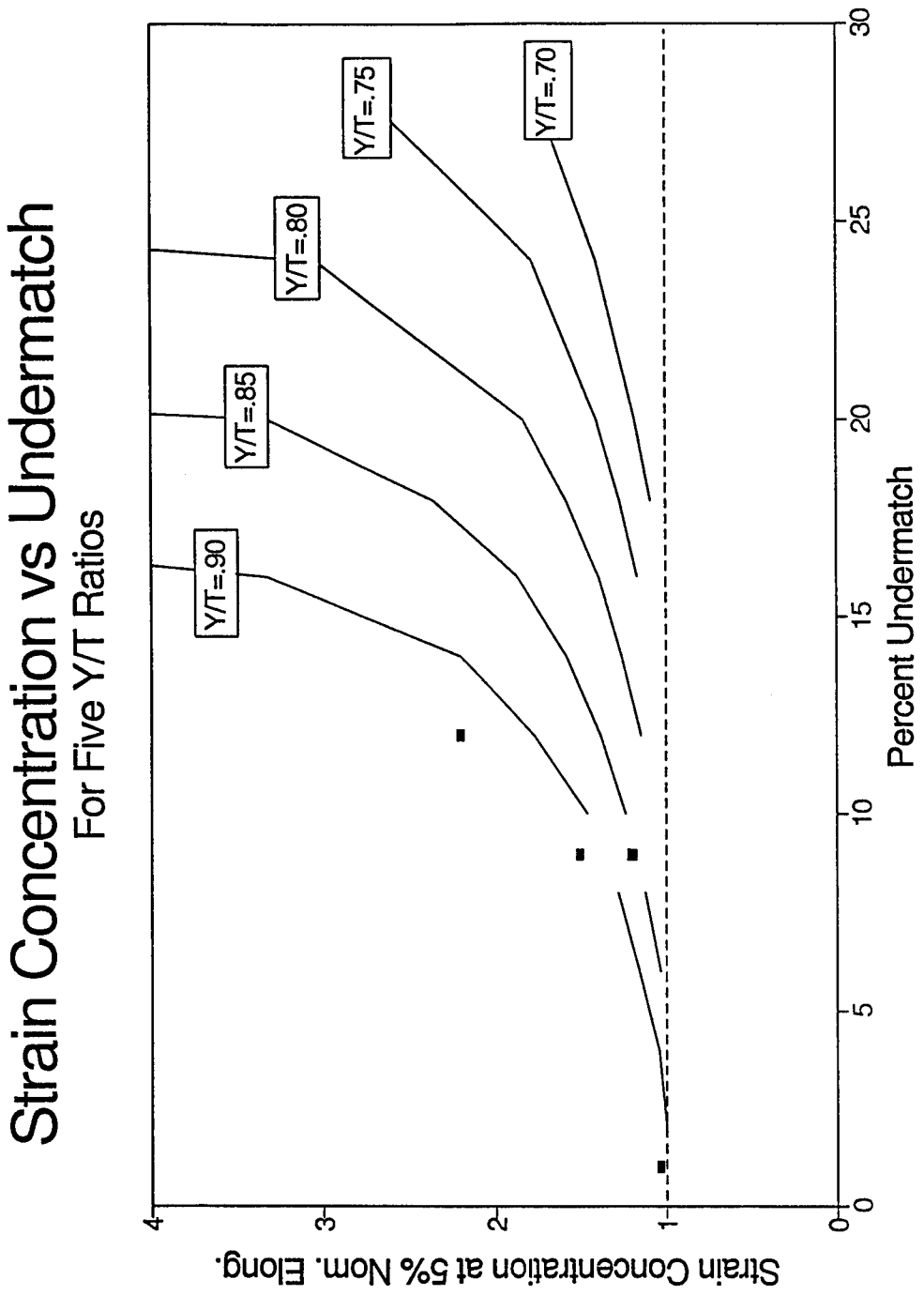

Figure 4-16 Parametric Study of the Effect of Y/T on the Computed Weld Strain as a Function of the Level of Undermatch. (Solid squares show wide-plate test results.)

5.0 GUIDELINES FOR USE OF UNDERMATCHED WELDS

The results of the experimental program, the finite-element analysis, and the survey of the relevant literature have been synthesized into a set of guidelines for the application of undermatched welds in high-strength steel structures.

5.1 Strength and Ductility

The following design guidelines are based on achieving strength and ductility at ultimate-load limit state which is comparable to the strength and ductility of similar joints which are overmatched. Therefore, in order to use the design guidelines, it is necessary for the designer to predict the possible failure modes and assess the adequacy of the undermatched weld for each individual condition.

1. Undermatched welds may be used without restrictions for:

    a. non-structural joints;

    b. joints never loaded beyond the elastic range (e.g. joints near the neutral axis of the hull); and

    c. joints loaded parallel to the weld axis (longitudinal joints).

2. Undermatched welds may be substituted for overmatched joints (as long as joint is redesigned to provide adequate strength), for:

    a. fillet and partial-penetration weld joints; and

    b. full-penetration tee and corner joints where reinforcing fillets or brackets can be added to provide the required strength.

Using undermatched welds in these applications may involve redesigning the joint (e.g. increasing weld size or adding reinforcement) to achieve the required strength. Whenever possible, the joint should be designed to force the yielding to occur away from the weld in the base plate.

3. In full-penetration butt joints loaded in shear or transverse tension, there must be a limit on the level of undermatching. The limit is given in terms of the actual undermatch, which requires that the actual yield strength of the base metal is known, e.g. from mill reports. Knowledge of the base metal yield strength might be available when weld procedures are being refined during construction. However, in design, only the minimum specified yield strength (MSYS) of the base metal is known. Examination of extensive mill report data fore HSLA-100 in Figure 2-1 reveals that the actual strength will be on average 8 percent greater than the MSYS but may occasionally be up to 18 percent greater than the MSYS. Therefore, if the base plate strength is not known, it is recommended that 18 percent be added to the allowable undermatch levels. Then the allowable undermatch can be considered in terms of the MSYS.

a. Butt-joints loaded in shear may be undermatched up to 28 percent in terms of the actual base plate strength (10 percent in terms of MSYS) and still have full strength and ductility comparable to overmatched welds.

Butt joints in shear may have significant bending stresses due to joint eccentricity. However, the tests described in Section 3.3 simulated worst-case conditions as far as combined shear and secondary bending and these joints achieved full base-plate shear strength. Therefore, panels loaded primarily in shear with secondary bending can be designed using the properties of the base plate without any special consideration of the welds.

b. Butt-joints in tension perpendicular to the weld axis with transverse plate widths greater than 12 times the thickness. These joints may be:

· undermatched up to 12 percent in terms of the actual base plate strength (overmatched by 6 percent in terms of the MSYS) and still have full strength and ductility comparable to overmatched welds (greater levels of undermatching can be tolerated if the weld reinforcement is not ground flush);

· undermatched up to 28 percent in terms of the actual base plate strength (10 percent in terms of the MSYS) and still have full strength but only limited ductility.

If the transverse plate width is less than 12 times the thickness, such as a butt weld in a girder or stiffener flange, undermatched welds may achieve less strength and/or ductility and should be designed on the basis of strength and ductility exhibited by standard 38 mm wide flat-strap transverse weld tension tests.

5.2 Defect Tolerance

The guidelines for the undermatching of butt-joints in tension presupposes there are no significant defects present in the weld. Because of the high fracture toughness of the low heat-input moderately-undermatched 100S-1 weld in HSLA-100, the following additional preliminary guidelines are applicable when defects are present:

a. Butt-joints with lack-of-fusion defects comprising up to 10 percent of the gross area will achieve the MSYS on the gross area but will have only limited ductility.

b. Butt-joints with misalignment of the plates up to 25 percent of the thickness will have full strength, but slightly reduced ductility.

c. Butt joints with undercut up to 12 percent of the depth will have full strength, but reduced ductility.

d. Additional guidance on defect tolerance may be obtained from the British Standards Institute published document PD 6493: "Guidance on Some Methods for the Derivation of Acceptance Levels for Defects in Fusion Welded Joints" [42] and from reference [35] regarding the Engineering Treatment Method (ETM).

5.3 Finite-element Analysis

For joints and loadings not explicitly described above, it is recommended that a finite-element analysis of the undermatched joint be conducted. The following guidelines apply to finite-element analyses of undermatched butt joints in transverse tension.

1. Small-strain theory may be used for computational efficiency;

2. Two-dimensional generalized plane-strain models using eight-noded elements with reduced (two-by-two) integration may be used for very wide joints, levels of undermatch below 20 percent, and constant properties through the width. These analyses may be suitable for modelling defects such as undercut which extend along the length of the weld.

3. Three-dimensional models using twenty-noded elements with reduced integration (two-by-two-by-two) must be used for levels of undermatch greater than 20 percent or variable properties through the width.

4. The Von-Mises yield criterion should be used. Isotropic hardening is more simple than kinematic hardening and will give good results for monotonic loading. For cyclic plasticity, kinematic models or mixed kinematic/isotropic constitutive models may have to be used, but these require extensive experimental data to get the parameters. For the isotropic models, the constitutive properties for the base plate and weld materials should be input as piecewise-linear, "effective" stress-strain curves obtained from uniaxial tension tests. The HAZ may be assumed to have the same properties as the base metal without significantly influencing the strain in the weld metal.

5. The model should include a length of the plate at least ten times the thickness from the weld centerline. An axial displacement boundary condition can be imposed at this length. There should be at least four elements through the thickness in the three-dimensional models in the region near the weld. (Greater refinement through the thickness can be easily afforded in two-dimensional models.) There should be at least fifteen elements (with a width that does not exceed two times the thickness or 20 mm) across the half-width of the plate in three-dimensional models.

6. The failure criteria of six percent weld strain or six percent nominal elongation may be applied to conservatively estimate the achievable strength and ductility. If the computed strength and ductility meet design requirements, the joint can be undermatched.

5.4 Optimum Weld Metal Properties for HSLA-100

In order to overmatch 690 MPa MSYS steel such as HSLA-100, filler metals (such as the 120S-1 wire) must have a higher alloy than the base metal. When these high-alloy weld metals cool, they tend to form a more crack-sensitive microstructure with a high proportion of martensite. Costly weld procedures must be strictly followed in order to prevent cracking of this 120S-1 weld metal.

Based on the results of this research, it is recommended that the 100S-1 weld metal be used with HSLA-100 in order to decrease the potential for hydrogen cracking. Because the 100S-1 requires less alloying, it transforms to a less crack-sensitive microstructure when it cools. It has been shown previously and was confirmed in this project that the HSLA-100 steel can be welded without preheat and interpass temperature requirements if the less-susceptible but slightly-undermatched 100S-1 weld metal is. used.

In this project, Bath Iron Works (BIW) reviewed the potential cost savings and other practical advantages of using the 100S-1 weld metal rather than the 120S-1 weld metal. The results estimate that at least a six percent reduction of the fabrication labor costs could be achieved. These results are very sensitive to the assumptions, e.g. the facility or the hull. In most cases, larger cost savings will probably be achieved.

For critical butt joints loaded in transverse tension which require good ductility, the heat input must be limited for the 100S-1 weld metal. The second and third series of tests were welded with the maximum permissible heat input for the 13 mm thick plate which is 1.8 kJ/mm and also with maximum preheat and interpass temperature, which is 150 degrees C. The weld metal yield strength was as low as the minimum allowable for the 100S-1 weld wire (565 MPa). Although these welds achieved adequate strength, the ductility was minimal. Optimal properties were obtained in the first series of wide-plate tests which were welded at heat inputs ranging from 0.55 to 1.2 kJ/mm for the fill passes and up to 1.7 kJ/mm for the root pass. The resulting yield strength of the weld metal ranged from 670 to 750 MPa with an average weld metal strength of 717 MPa. The base plate strength in these tests was at the high end of the expected strength level for HSLA-100, therefore these weld parameters are expected to give very good results for any HSLA-100.

5.5 Computer Program for Selection of Weld Metal Properties

A very simple computer program was developed to facilitate the choice of optimum weld metal properties based on the loading and the type of joint. The program was written in Visual Basic 3.0. The program has a graphical user interface which allows the user to select options by pointing and clicking with a mouse. The program is called OPTIMATT and it is provided on a disk with a file VBRUN300.DLL needed to run it. The program can be executed from windows by choosing File, Run. The source code consists of numerous files that are provided on another disk.

The operation of the program is self explanatory. It begins with a welcoming screen and a general information screen. The next screen is for selection of the type of joint (e.g. butt joint or tee and corner joint). Based on the type of joint, the next screen is for selection of the type of loading. The joint types are shown in isometric views and the loading directions are shown with arrows (such as in Figures 2-4 and 2-5).

In accordance with the guidelines in Section 5.1, some of these joint types and loadings will be accepted without qualification at this point, while other will lead to a screen where the materials must be specified. After the materials are input, width and thickness data and also weld-joint preparation data are input. All of these values are checked to see if they are reasonable. Warnings are issued if the values are not reasonable. At this point, the user is asked if default properties for the weld metal are to be used or if the weld metal strength is to be calculated. If it is to be calculated, another screen asks for the welding parameters including process, voltage, amperage, travel speed,. and preheat temperature. These values are checked to see if they are reasonable. The heat input, predicted cooling rate, and yield strength are displayed.

The cooling rates and yield strength are presently calculated based on interpolation among the few data generated in this project. Unfortunately, we were not able to obtain a general algorithm to predict the yield strength, although it is known that such algorithms exist. The provisions for substituting an improved algorithm have been made. In any case, the final values are displayed and a calculation of the undermatch is made. Depending on the guidelines in Section 5.1, a judgement is made on the acceptability of the weld metal yield strength. The user can then return to the beginning for analysis of another joint or quit.

At present, this computer program probably does not offer significant advantages relative to just reading and applying the criteria presented in Section 5.1. However, with the addition of a weld metal strength algorithm and additional strength data, this program could become a useful tool.

6.0 CONCLUSIONS AND RECOMMENDATIONS

6.1 Conclusions

1. There are many welded joints in surface ships which can be undermatched without concern (e.g. fillet welds or any weld parallel to the primary loading direction). However, undermatched butt-joints which are transverse to the primary loading direction could be a potential weak link and must be checked to be sure that full strength of the base plate and reasonable ductility can be achieved.

2. Butt welds in shear can be undermatched up to 28 percent in terms of the actual base plate strength without reducing the shear strength or ductility of the welded panel.

3. Despite low strain hardening (i.e. high Y/T), undermatched welds can achieve higher apparent strength due to constraint.

4. Provided the transverse width is greater than 12 times the thickness, plates with transverse butt welds can be undermatched up to 12 percent with respect to the actual base plate strength without a reduction in strength or ductility relative to comparable overmatched welds.

5. Provided the transverse width is greater than 12 times the thickness, plates with transverse butt welds can be undermatched without a reduction in strength, but ductility relative to comparable overmatched welds is significantly affected.

6. Traditional flat-strap cross-weld specimens exhibit lower strength and ductility for undermatched welds than is exhibited in wide-plate specimens due to loss of constraint in the transverse (width) direction.

6.2 Recommendations

1. Preliminary tests showed that the HSLA-100 steel with the overmatched and undermatched welds is remarkably tolerant to misalignment, lack-of-fusion defects, and undercut. More combined experimental/numerical studies should be performed on the comparative behavior (ultimate strength and fatigue strength) of overmatched and undermatched welded structural components with realistic welding defects (including slag and porosity). All previous studies of the ultimate strength of welds with defects have dealt only with idealized surface cracks or through-thickness cracks at the weld centerline rather than realistic defects. The proposed study will establish fitness-for-purpose guidelines for tolerable defect sizes. Note that such a study has never been done for even overmatched welds.

2. Further experiments should be performed with undermatched welds in different types of joints (e.g. corner and tee joints) under a variety of combinations of shear and bending loading to establish interaction curves for such combined loading. In corner and tee joints, it should be possible to force the yielding to occur in the base plate by adding reinforcing fillets.

3. As ubiquitous as fillet welds are, a surprisingly small amount of test data and analyses are available pertaining to their ultimate strength. It is not clear why longitudinal fillet welds exhibit about 0.8 times the ultimate strength in uniaxial tension, where the Von-Mises yield surface, if extrapolated to ultimate strength, would predict the shear strength to be 0.57 times the uniaxial strength. Even less is known about the behavior of groove welds in shear. A fundamental investigation of welds in shear and in combined shear and bending should be performed. The following effects should be clarified: 1) the effect of weld process and geometry on cooling rate and weld strength; 2) the effect of the actual failure plane as opposed to the idealized path through the weld throat; 3) the effect of shear lag; 4) the effect of weld size (scale effects); and, 5) the effect of statistical variation of weld profile.

7.0 REFERENCES

1. American Welding Society, B4.0, Standard Methods for Mechanical Testing of Welds, 1984.
2. American Welding Society, D1.5, Bridge Welding Code, 1998.
3. American Welding Society, D1.1, Structural Welding Code, 1992.
4. Aronson, A., H., "The Weldability of Columbium-bearing High-Strength Low-Alloy Steel," Welding Journal-Welding Research Supplement, pp. 266s-271s, 1966.
5. Bates, K.S., et al., Weld Undermatch in Thin-Section HY100 Steel, General Dynamics Corp., Electric Boat Division, Report No. PDE-283, 1992.
6. Denys, R.M., Fracture Behavior of Large Diameter Pipeline Girth Welds: Effect of Weld Metal Yield Strength, Pipeline Research Committee, American Gas Association, 1990.
7. Dexter, R.J., and Lundin, C.D., "Plastic Behavior of Pipeline Girth Welds with Softened Heat-Affected Zones and Undermatched Weld Metal," Mis-Matching of Welds, ESIS-17, Mechanical Engineering Publications, London, pp. 741-755, 1994.
8. Easterling, K., Introduction to the Physical Metallurgy of Welding, Butterworths Monographs in Materials, London, 1983.
9. Fisher, J.W., et al., Effect of Weldments of the Fatigue Strength of Steel Beams, National Cooperative Highway Research Program (NCHRP) Report 102, Highway Research Board, Washington, D.C., 1970.
10. Fisher, J.W., et al., "Load and Resistance Factor Design Criteria for Connectors," Journal of the Structural Division, Vol. 104, ST9, pp. 1427-1441, Sept. 1978.
11. Fisher, J.W., et al., Structural Failure Modes of Advanced Double-Hull, Fatigue and Fracture Failure Modes, TDL 91-01, Vol. 3a, Lehigh University, Bethlehem, PA, 1992.
12. Frank, K.H., University of Texas, Personal Communication, 1994.
13. Glover, A., G., Effect of Weld Metal Strength on the Control of Root Pass Cracking, Welding Institute of Canada, 1984.
14. Hartbower, C.E., and Pellini, W.S., "Explosion Bulge Test Studies of the Deformation of Weldments," Welding Journal-Welding Research Supplement, pp.307s-318s, June 1951.
15. Hartbower, C.E., and Pellini, W.S., "Investigation of Factors which Determine the Performance of Weldments, " Welding Journal-Welding Research Supplement, pp. 499s-511s, October 1951.
16. Hasimoto, T., et al., "Recent Development of Large Diameter Line Pipe of Grade X-80 and X-100," Proceedings of the Seventh International Conference on Offshore Mechanics and Arctic Engineering, American Welding Society, Miami, Vol.3, pp. 179-185, 1988.
17. Howden, D. G., et al., Effective Use of Weld Metal Yield Strength for HY Steels, National Materials Advisory Board Report, Report No. NMAB-380, January 1983.
18. Ikeda, A., et al., "On the Evaluation Method of Sulfide Stress Cracking Susceptibility of Carbon and Low-Alloy Steels," Corrosion Science, Vol. 27, pp. 1099-1115, 1987.

19. Kocak, M., et al., "Fracture Aspects of the Under- and Overmatched Weld Joints," Engineering Design in Welded Constructions, Oxford, 1992.
20. Kulak, G.L. and Fisher, J.W., "Behavior of Large A514 Steel Bolted Joints," Journal of the Structural Division, ASCE, Vol. 95, No. ST9, 1969.
21. Lundin, C.D., et al., Carbon Equivalence and Weldability of Microalloyed Steels, Ship Structure Committee Report, SSC-357, 1991.
22. Mil-S-24645A(SH), Steel Plate, Sheet or Coil, Age-Hardening Alloy, Structural, High Yield Strength (HSLA-80 and HSLA-100), 1990.
23. Mil-Std-1689A(SH), Fabrication, Welding and Inspection of Ships Structure, 1990.
24. Null, C., NAVSEA, Personal Communication, 1994.
25. Ohsawa, Y., et al., Evaluation of Elasto-Plastic Behavior of Soft Welded Joints for High Strength Steel Pipes, Nippon Kokan Technical Report, pp. 117-125, 1984.
26. Petrovski, B., et al., "Fracture Behavior of Undermatched Weld Joint with Short Surface Crack," Proceedings of the Tenth International Conference on Offshore Mechanics and Arctic Engineering, pp. 101-107, 1991.
27. Prinaris, A.A. and Saouma, V.E., Elasto-Plastic Fracture Analysis of Welded Plates, Structural Research Series Report 88-09, University of Colorado, Boulder, 1988.
28. Satoh, K., and Toyoda, M., "Joint Strength of Heavy Plates with Lower Strength Weld Metal," Welding Journal-Welding Research Supplement, pp. 311s-319s, September 1975.
29. Satoh, K., et al., "Prevention of Weld Crack in HT80 Plates with Undermatching Electrodes in Application to Fabricating Penstock," Trans. Japan Welding Society, Vol. 9, No.1, pp.17-21, April 1978.
30. Satoh, K., and Toyoda, M., "Static Tensile Properties of Welded Joints Including Soft Interlayer," Trans. Japan Welding Society, pp. 7-12, April 1970.
31. Satoh, K., et al., "Undermatching Electrode Applied to Heavy Penstock," Welding Journal-Welding Research Supplement, pp. 25s-33s, February 1979.
32. Satoh, K., and Toyoda, M., "Static Strength of Welded Plates Including Soft Interlayer Under Tension Across a Weld Line," Trans. Japan Welding Society, pp. 10-17, September 1970.
33. Sbarskaya, N.,P., et al., "The Weldability of Low-Alloy Pipe Steels Strengthened by Heat Treatment," Welding Production, Vol. 25, pp. 34-35, 1978.
34. Schwalbe, K.-H. and Kocak, M., ed., Mis-Matching of Welds, ESIS-17, Mechanical Engineering Publications, London, 1994.
35. Schwalbe, K.-H., "Effect of Weld Metal Mis-match on Toughness Requirements: Some Simple Analytical Considerations Using the Engineering Treatment Model (ETM)," International Journal of Fracture, Vol 56, pp. 257-277, 1992.
36. Smirnov, B., A., and Borisov, P.,P., "Determination of the Properties of Welded Joints in Pipes from Steel," Welding Production, Vol. 21, pp. 39-42, 1974.
37. Wiggs, A., Naval Surface Warfare Center, Personal Communication, 1994.
38. Youn, J.G. and Kim, H.J., "Characteristics of TMCP Steel and its Softening," Welding Metallurgy of Structural Steels, 1987.

39. ASCE-WRC, Plastic Design in Steel, A Guide and Commentary, Second Edition, Joint Committee of the Welding Research Council and the American Society of Civil Engineers, ASCE, New York, 1971.
40. Denys, R. M., 1995, "Toughness Requirements for Pipeline Integrity", Proceedings of the 14th International Conference on Offshore Mechanics and Arctic Engineering Conference (OMAE), 18-22 June 1995, Copenhagen Denmark, Salama et al, eds., ASME, Vol. III, Materials Engineering, pp 93--100.
41. Ghose, D.J., Nappi, N.S., and Wiernicki, C.J., Residual Strength of Damaged Marine Structures, Report SSC-381, Ship Structure Committee, Washington, D.C., September, 1994.
42 BSI, "PD6493 Guidance on Some Methods for the Derivation of Acceptance Levels for Defects in Fusion Welded Joints", British Standards Institute, London, 1991.

PROJECT TECHNICAL COMMITTEE MEMBERS

The following persons were members of the committee that represented the Ship Structure Committee to the Contractor as resident subject matter experts. As such they performed technical review of the initial proposals to select the contractor, advised the contractor in cognizant matters pertaining to the contract of which the agencies were aware, and performed technical review of the work in progress and edited the final report.

Mr. Allen Manuel	Naval Sea Systems Command
Mr. John Allison	Naval Sea Systems Command
Mr. David Ku	American Bureau of Shipping
Mr. Walter Reuter	Idaho National Engineering Labs
Mr. James Sawhill	Newport News Shipbuilding
Mr. William Sickierka	Naval Sea Systems Command, Contracting Officer's Technical Representative
Dr. Robert Sielski Mr. Alexander Stavovy	National Academy of Science, Marine Board Liaison
CDR Steve Sharpe	U.S. Coast Guard, Executive Director Ship Structure Committee

COMMITTEE ON MARINE STRUCTURES

Commission on Engineering and Technical Systems

National Academy of Sciences – National Research Council

The COMMITTEE ON MARINE STRUCTURES has technical cognizance over the interagency Ship Structure Committee's research program.

John Landes, University of Tennessee, Knoxville, TN
Howard M. Bunch, University of Michigan, Ann Arbor, MI
Bruce G. Collipp, Marine Engineering Consultant, Houston, TX
Dale G. Karr, University of Michigan, Ann Arbor, MI
Andrew Kendrick, NKF Services, Montreal, Quebec
John Niedzwecki, Texas A & M University, College Station, TX
Barbara A. Shaw, Chairman, Pennsylvania State University, University Park, PA
Robert Sielski, National Research Council, Washington, DC
Stephen E. Sharpe, Ship Structure Committee, Washington, DC

DESIGN WORK GROUP

John Niedzwecki, Chairman, Texas A&M University, College Station, TX
Bilal Ayyub, University of Maryland, College Park, MD
Ovide J. Davis, Pascagoula, MS
Maria Celia Ximenes, Chevron Shipping Co., San Francisco, CA

MATERIALS WORK GROUP

Barbara A. Shaw, Chairman, Pennsylvania State University, University Park, PA
David P. Edmonds, Edison Welding Institute, Columbus, OH
John F. McIntyre, Advanced Polymer Sciences, Avon, OH
Harold S. Reemsnyder, Bethlehem Steel Corp., Bethlehem, PA
Bruce R. Somers, Lehigh University, Bethlehem, PA

RECENT SHIP STRUCTURE COMMITTEE PUBLICATIONS

Ship Structure Committee Publications – A Special Bibliography

SSC–384 Post–Yield Strength of Icebreaking Ship Structural Members C. DesRochers, J. Crocker, R. Kumar, D. Brennan, B. Dick, S. Lantos 1995

SSC–383 Optimum Weld–Metal Strength for High Strength Steel Structures R. Dexter and M. Ferrell 1995

SSC–382 Reexamination of Design Criteria for Stiffened Plate Panels by D. Ghose and N. Nappi 1995

SSC–381 Residual Strength of Damaged Marine Structures by C. Wiernicki, D. Ghose, N. Nappi 1995

SSC–380 Ship Structural Integrity Information System by R. Schulte–Strathaus, B. Bea 1995

SSC–379 Improved Ship Hull Structural Details Relative to Fatigue by K. Stambaugh, F. Lawrence and S. Dimitriakis 1994

SSC–378 The Role of Human Error in Design, Construction and Reliability of Marine Structures by R. Bea 1994

SSC–377 Hull Structural Concepts For Improved Producibility by J. Daidola, J. Parente, and W. Robinson 1994

SSC–376 Ice Load Impact Study on the NSF R/V Nathanial B. Palmer by J. St. John and P. Minnick 1995

SSC–375 Uncertainty in Strength Models for Marine Structures by O. Hughes, E. Nikolaidis, B. Ayyub, G. White, P. Hess 1994

SSC–374 Effect of High Strength Steels on Strength Consdierations of Design and Construction Details of Ships by R. Heyburn and D. Riker 1994

SSC–373 Loads and Load Combinations by A. Mansour and A. Thayamballi 1994

SSC–372 Maintenance of Marine Structures: A State of the Art Summary by S. Hutchinson and R. Bea 1993

SSC–371 Establishment of a Uniform Format for Data Reporting of Structural Material Properties for Reliability Analysis by N. Pussegoda, L. Malik, and A. Dinovitzer 1993

SSC–370 Underwater Repair Procedures for Ship Hulls (Fatigue and Ductility of Underwater Wet Welds) by K. Grubbs and C. Zanis 1993

SSC–369 Reduction of S–N Curves for Ship Structural Details by K. Stambaugh, D. Lesson, F. Lawrence, C–Y. Hou, and G. Banas 1993

SSC–368 Probability Based Ship Design Procedures: A Demonstration by A. Mansour, M. Lin, L. Hovem, A. Thayamballi 1993

SSC–367 Fatigue Technology Assessment and Strategies for Fatigue Avoidance in Marine Structures by C. C. Capanoglu 1993